AFRL-RH-WP-TR-2019-0091

MODELING REAL-TIME OCCUPATIONAL NAPHTHALENE EXPOSURES TO PREDICT URINARY BIOMARKERS

Elaine A. Merrill
Applied Biotechnology Branch

Teresa R. Sterner
Peter J. Robinson
Henry M. Jackson Foundation
for the Advancement of Military Medicine

Janis E. Hulla
U.S. Army Corps of Engineers-Sacramento District-EDE

Susan P. Proctor
U.S. Army Research Institute of Environmental Medicine

SEPTEMBER 2019
Interim Report

AIR FORCE RESEARCH LABORATORY
711TH HUMAN PERFORMANCE WING,
AIRMAN SYSTEMS DIRECTORATE,
WRIGHT-PATTERSON AIR FORCE BASE, OH 45433
AIR FORCE MATERIEL COMMAND
UNITED STATES AIR FORCE

NOTICE AND SIGNATURE PAGE

Using Government drawings, specifications, or other data included in this document for any purpose other than Government procurement does not in any way obligate the U.S. Government. The fact that the Government formulated or supplied the drawings, specifications, or other data does not license the holder or any other person or corporation; or convey any rights or permission to manufacture, use, or sell any patented invention that may relate to them.

This report was cleared for public release by the 88th Air Base Wing Public Affairs Office and is available to the general public, including foreign nationals. Copies may be obtained from the Defense Technical Information Center (DTIC) (http://www.dtic.mil).

AFRL-RH-WP-TR-2019-0091 HAS BEEN REVIEWED AND IS APPROVED FOR PUBLICATION IN ACCORDANCE WITH ASSIGNED DISTRIBUTION STATEMENT.

MATTIE.DAVID.R.1230101880 Digitally signed by MATTIE.DAVID.R.1230101880 Date: 2020.01.14 14:50:19 -05'00'

DAVID R. MATTIE, Work Unit Manager
Applied Biotechnology Branch
Airman System Directorate
711th Human Performance Wing
Air Force Research Laboratory

SIMPSON.RICHARD.D.1091443429 Digitally signed by SIMPSON.RICHARD.D.1091443429 Date: 2020.02.03 16:34:01 -05'00'

RICHARD D. SIMPSON, NH-04, DAF
Chief, Airman Bioengineering Division
Airman Systems Directorate
711thHuman Performance Wing
Air Force Research Laboratory

This report is published in the interest of scientific and technical information exchange and its publication does not constitute the Government's approval or disapproval of its ideas or findings.

REPORT DOCUMENTATION PAGE

Form Approved
OMB No. 0704-0188

1. REPORT DATE *(DD-MM-YY)*	2. REPORT TYPE	3. DATES COVERED *(From - To)*
30-09-19	Interim	January 2019 – September 2019

4. TITLE AND SUBTITLE
Modeling Real-Time Occupational Naphthalene Exposures to Predict Urinary Biomarkers

5a. CONTRACT NUMBER
FA8650-15-2-6608

5b. GRANT NUMBER

5c. PROGRAM ELEMENT NUMBER
62202F

6. AUTHOR(S)
Elaine A. Merrill[1]
Teresa R. Sterner, Peter J. Robinson[2]
Janis E. Hulla[3]
Susan P. Proctor[4]

5d. PROJECT NUMBER

5e. TASK NUMBER

5f. WORK UNIT NUMBER
H0D1 (7757HD05)

7. PERFORMING ORGANIZATION NAME(S) AND ADDRESS(ES)
HJF
2728 Q Street, B837
Wright-Patterson AFB OH 45433

U.S. Army Corps of Engineers
Sacramento District-EDE
1325 J St., Sacramento CA 95814

8. PERFORMING ORGANIZATION REPORT NUMBER

9. SPONSORING/MONITORING AGENCY NAME(S) AND ADDRESS(ES)
[1]Air Force Materiel Command
Air Force Research Laboratory
711th Human Performance Wing
Airman Systems Directorate
Airman Bioengineering Division
Applied Biotechnology Branch
Wright-Patterson AFB, OH 45433

10. SPONSORING/MONITORING AGENCY ACRONYM(S)
711 HPW/RHBB

11. SPONSORING/MONITORING AGENCY REPORT NUMBER(S)
AFRL-RH-WP-TR-2019-0091

12. DISTRIBUTION/AVAILABILITY STATEMENT
Distribution A: Approved for public release.

13. SUPPLEMENTARY NOTES
Report contains color. PA Clearance: MSC/PA-2019-0463; 88ABW-2019-5995. Cleared on 19 December 2019

14. ABSTRACT
A novel real-time naphthalene dosimeter (NaDos) prototype, sponsored by the U.S. Army, provides the capability for close monitoring of naphthalene concentration measurements to identify changes in occupational exposures. Quantitative real-time monitoring has the potential to be more accurate than traditional dosimeters that rely on sorbent tubes to provide a time weighted average of exposure concentrations following laboratory analysis. Continuous data (every 3 minutes) were collected from military fuel workers wearing the NaDos prototype monitors. Data included biometric information (height, weight and sex), traditional work day naphthalene breathing zone measurements, and spot urine samples during 3 consecutive work days. Urine was analyzed for 1- and 2-naphthol and creatinine content. Additionally, hand wash wipe and exhaled breath samples were collected post-shift; however, there were few results above the naphthalene limit of detection. In order to simulate real-time exposure data, a novel physiologically-based pharmacokinetic (PBPK) model was written to simulate the changing concentrations inhaled over time. The model structure accounted for naphthalene metabolism in the lung and liver, as well as production, distribution and urinary elimination of metabolites (combined naphthols). To predict urinary concentration, the model estimated urinary flow and creatinine production based upon sex, age and body mass index. Given data limitations, the naphthalene model satisfactorily simulated urine naphthol concentrations or creatinine normalized naphthol concentrations for most individual datasets.

15. SUBJECT TERMS
Uaphthalene, PBPK occupational exposure, biological model, dosimeter, real-time

16. SECURITY CLASSIFICATION OF:			17. LIMITATION OF ABSTRACT:	18. NUMBER OF PAGES	19a. NAME OF RESPONSIBLE PERSON (Monitor)
a. REPORT	b. ABSTRACT	c. THIS PAGE			Elaine A. Merrill
Unclassified	Unclassified	Unclassified	SAR	76	19b. TELEPHONE NUMBER *(Include Area Code)* N/A

TABLE OF CONTENTS

LIST OF FIGURES

LIST OF TABLES

PREFACE

Naphthalene dosimeter project efforts have been supported and overseen since 2009 by the Exposure Dosimeter Working Group, chartered through the Office of the Assistant Secretary of Defense (OASD) for Environment, Safety, and Occupational Health and reported quarterly to the Materials of Emerging Regulatory Interest Team (MERIT), Chemical and Material Risk Management Program, Office of the Assistant Secretary of Defense for Energy, Installations & Environment (DUSD(EIE)).

Initial funding for the project "Pharmacokinetic (PK) modeling of naphthalene biomarkers to support risk relevant human internal dose estimation" was obtained from the Military Operational Medicine Research Program (Joint Program Committee 5, JPC5 Award 21590); Dr. Susan Proctor (U.S. Army Research Institute of Environmental Medicine (USARIEM)) served as the principal investigator. The original project was submitted in partnership between the U.S. Army coauthors and the NAMRU Dayton Environmental Health Effects Research Laboratory. Supplemental support for the research described herein was provided through the Aerospace Toxicology Program in the Air Force Research Laboratory, 711th Human Performance Wing, Airman Systems Directorate, Airman Bioengineering Division, Applied Biotechnology Branch, 711 HPW/RHBB (formerly Human Centered ISR Division, Molecular Mechanisms Branch, 711 HPW/RHXJ) at Wright-Patterson Air Force Base OH.

This research was conducted under cooperative agreement FA8650-15-2-6608 with the Henry M. Jackson Foundation for the Advancement of Military Medicine (HJF). The program manager for HJF was Armando Soto (711 HPW/RHBB). Elaine A. Merrill, PhD (711 HPW/RHBBF), was the technical manager for this project.

The de-identified data provided for this modeling effort was obtained under the human use protocol "Measuring Naphthalene & Biological Markers of Exposure Among Military Fuel-Worker Personnel: The Naphthalene Dosimeter Field Validation Study (Phase II)", which was approved by the U.S. Army (MRDC IRB # M-10630; USARIEM #12-10HC (H10-10b); HRPO #A-17184.ii). Dr. Susan Proctor (USARIEM) served as the principal investigator; co-investigators were Dr. Jan Hulla (U.S. Army Corps of Engineers) and Dr. John Snawder (National Institutes of Occupational Safety and Health (NIOSH)). The study was performed in compliance with DODI 3216.02.

The views expressed in this report are those of the author and do not necessarily reflect the official policy or position of the U.S. Air Force, U.S. Army Corps of Engineers, U.S. Army, Department of the Navy, Department of Defense, nor the U. S. Government.

The authors would especially like to thank Tammie R. Covington (HJF, 711HPW/RHMO) for assistance with dosing codes.

1.0 SUMMARY

Development of a novel real-time (RT) naphthalene dosimeter (NaDos) prototype was sponsored by the U.S. Army through a Small Business Innovative Research contract. This dosimeter provides the capability for RT monitoring of naphthalene concentration measurements to identify changes in occupational exposures. The dosimeter logs naphthalene air concentrations in the breathing zone every 3 minutes by reading native fluorescence of the molecule when excited by ultraviolet (UV) light. Quantitative RT monitoring has the potential to be more accurate than traditional dosimeters that rely on sorbent tubes to provide a time weighted average of exposure concentrations following laboratory analysis.

The objective of the modeling project was to determine if RT data could be used to predict urinary naphthol concentrations in occupationally exposed personnel and thus provide validation of a physiologically-based pharmacokinetic (PBPK) model of naphthalene exposure biomarkers in humans.

De-identified data collected from 9 military fuel workers wearing the NaDos prototype were utilized to develop a PBPK model of naphthalene urinary biomarkers. Additional data utilized included biometric information (height, weight and sex). Workday naphthalene breathing zone measurements were recorded every 3 minutes over 3 consecutive work days. The NaDos reliably measured naphthalene levels within the subject's breathing zone in most cases. However, some sampling periods with high temperatures and/or high humidity rendered the naphthalene measurements as "exempt" or outside the limits at which the dosimeter had been calibrated. Spot urine samples were collected daily over the 3 days and on the fourth morning. Urine was analyzed for 1- and 2-naphthol plus creatinine content. All spot urine samples provided detectable levels of the metabolic biomarkers, 1- and 2-naphthol. Additionally, end-of-shift hand wash wipe and exhaled breath samples were collected; however, there were few analyses above the naphthalene limit of detection.

In order to simulate real-time exposure data, a novel dosing code was incorporated to capture the changing concentrations inhaled over time. The model structure accounted for naphthalene metabolism in the lung and liver as well as production, distribution and urinary elimination of metabolites (1- and 2-naphthol, combined). As spot urine samples did not provide measurements of collection volume or time from last void, individual urinary production rates could not be simulated. To predict instantaneous urinary concentration, the model estimates an average urinary flow and creatinine production based upon sex, age and body mass index. Given the limitations of the available data and creatinine normalization, the model satisfactorily simulates urine time course data for most subjects.

Future model improvements could include Monte Carlo analysis to better predict a range of individual urinary naphthols using population variability. A sensitivity analysis would help determine which parameters would need further research to improve the predictability of naphthols in urine.

Naphthols in urine were found to be good indicators of naphthalene exposure. However, exposure to naphthalene also occurs in common non-occupational activities involving petroleum fuels and cigarette smoking. Exposures outside the workplace need to be considered in finalizing models examining urinary naphthols as biomarkers of occupational naphthalene exposure.

2.0 INTRODUCTION

The ability to monitor exposures in near real-time (RT) is advantageous when assessing occupational risk for workers exposed to hazardous vapors, as transient high spikes in levels are captured. Traditional methods using sorbent tubes, which are analyzed by gas chromatograph (GC) or other laboratory intensive methods, may be sensitive and highly specific, but do not provide temporally or spatially resolved exposure information. The variability in time, concentrations or locations of exposure cannot be resolved with traditional methods, which are typically used to provide time weighted average (TWA) concentrations. Near RT monitors benefit workers, as the units are coupled with an audible alarm system that provide warning when a set exposure level is exceeded. Providing fast access to actionable data allows workers to modify engineering controls or personal protective equipment to avoid excessive exposures (Negi *et al.*, 2011).

A near RT dosimeter prototype for naphthalene, called NaDos, has been developed under Army SBIR #07-072, with the goal of delivering laboratory-quality data for qualitative and quantitative analysis. The NaDos sensor technology measures the native fluorescence of molecules when excited by ultraviolet light and has been demonstrated to perform across a range of naphthalene concentrations from 10 $\mu g/m^3$ to over 100 mg/m^3 (Reid *et al.*, 2018).

A physiologically-based pharmacokinetic (PBPK) model was required to link exposure data with naphthol in the urine. Several published PBPK naphthalene models exist (Sweeney *et al.*, 1996; Quick and Shuler, 1999; Willems *et al.*, 2001; Kim *et al.*, 2007; Campbell *et al.*, 2014). Each of these models predicted naphthalene dosimetry in either mice, rats or humans. All included the elimination of the parent compound by metabolism. However, none of the models explicitly address quantification of the urinary metabolites, 1- and 2-naphthol. Therefore, these models were reviewed and relevant portions were applied to the model presented here.

Naphthalene is an occupational exposure concern as it is currently listed by the U.S. Environmental Protection Agency as a possible human carcinogen (U.S. EPA, 1998). Naphthalene is a common exposure in the DoD as it is a component (up to 1 percent) of the single battle fuel, JP-8 (Egeghy *et al.*, 2003). JP-8 is the largest chemical exposure experienced by warfighters (NRC, 2003). Development of the NaDos was funded to aid in managing potential health risks from excessive naphthalene exposures.

Naphthalene toxicity is related to cytochrome P450 dependent metabolism to reactive intermediates, which can form DNA adducts or be detoxified by glutathione. Naphthalene has been shown to cause injury to nasal olfactory epithelium and Clara cells lining airway epithelia in mice (Van Winkle *et al.*, 1995). In rats, injury occurs to both respiratory and olfactory nasal epithelia, but in contrast to mice, there is no detectable injury to conducting airway epithelial Clara cells (Dodd *et al.*, 2012; Lee *et al.*, 2005). The abundance and high catalytic metabolism of naphthalene by CYP2F2 in mouse lung is likely responsible for the susceptibility of murine Clara cells. In rat airway microsomes, the catalytic efficiency of this enzyme is 10 to 20 percent that of the murine Clara cells (Buckpitt *et al.*, 2013; Li *et al.*, 2011). The human ortholog, CYP2F1, shares approximately 80 percent of the sequence identity but has dramatically reduced activity (Lanza *et al.*, 1999). Microsomes prepared from lung of rhesus macaques or humans metabolize naphthalene at less than 1 percent of the rate observed in rodent tissues (Buckpitt *et al.*, 2013).

2.1 Objectives

The objectives of this PBPK modeling effort were to determine if RT data could be used to predict urinary naphthol concentrations and if urinary naphthols are a good biomarker of occupational exposure to naphthalene. An additional objective was to provide a model that quantitatively addresses both exposure and elimination pathways for humans, to inform future risk assessments. Previous PBPK models for naphthalene have not quantitatively simulated naphthalene in exhaled breath nor the production of naphthols.

3.0 APPROACH

3.1 PBPK Model Structure

A PBPK model is a mix of algebraic and ordinary differential equations (ODEs). The latter are mass balance equations, which describe the rate of change of a chemical within a model compartment. Taken together, the mass balance equations for all compartments describe how the chemical distributes within the body. The amount of a chemical within a single tissue compartment at any time should equal the amount of that chemical entering the compartment in the arterial blood stream, minus the amount leaving the compartment in venous blood stream, plus the amount taken up within the compartment, minus any amount excreted (or metabolized). A schematic (Figure 1) visually diagrams the transfer of the chemical. This model was adapted from Clewell *et al.* (2001) and coded in acslX (AEgis Technologies, Huntsville AL).

Equation 1 is a mass balance equation for a compartment without metabolism or excretion and whose concentration is limited by arterial blood concentration and blood flow.

$$V_{Tiss}\, {dC_{Tiss}}/{dt} = Q_{Tiss}(C_{Art} - CV_{Tiss}) \qquad \text{Equation 1}$$

V_{Tiss} represents the tissue volume, Q_{Tiss} is tissue blood flow and the subscript, $_{Tiss}$, represents the particular tissue. C_{Art} is arterial concentration and CV_{Tiss} is the venous blood concentration within the tissue, equivalent to the concentration in the tissue (C_{Tiss}) and divided by the tissue:blood partition coefficient (P_{Tiss}). In the current model, the rapidly perfused tissue compartment is assumed to be best represented as a simple "flow limited" compartment, represented by Equation 1.

The rate of change in the amount of chemical in compartments in which the concentration is limited by diffusion is described as being proportional to the cell membrane permeability coefficient (PA_{Tiss}), as shown in the Equations 2 and 3. These equations are used to describe the slowly perfused and fat compartments in this PBPK model.

$$V_{TissB}\, {dCV_{Tiss}}/{dt} = Q_{Tiss}(C_{Art} - CV_{Tiss}) + PA_{Tiss}\left({C_{Tiss}}/{P_{Tiss}} - CV_{Tiss}\right) \qquad \text{Equation 2}$$

V_{TissB} is the volume of blood in the tissue and CV_{Tiss} is the concentration in the tissue's venous blood (capillary bed). The tissue concentration (C_{Tiss}) can then be derived from the tissue blood concentration (CV_{Tiss}) using Equation 3.

$$V_{Tiss}\, {dC_{Tiss}}/{dt} = PA_{Tiss}\left(CV_{Tiss} - {C_{Tiss}}/{P_{Tiss}}\right) \qquad \text{Equation 3}$$

To model the formation of naphthalene oxide and its subsequent conversion to the naphthols, naphthalene metabolism and elimination occurs in the lung and liver compartments. The rate of change in naphthalene concentration within the liver is described using flow limitation and saturable metabolism to naphthalene oxide as an intermediate product.

$$V_{Liv}\, {dC_{Liv}}/{dt} = Q_{Liv}\left(CA - {C_{Liv}}/{P_{Liv}}\right) - \frac{V_{MaxLiv} \times CV_{Liv}}{K_{mLiv} + CV_{Liv}} \qquad \text{Equation 4}$$

CV_{Liv} is the concentration of naphthalene in the liver capillary bed ($CV_{Liv} = C_{Liv}/P_{Liv}$). V_{MaxLiv} and K_{mLiv} are the Michaelis Menten maximum velocity and affinity constants for the conversion of naphthalene to naphthalene oxide, respectively. The lung compartment is modeled using the same approach. Note that in either tissue, V_{Max} is the result of converting the respective *VMaxC* value using body weight of the animal or human ($V_{Max} = V_{MaxC} * BW$). Because rat and human microsomal values were used for the appropriate species, V_{MaxC} is not scaled using allometry ($V_{MaxC}*BW^{0.75}$), as is customary in PBPK models when species to species extrapolation of metabolic parameters is performed.

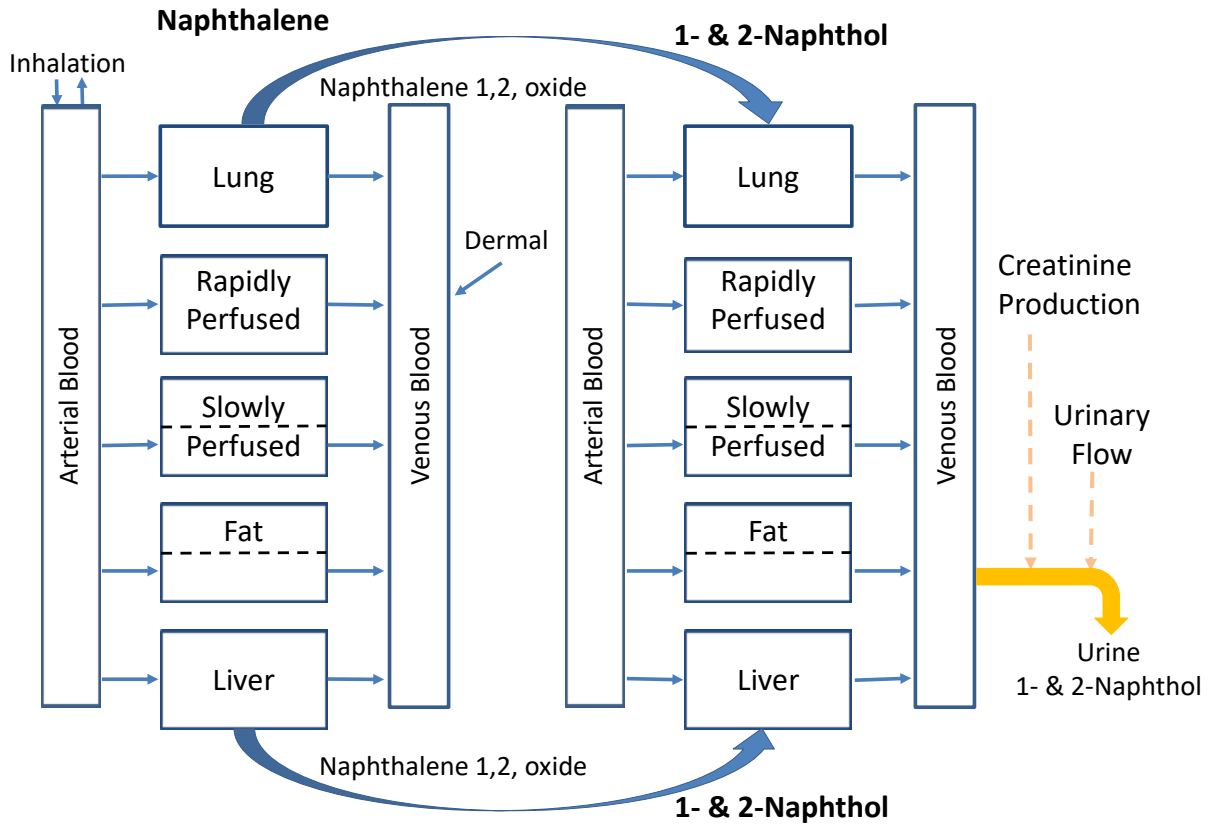

Figure 1. PBPK Model Structure for Naphthalene and its Metabolites, 1- and 2-Naphthol

Only a portion of the naphthalene dose is converted to 1- and 2-naphthol. The kinetics of other metabolites resulting from naphthalene oxide are not incorporated into this project. The fraction of naphthalene oxide converted to naphthols within the liver and lung are tracked within a parallel metabolites (naphthols) model (featured on the right side of Figure 1). Equation 5 shows the metabolite description for the liver. The metabolite lung compartment is coded likewise. The distribution of naphthols throughout all other compartments is modeled as shown for

naphthalene (Equations 1 through 4). Note that variables specific to the metabolite portion of the model are labeled with a subscript (1).

$$V_{Liv}\, {dC_{Liv1}}/{dt} = Q_{Liv}\left(C_{Art1} - {C_{Liv_1}}/{P_{Liv_1}}\right) + FOH_{Liv} * Stoch\left(\frac{V_{MaxLiv}\times CV_{Liv}}{K_{mLiv}+CV_{Liv}}\right)$$

Equation 5

C_{Liv1} and P_{Liv1} indicate the liver concentration and liver:blood partition coefficient for combined naphthols. FOH_{Liv} is the fraction of naphthalene oxide spontaneously reduced to 1- and 2-naphthol, combined, in the liver. *Stoch* facilitates the stochastic conversion of naphthalene to naphthol (MW_1/MW, where MW = molecular weight).

The model includes 3 routes of exposure, inhalation, intravenous injection (IV) and dermal. IV injection was modeled as a zero-order rate into venous blood, based upon the length of the injection time. Inhalation was modeled using the species-specific ventilation rate times the air concentration, diffusing in and out of arterial blood, based upon the blood:air partition coefficient of 571 (NTP, 2000). Dermal uptake is modeled based on the surface area of exposed skin, dermal permeability to naphthalene and blood flow to the exposed skin area. The dermal uptake route was not parameterized or simulated in this modeling effort, as exposure data for that route was not available; only a few hand wash wipe analyses were greater than the limit of detection. However, this dosing route capability was retained in the code for future use.

Urinary clearance of naphthalene itself is very low (0.3 percent of total administered dose in rats; Turkall *et al.*, 1994) and was assumed to be essentially zero in the model. Urinary clearance of the naphthol metabolites (RA_{Urine1}) was described in Equation 6 using a first order rate Cl_{Ur1} multiplied by the concentration of metabolite in arterial blood (C_{Art1}).

$$RA_{Urine1} = Cl_{Ur1} \times C_{Art1}$$

Equation 6

Urinary production (K_{Urn}, L/hour) was estimated using a urinary flow rate (0.00065 (L/hour)/kg) based on body weight (BW) for each individual, normalized to a 70 kg default human body weight (Equation 7). This estimation was developed by Hays *et al.* (2015).

$$K_{Urn} = 0.00065 \times BW \times {BW}/{70}$$

Equation 7

Using K_{Urn}, the instantaneous concentration of naphthols ($C_{UrnMetOH}$, mg/L) can then be estimated as shown in Equation 8.

$$C_{UrnMetOH} = \frac{RA_{Urine1}}{K_{Urn}}$$

Equation 8

To estimate the urinary concentration normalized to creatinine, an empirical equation that considers the age, sex and body mass index (BMI) is used to calculate the creatinine production (MCR, Equation 9) in µmol creatinine/(kg BW*day) for each subject. This equation was developed by Forni Ogna *et al.* (2015).

$$MCR = \beta_0 + \beta_1 \times sex + \beta_2 \times BMI + \beta_3 \times age + B_4 \times age^2$$

Equation 9

The values for β_0, β_1, β_2, β_3, and β_4 were calculated to be 266.16, -47.71, -2.33, 0.66, and -0.017, respectively, by Forni Ogna *et al.* (2015). The parameter *sex* is set to 0 for men and 1 for women. The resulting estimate is then converted into K_{Creat}, expressed in units of g creatinine/hour, and used in Equation 10 with the rate of change in the amount of naphthols

eliminated in urine (RA_{Urine1}) to estimate the creatinine normalized concentration of naphthols ($C_{UrnNormOH}$, mg naphthols/g creatinine) at a given moment.

$$C_{UrnNormOH} = \frac{RA_{Urine1}}{K_{Creat}} \quad \text{Equation 10}$$

3.2 Model Development with Rat Literature Studies

The PBPK model was developed using literature data from rat studies. Two main naphthalene kinetic data sets have been identified for exposure routes of interest (IV and inhalation). Research Triangle Institute (RTI) conducted a rat IV study in 1996 for the National Toxicology Program (NTP). These data were never published by the NTP; however, the data were used in published models by Quick and Shuler (1999), Willems *et al.* (2001), and Campbell *et al.* (2014). In this study, 12 male and 12 female Fischer 344 (F344) rats weighing 143 to 270 g were cannulated in the jugular vein under anesthesia for serial blood sampling. Rats were dosed intravenously with 1, 3 or 10 mg/kg naphthalene. Injection volumes were 2 mL/kg. The sample vehicle was 10 percent Emulphor®, 10 percent ethanol, and 80 percent deionized distilled water. Serial samples were drawn at 10 time points over 8 (low and mid doses) to 12 hours (high dose). Sample sizes were 125 µL for the first 4 samples and 250 µL for the remaining 6 samples. Unexposed sex-matched F344 rat plasma was replaced (250 µL) via the cannula following the fifth through the ninth draw due to the larger volume drawn at these time points. Blood sample analysis was performed utilizing a validated high-performance liquid chromatography (HPLC) system with ultraviolet (UV) detection at 260 nm.

The NTP (2000) inhalation study is available online, contains a PBPK model within the report, and has been utilized for development of two published models (Willems *et al.*, 2001; Campbell *et al.*, 2014). Male and female F344 rats (9 per sex per group) were exposed to 10, 30 or 60 ppm naphthalene 6 hours per day, 5 days per week, for up to 18 months during the NTP kinetic study. Male rats weighed 239.8 to 270.2 g at the start of the study; female rats weighed 143.4 to 168.3 g. Blood samples were drawn from the retro-orbital sinus on 5 sampling days (2 weeks, 3, 6, 12 and 18 months). On each sampling day, blood was drawn at 6 time points over 8 (10 ppm group) or 16 hours (30 and 60 ppm groups) following the end of exposure, with an n of 3 per sex at each time point. Each rat was sampled twice on a sampling day, once from each sinus. The male rat data from the 2-week sampling day was simulated herein. An additional group of 12 male and 12 female rats were exposed once to the same concentrations for 6 hours; blood was collected 8 times over 8 hours with an n of 3 per sex per time point. Blood samples were analyzed using HPLC with UV light detection at 260 nm. Male rat data from this group were used in the model.

3.3 Model Refinement with Human Literature Studies

Conventional kinetic studies for humans were not found in the literature. However, 2 studies were instrumental in refining the rat model for humans. First, Egeghy *et al.* (2003) measured benzene and naphthalene in exhaled breath from U.S. Air Force workers exposed for 4 hours to low, moderate and high levels (fuel maintenance workers) of JP-8 jet fuel. Expired naphthalene levels were reported for fuel maintenance workers exposed to an average concentration of 485 µg naphthalene/m^3. Exhaled breath samples were collected on glass bulbs, transferred to sorbent

tubes, desorbed in the laboratory and analyzed using gas chromatography with a photo-ionization detector. Body weights were not listed in the study; the model was run with an assumed 70 kg average.

A study by Bieniek (1994) measured 1-naphthol concentrations in the urine of coke plant and naphthalene oil plant workers. Grab samples were collected from 26 workers, presumably at each site, over approximately 17 hours from the start of a work shift. Average exposure concentrations in each plant were not stated in the article. Naphthalene oil contained 73.6 percent naphthalene, some 1-naphthol and other hydrocarbons. Coke plant atmospheres contained naphthalene and other hydrocarbons but no naphthol. 1-Naphthol was quantified using thin layer chromatography followed by spectrophotometry. Body weights were not listed in the study; a 70 kg average was assumed.

3.4 Real-time Human Data

Urine data (naphthols and creatinine concentrations) for 17 subjects, collected as part of the parent study, were received for this modeling effort. These represented 1 female and 16 male active duty members. All were actively engaged in jobs with regular, daily exposure to jet fuel (JP-8 or JP-5). Approximately 70 percent (12) subjects were active duty Air Force (AF) personnel; the remainder (5) were active duty Navy. All participants were not current tobacco smokers, per the study design. AF subjects were studied over 3.5 days during their occupational work week at an AF base in the Midwest while performing fuel cell repair activities. Navy personnel were studied for 3.5 days during a standard work week period while conducting off-shore exercises on an aircraft carrier. During the parent study, neither volumes of urine voids nor the time from last void were recorded, so individual urinary flow rates could not be established. However, height, body weight and age were reported for these individuals. These data were used to estimate average creatinine excretion rates in the model using an algorithm published by Forni Ogna *et al.* (2015). Average creatinine concentrations from each of these 17 individuals were used to evaluate the predictability of this algorithm.

Real-time breathing zone concentration data were received to correlate with the urine data. Subjects were down-selected for modeling based on several criteria. All subjects wore a NaDos RT monitor as well as a conventional personal monitoring device (Chromosorb 106 tubes or polytetrafluoroethylene (PTFE) filtered XAD® resin tubes). One subject (#12) was excluded as no RT data were available to correlate to this subject's urine data. For this modeling project, subjects were excluded if the RT data collection period was shorter by more than 1 hour than the conventional collection period, as in these instances, the RT data would not capture the total occupational naphthalene exposure, as the conventional monitors would not have been running if the subjects were not working.

The NaDos RT monitor reads the native fluorescence of the molecule when excited by UV light and reports a concentration based on an internal table that takes into account ambient temperature and humidity. NaDos will report a data point that falls outside the table as a concentration but labels the value as "exempt". For this modeling study, a day's data were considered acceptable if less than 50 percent of the data points were exempt. A subject was retained only if the acceptable day(s) fell on Day 1, Days 1 and 2, or Days 1 through 3 of the work week. Data from 9 subjects fit these criteria for modeling. Following model building, 3

additional subjects were simulated whose data fit all other criteria, but due to temperature and/or humidity, all or most data points were labeled exempt; these simulations are found in Appendix A.

Inhalation data from individuals fitting these criteria were then smoothed utilizing a simple moving average with an n of 2. Briefly, the first two concentrations registered by NaDos were averaged to become the first smoothed concentration used by the model. Then the second and third concentration registered are averaged to become the second model concentration, and so on. Simple moving averages are used with many types of RT data to smooth out short-term fluctuations, reduce noise and highlight longer-term trends (Hu *et al.*, 2015).

End-of-shift measurements of exhaled air were collected and analyzed for naphthalene using thermal desorption followed by gas chromatography followed by time of flight mass spectrometry (MS) using the National Institute of Occupational Safety and Health (NIOSH) method 2549 at Taft Laboratories, (Cincinnati OH). Hand wipe samples were collected post-shift to assess dermal exposure and analyzed for total polycyclic aromatic hydrocarbons (2- to 4-ring and 4- to 6-ring) using NIOSH method 5800. The NIOSH Manual of Analytical Methods (5^{th} Edition) can be found online (<https://www.cdc.gov/niosh/nmam/default.html>). Detection of naphthalene and polycyclic aromatic hydrocarbons were not consistently detected in these samples; dermal and exhaled breath were not included in the modeling effort.

Subjects were asked to collect urine samples at the beginning of the shift on Day 1, upon waking on Days 2, 3 and 4, immediately following the shift on Days 1 through 3, and near 2100 on Days 1 through 3. Urine samples were refrigerated immediately, shipped to NIOSH and then to the Centers for Disease Control (CDC, Atlanta GA). There they were analyzed for 1- and 2-naphthol by GC-MS as described by Serdar *et al.* (2003).

3.5 Model Parameterization

The rate of entry of any chemical into a tissue depends on blood flow to the tissue, the tissue volume, and partition characteristics between blood and tissue. Equilibrium in distribution (when entry and exit rates are the same) between blood and tissue is reached more quickly in rapidly perfused areas (e.g., kidney and brain), unless diffusion across cell membranes is the rate-limiting step. After equilibrium, drug concentrations in tissues and in extracellular fluids are reflected by the blood concentration. Metabolism and excretion also occur simultaneously with distribution, making the process dynamic and complex.

Parameters used to describe these processes within the PBPK model are species and chemical specific. Physiological parameters, describing blood flows and tissue volumes, for rat and human were obtained from experimentally measured data as stated in Table 1. To account for variation associated with size, all rate constants are scaled by $BW^{0.75}$ unless otherwise noted; this practice is known as allometric scaling.

The physicochemical specific parameter list for each chemical (naphthalene and its metabolites) includes tissue:blood partition coefficients (*PCs*), permeability coefficients (*PAs*), Michaelis-Menten metabolic constants (V_{max} and K_m values), and clearance (*Cl*) rates. Tissue:blood partition coefficients are critical parameters in PBPK modeling as they govern steady state chemical distribution and generally are fairly consistent across species. Measured PC values in

mouse tissue, utilized in the Campbell *et al.* (2014) human and rat model, were chosen for the model herein (Table 2). Measured rat PCs are not available. For the naphthols, a mechanistic tissue composition model for the prediction of steady-state tissue:plasma PCs was utilized that uses chemical lipophilicity, *pKa*, phospholipid membrane binding, and the unbound plasma fraction, together with tissue fractions of water, neutral lipids, neutral and acidic phospholipids, proteins, and pH (Ruark *et al.*, 2014). Inputs included measured tissue composition data from the rat compiled by Ruark and others (2014), *LogKow* (*logP*, *logD*) taken from ChemSpider database (www.chemspider.com), and the assumption of negligible active transport. The tissue:plasma PC values calculated were assumed to be sufficiently similar to tissue:blood PCs (Table 2). PCs for both 1- and 2-naphthol were average together for each tissue in the model, as they were not simulated separately.

The rat Michaelis Menten affinity constant (K_m) used for lung tissue was the weighted average of two K_m values published for rat lung microsomes by Buckpitt *et al.* (2013). For the liver K_m, the lung value was used as no rat liver microsomal values could be found in the literature. For the human model, the liver K_m was the lowest value published in the Cho *et al.* (2006) human liver microsome study. The lung K_m used was the weighted average of lung affinity constants published by Buckpitt *et al.* (2013) for non-human primate (NHP) lung microsomes. K_m values in Table 3 have been converted to model relevant units, which differ from the published units.

Table 1. Physiological Constants

Parameter (Constants)	Name	Rat	Human
BW	Body weight (kg)	0.22	[a]
QCC	Cardiac output (blood flow) (L/hour*kg)	14.6	12.89
Tissue Blood Flows [fraction of Cardiac Output (*QCC*), L/hour*kg)]			
QPC	Alveolar (Pulmonary)	24.75	27.75
QFatC	Fat	0.07	0.052
QLivC	Liver	0.183	0.227
QLuC	Lung	0.021[b]	0.025[b]
QRapC	Rapidly perfused	0.557	0.419
QSknC	Skin	0.058	0.058
QSlwC	Slowly perfused	0.17	0.188
Tissue Volumes [fractions of BW, kg = L]			
VAlvC	Alveolar blood	0.007	0.0079
VFatC	Fat	0.10	0.214
VLivC	Liver	0.034	0.026
VLuC	Lung	0.005[b]	0.0076[b]
VRapC	Rapidly perfused	0.045[c]	0.0484[c]
VSkn	(Calculated based on surface area of application and *Depth*, then subtracted from *VSlw; Not a constant*)		
VSlwC	Slowly perfused	0.65	0.536
Tissue blood volumes [fraction of tissue volumes, L]			
VFatBC	Blood fraction of fat	0.02[b,d]	0.02[b]
VSlwBC	Blood fraction slowly perfused	0.033[b,e]	0.04[b,e]
Dermal Thickness (cm)			
Depth	Skin depth	0.1	0.1

Notes: All tissue volumes and blood flows taken from Clewell *et al.* (2001), unless noted otherwise. [a]Model used subject specific BW. [b]Source: Brown *et al.* (1997). [c]Clewell *et al.* (2001) value, with brain volume added and lung subtracted. [d]Human value. [e]Mean of slowly perfused tissue values except fat.

Table 2. Physicochemical Specific Tissue:Blood Partition Coefficients and Cell Membrane Permeability Coefficients

Parameter (Constants)	Naphthalene	1-Naphthol[a]	2-Naphthol[a]
Blood:Air (*PB*)	571[b]	10000[c]	
Tissue:Blood Partition Coefficients (PC, unitless)[b]			
Fat (*PFat*)	49	10.2	7.3
Liver (*PLiv*)	1.6	0.88	0.55
Lung (*PLu*)	3.5	0.88	0.54
Rapidly Perfused (*PRap*)	3.5	0.72	0.46
Slowly Perfused (*PSlw*)	3.5	0.45	0.24
Cell Membrane Permeability Coefficient Constants (PA, L/(hour*kg$^{0.75}$))[d]			
Fat (*PAFatC*)	0.4	0.4	
Slowly Perfused (*PASlwC*)	4.0	4.0	

Notes: [a]PCs for the naphthols were averaged together for use in the model; [b]Naphthalene PCs published by Campbell *et al.* (2014) and naphthol values calculated using Ruark *et al.* (2014); [c]High value = non-volatile; [d]Fit to data

Table 3. Metabolic and Clearance Parameters

Parameter	Units	Rat Value	Human Value
Lung K_m	mg/L	2.18	8.7
Liver K_m	mg/L	2.18	2.94
Lung V_{MaxC}	mg/(hour*kg)	0.45	0.0035
Liver V_{MaxC}	mg/(hour*kg)	8.28	0.775
Cl_{UrC} Naphthalene	L/(hour*kg$^{0.75}$)	0	0
Cl_{UrC} Naphthols	L/(hour*kg$^{0.75}$)	[a]	0.4

Notes: [a]Parameter set same as human value

Lung $V_{Max}C$ values based on rat microsomal metabolic activity were located in Buckpitt *et al.* (2013); two values were estimated, indicated more than one metabolic process, so these values were added for an approximate total $V_{Max}C$. Again, rat liver microsomal studies were not found in the literature; instead a ratio of liver:lung microsomal activity was calculated from rat data in Buckpitt *et al.* (1987). That ratio (1.88) was used with the Buckpitt *et al.* (2013) lung total activity to estimate liver microsomal activity. Human $V_{Max}C$ values were more readily available. Liver $V_{Max}C$ was set to the sum of the metabolite values reported in Cho *et al.* (2006). Lung $V_{Max}C$ was converted from the lowest NHP $V_{Max}C$ value reported in Buckpitt *et al.* (2013) and used by Campbell *et al.* (2014). To convert microsomal metabolic activity, the protein content values used by Campbell *et al.* (2014) were utilized; these values are 45 and 4.6 mg/g for the rat liver and lung; and 32 and 2.3 mg/g for the human liver and lung, respectively.

The rat $V_{Max}C$ values were utilized in the model using the NTP (2000) rat inhalation data. The *in vitro* derived values were found to be too high to describe the rat data. Through iterative fitting, lung and liver $V_{Max}C$ values had to be decreased by a factor of 100 in order to match the concentration of parent compound (naphthalene) in the blood of this kinetic study. The IV study blood concentration data from RTI (1996) were then used to confirm this reduction of metabolic capacity. As this approach worked for two rat data sets and as human blood time course data were unavailable, the human $V_{Max}C$ values based on the same type of *in vitro* study were also decreased by a factor of 100. Next, PA values for the fat and slowly perfused tissues were fit to the NTP (2000) time course data.

Detailed pathways of naphthalene metabolism have been reviewed in ATSDR (2005), Buckpitt and Franklin (1989), Buckpitt *et al.* (2002), and Cho *et al.*, (2006), among others. Naphthalene is metabolically converted by cytochrome-P450-dependant monooxygenases to naphthalene epoxide, which exists in two chiral forms (naphthalene-1R,2S epoxide or naphthalene-1S,2R epoxide). Many biochemical pathways occur from this point. The epoxide is speculated to covalently bind DNA. Glucuronidation yields three potential GSH conjugates. Spontaneous rearrangement of the epoxide results in 1- and 2-naphthols. Finally, epoxide hydrolase produces 1,2-dihydro-1,2-dihydroxy naphthalene (Buckpitt and Bahnson, 1986; Cho *et al.,* 2006). Under *in vitro* conditions, human liver microsomal enzymes produce from naphthalene approximately 10 percent naphthols, of which 90 percent is 1-naphthol (Cho *et al.*, 2006). Buckpitt *et al.* (2013) reported 5.5 percent of the metabolites to be 1-naphthol; 2-naphthol was not measured. These reported *in vitro* values served as a starting point for estimating naphthols production in humans.

A urinary clearance rate for naphthols (Cl_{UrC1}) in humans was estimated to be 0.4 L/(hour*kg$^{0.75}$). This was determined by fitting the clearance parameter to the shape of the urinary naphthol data reported by Bieniek (1994). Urinary clearance of naphthalene itself is so low as to be assumed zero (Turkall *et al.*, 1994).

4.0 RESULTS

The model code and m files are found in Appendices B through J. Inclusion of these lengthy files ensures the ability to reconstruct the model and incorporation of all data used in model development and individual subject predictions.

4.1 Rat Literature Data Simulations and Predictions

As a first step, the model was fit to the NTP (2000) rat study. Blood time course data were available for a single 6-hour inhalation exposure to 10, 30, or 60 ppm. Following fitting of the $V_{Max}C$ magnitude (1/100 the *in vitro* microsome value), the peak concentration simulated in the blood adequately matched the data. Following fitting of the slowly perfused and fat PA values, the width of the time course data curve was adequately described (Figure 2). Special attention was paid to the 10 ppm exposure data, as this lower concentration is closer to human occupational exposures (Figure 2 inset).

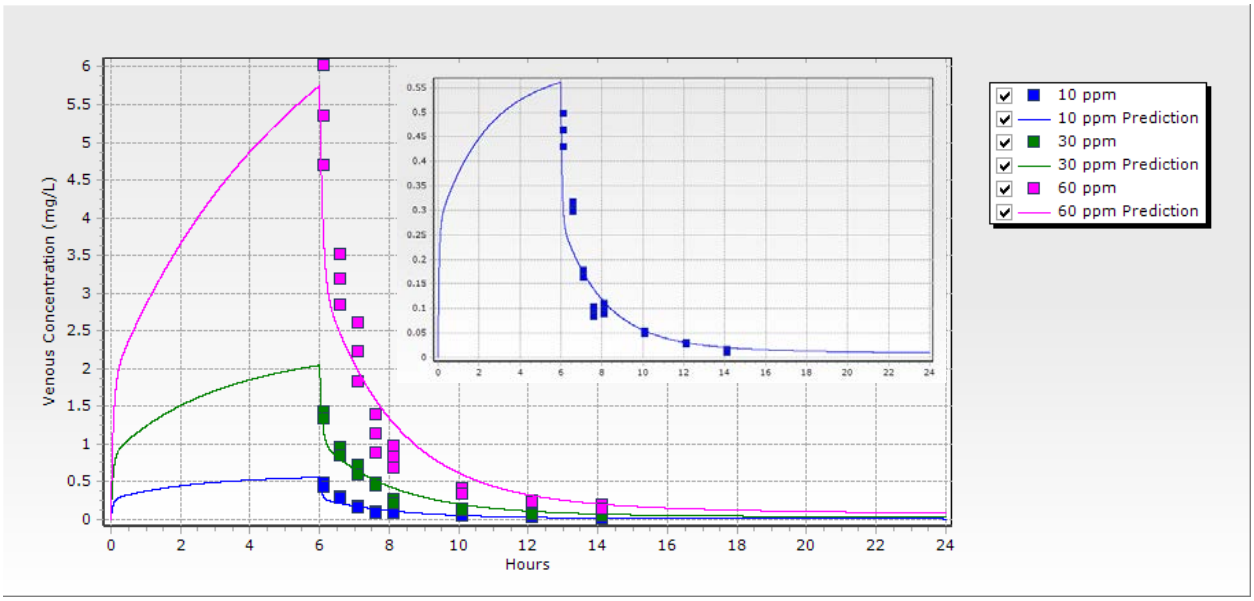

Figure 2. Simulation of NTP (2000) Single Inhalation Naphthalene Exposure Data

Simulation colors (solid lines) correspond to reported data values (squares) representing mean ± standard error (SE) for three naphthalene exposure concentrations: 10, 30 and 60 ppm. The inset shows the 10 ppm simulation and data alone.

Next the RTI IV data were used to determine if the rat model parameters were sufficient to predict blood naphthalene levels, given that a previous naphthalene model (Willems *et al.*, 2001) was unable to simulate both this IV data set and the NTP inhalation set with the same parameter values. The model and parameters described herein were found to perform adequately to predict the general magnitude of the IV data in male (Figure 3) and female (Figure 4) rats without

alteration. More importantly, insets in Figures 3 and 4 indicate a better fit to data from the lowest IV concentration (1 mg naphthalene/kg).

The NTP (2000) study also provided repeated 6-hour exposure (5 days/week for 2 weeks) time course data. The decreased peak height of these data indicate that up-regulation of the metabolic enzymes likely occurred. Following repeated naphthalene doses, Elovaara *et al.* (2007) measured up to 6.4 fold increases of glucuronidation in the rat liver and up to 1.9 fold increases in the rat lung; the liver:lung up-regulation ratio was therefore 3.4. Up-regulation was fit to the repeated exposure data while keeping the ratio constant; the repeated $V_{Max}C$ value was 1.40 times the single exposure value in the liver and 1.12 in the lung (Figure 5).

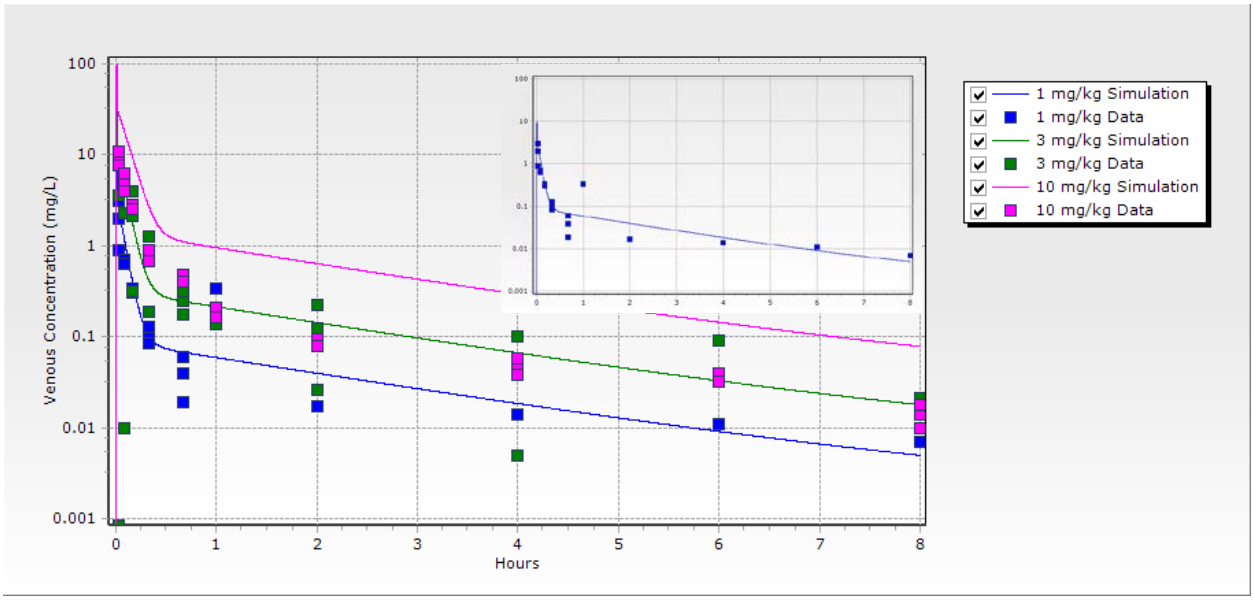

Figure 3. Prediction of Naphthalene Blood Concentrations following a Single Intravenous Injection of Naphthalene Administered to Male Rats

Prediction colors (solid lines) correspond to RTI (1996) data values (squares) representing mean ± SE for three naphthalene exposure concentrations: 1, 3 and 10 mg/kg. The inset shows the 1 mg/kg prediction and data alone.

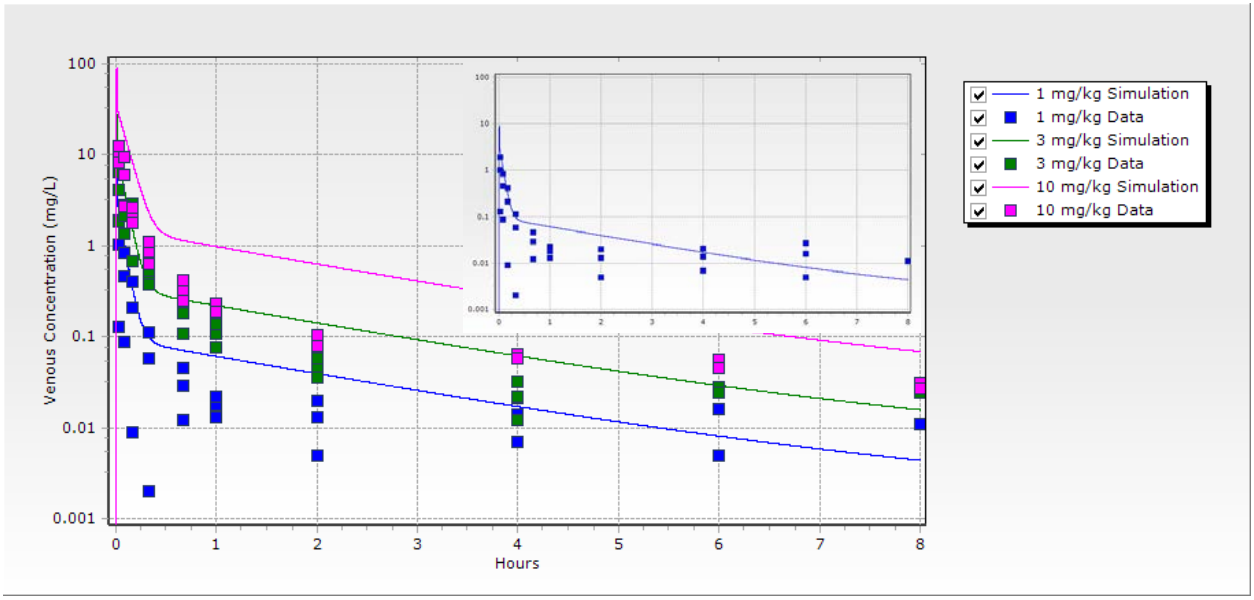

Figure 4. Prediction of Naphthalene Blood Concentrations following a Single Intravenous Injection of Naphthalene Administered to Female Rats

Prediction colors (solid lines) correspond to RTI (1996) data values (squares) representing mean ± SE for three naphthalene exposure concentrations: 1, 3 and 10 mg/kg. The inset shows the 1 mg/kg prediction and data alone.

A

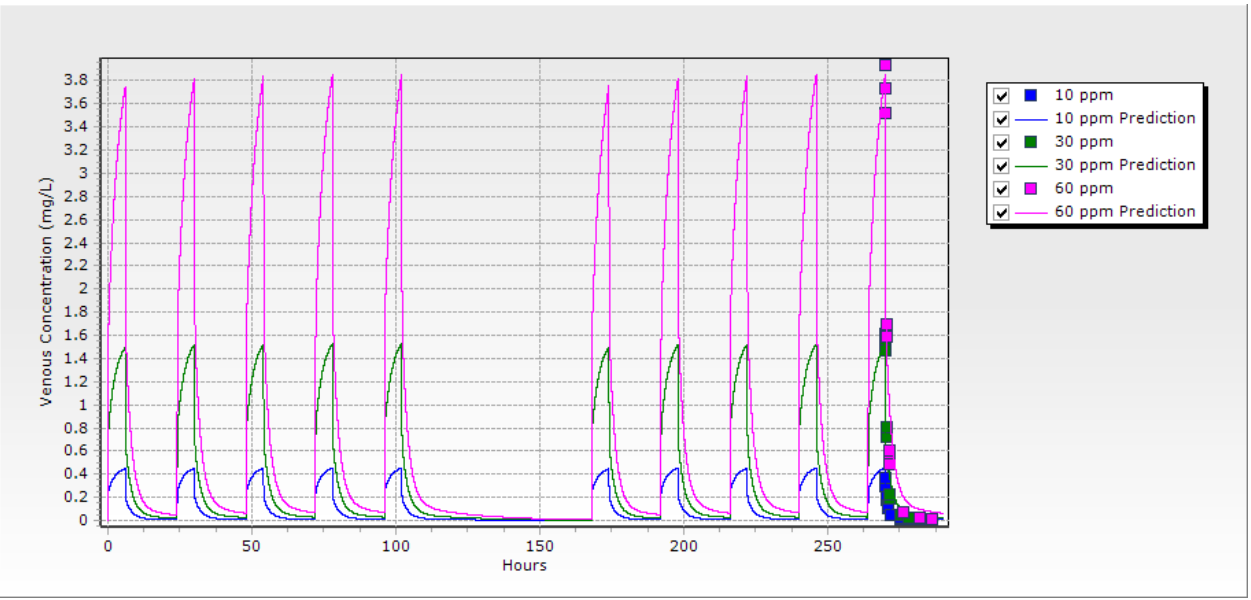

B

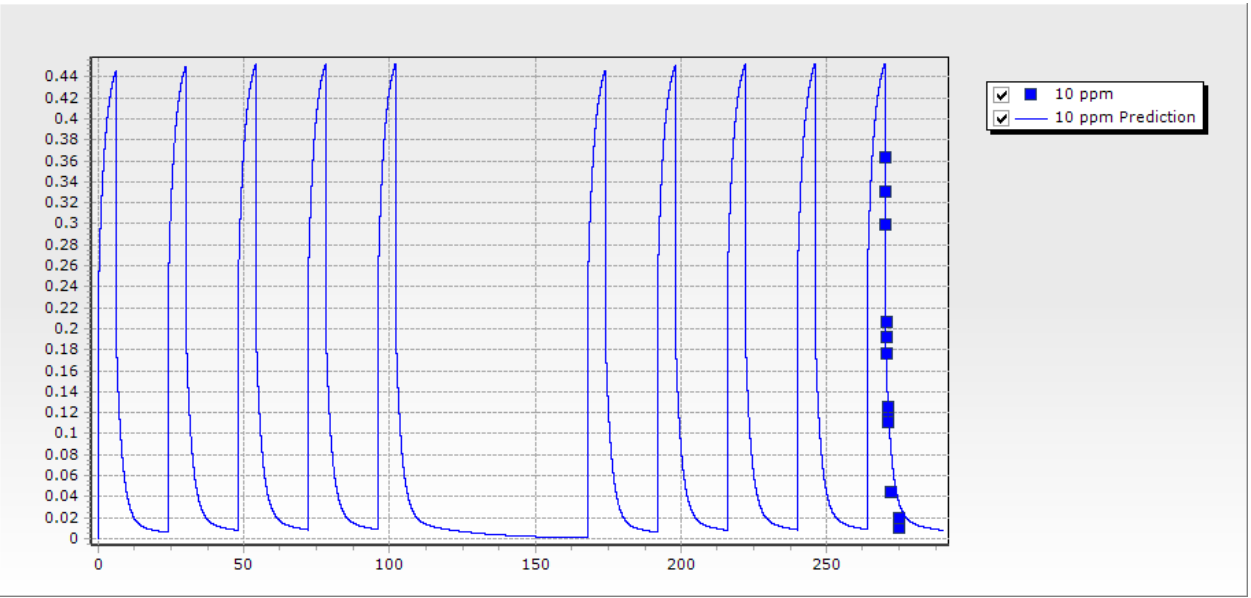

Figure 5. Simulation of NTP (2000) Repeated Inhalation Naphthalene Exposure Data

(A) Simulation colors (solid lines) correspond to reported data values (squares) representing mean ± SE for three naphthalene concentrations (10, 30 and 600 ppm) over two weeks of exposure. (B) The 10 ppm simulation and data are shown alone.

4.2 Human Literature Data Simulations

Human simulations were run utilizing human physiological (Table 1) and rat model physicochemical specific parameters, whenever human values weren't available (Tables 2 and 3). Rat urine data were not available to estimate metabolite urinary clearance. Human occupational data were available, however, from Bieniek (1994). Urinary clearance was estimated to be approximately 0.4 L/(hour*kg$^{0.75}$) based on fitting to excretion patterns shown in Figures 6 and 7 and the assumption of 1-naphthol being formed from 10 percent of the liver metabolites and 5.5 percent of the lung metabolites, as explained in the Approach section above.

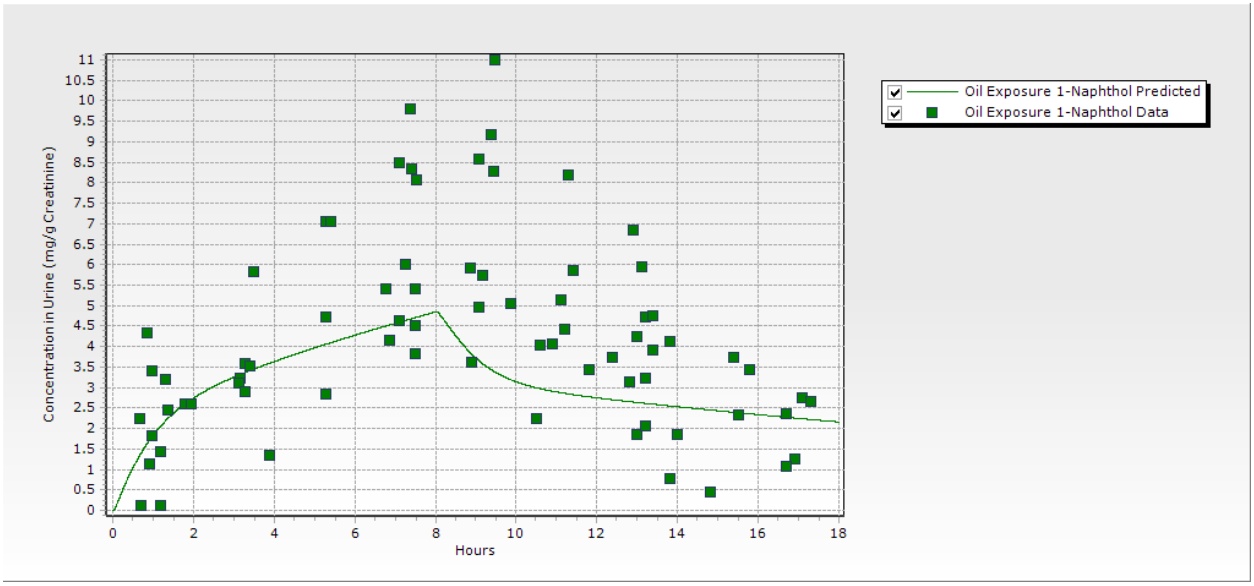

Figure 6. Simulation of 1-Naphthol Excretion following Naphthalene Occupational Exposures in a Naphthalene Oil Plant

The simulation (solid line) indicates the general pattern of excretion in urine compared to data (squares) from Bieniek (1994). Average urine production (Hays et al., 2015) and creatinine production (Forni Ogna et al., 2015) were assumed for this simulation.

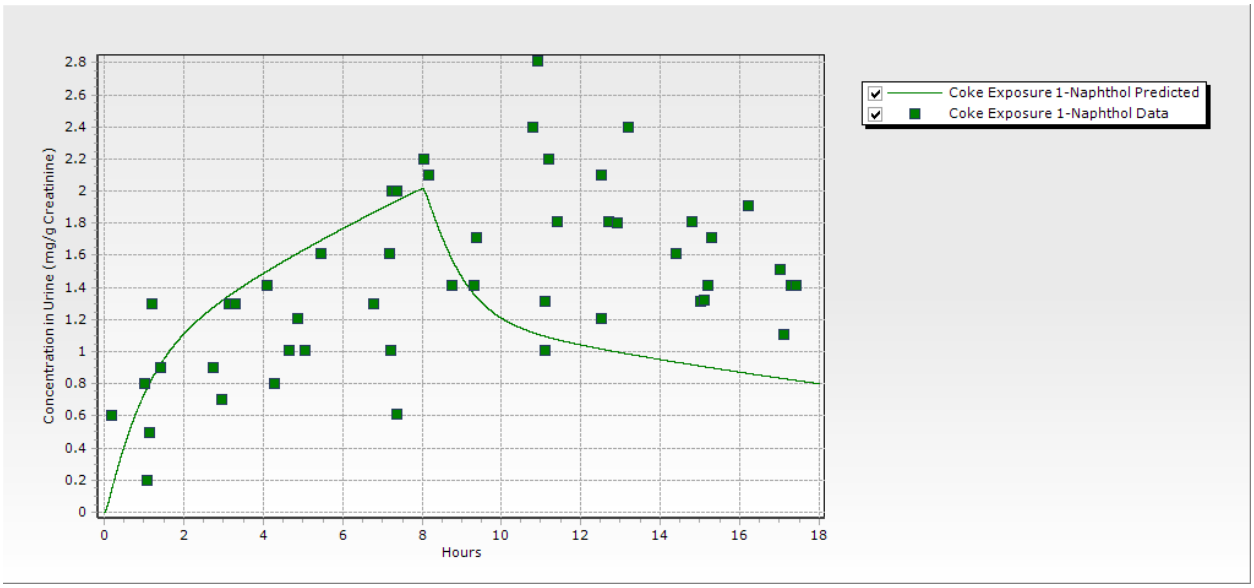

Figure 7. Simulation of 1-Naphthol Excretion following Naphthalene Occupational Exposures in a Coke Plant

The simulation (solid line) indicates the general pattern of excretion in urine compared to data (squares) from Bieniek (1994). Average urine production (Hays et al., 2015) and creatinine production (Forni Ogna et al., 2015) were assumed for this simulation.

Data from Egeghy *et al.* (2003) were used to verify model assumptions affecting naphthalene in exhaled breath, namely the blood:air PC. A prediction of naphthalene in exhaled air for the highest exposure group (military JP-8 fuel handlers) is shown in Figure 8, which indicates sufficient confidence in the blood:air partition coefficient and other exhalation assumptions.

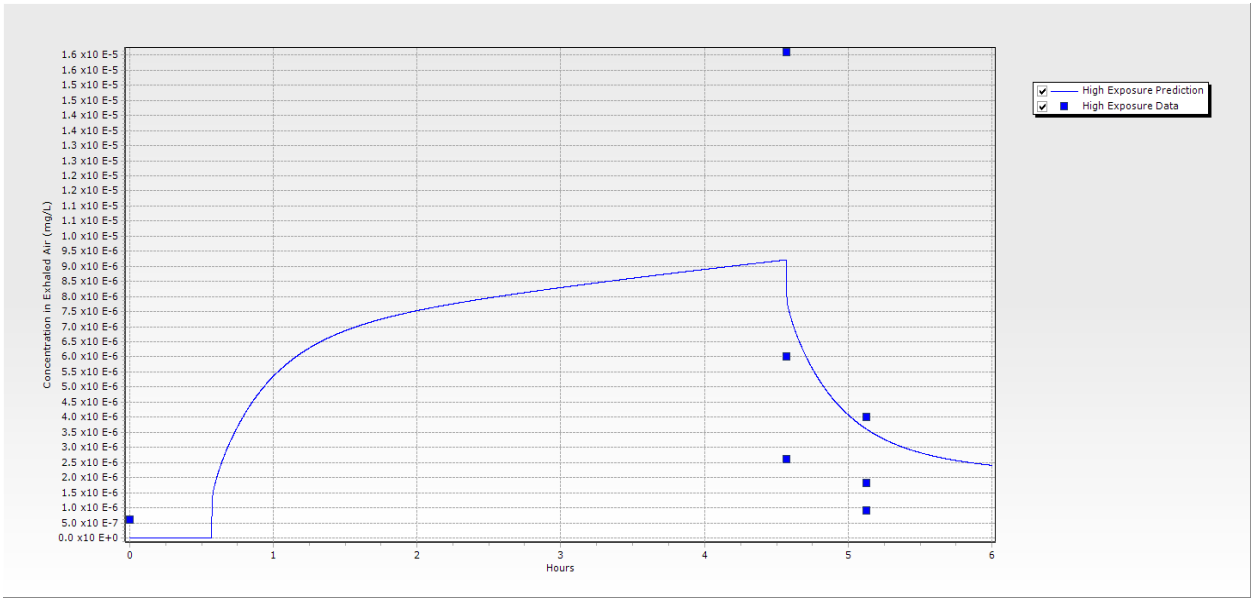

Figure 8. Prediction of Naphthalene in Exhaled Breath Excretion following Military Fuel Handler Exposure to JP-8

The simulation (solid line) indicates the predicted exhaled concentration compared to median and upper and lower quartile data (squares) from Egeghy et al. (2003). Fuel handlers were exposed to a time weighted average of 485 µg/m^3 naphthalene.

4.3 NaDos Real-time Data Analysis

Urinary excretion data from 17 subjects was examined and summarized in Table 4. Data in this table were sorted by the average 1-:2-naphthol ratio in each subject's urine sample. *In vitro* naphthalene metabolic studies using human liver microsomes indicated that 1-naphthol was produced in a quantity 10 times greater than 2-naphthol (Cho *et al.*, 2006). This ratio is not upheld in the subject data. Six subjects produced more 1-naphthol than 2-naphthol; the remaining 11 showed the opposite trend. Due to this variability in the observed data, 1- and 2-naphthol concentrations in urine were added together at each time point and the naphthol production predictions, generated using the average naphthol PCs shown in Table 2, were summed in the model.

Average creatinine concentration by subject and each subject's predicted daily creatinine production (Forni Ogna *et al.*, 2015) are listed in Table 5; data in this table are ordered by average creatinine concentration. Figure 9 shows these same data in a graph together. Observed average creatinine concentrations do not correlate with predicted values.

Table 4. Individual Urinary Naphthols Variation

Subject	1-: 2-Naphthol	
	Ratio	**Range**
05*	0.24	0.07 – 0.42
09	0.30	0.10 – 0.68
18	0.40	0.14 – 0.63
11	0.41	0.12 – 0.68
19	0.40	0.25 – 0.53
17	0.54	0.01 – 1.36
16	0.55	0.15 – 1.55
13	0.70	0.37 – 0.99
10	0.72	0.18 – 1.60
14	0.66	0.20 – 1.22
12	0.88	0.23 – 1.45
20	1.27	0.38 – 2.35
02	1.60	0.57 – 2.03
06	2.06	0.38 – 4.17
01	2.06	1.18 – 2.53
08	3.26	0.54 – 5.43
04	4.09	1.12 – 6.95
Average	1.20	0.01 – 6.95

Note: *Female – all other subjects are male

Table 5. Individual Urinary Average Creatinine Variation

Subject	Sex	BMI (kg/m^3)	Creatinine Concentration (g/L)		Creatinine Production (µmol/(kg*day)
			Average	SD	Predicted Value[a]
20	M	26.5	0.819	0.864	210
16	M	25.1	0.823	0.413	213
17	M	23.2	0.836	0.458	218
18	M	21.3	0.852	0.436	223
14	M	28.8	1.156	0.498	205
13	M	22.0	1.215	0.572	221
01	M	25.9	1.422	0.733	212
12	M	25.3	1.516	0.624	213
08	M	34.3	1.524	0.638	186
04	M	30.1	1.605	0.473	202
19	M	38.8	1.636	0.886	182
02	M	27.6	1.767	0.747	208
10	M	26.4	2.062	0.644	211
11	M	23.6	2.116	1.110	217
06	M	23.1	2.289	2.791	219
05[b]	F	22.8	2.383	0.298	171
09	M	22.6	2.999	1.008	220

Notes: SD = standard deviation; [a]Predicted based on the work of Forni Ogna *et al.* (2015); [b]Female – all other subjects are male

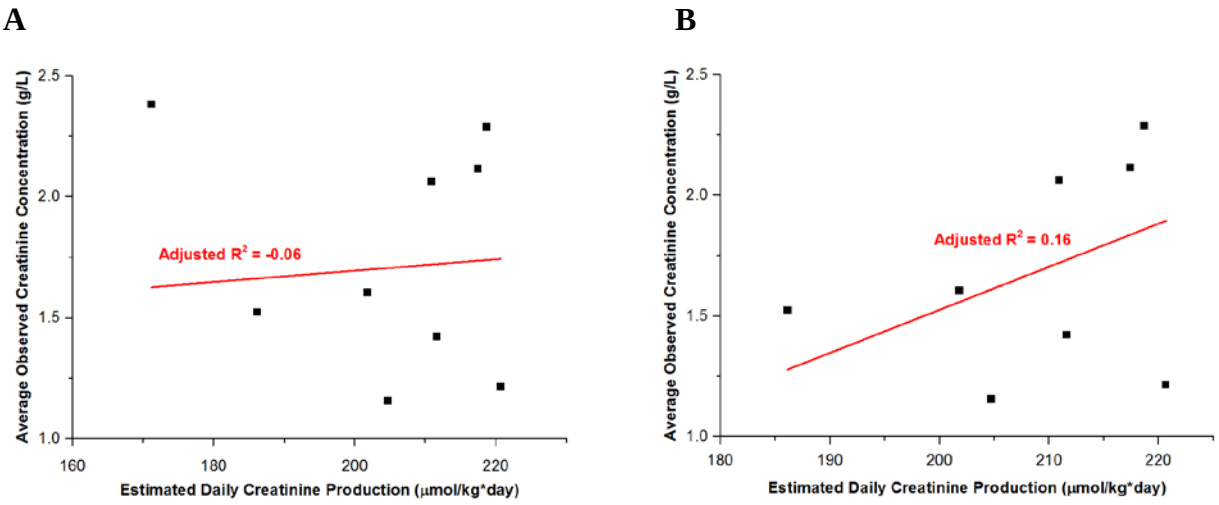

Figure 9. Relationship of Predicted Daily Creatinine Production and Measured Average Creatinine Concentration in Urine Samples of 17 Subjects

Daily creatinine production was predicted using the work of Forni Ogna et al. (2015). (A) Data included the single female subject. (B) Data excluded the single female subject.

4.4 Human Real-time Data Predictions

Given the variability inherent in the real-time subject urine data discussed above, a range of urinary naphthols was predicted for each of the nine subjects with paired real-time and urine data that met the requirements laid out in the Approach section. This lower prediction of this range was set as discussed, with naphthols constituting 10 percent of liver metabolites (Cho *et al.,* 2006) and 5.5 percent of lung metabolites (Buckpitt *et al.,* 2013). The upper prediction of the range was set at 20 percent of liver metabolites and 11 percent of lung metabolites by simple doubling.

A novel array dosing code was utilized to input the real-time data. Two arrays were constructed for each subject, one listing the time spent at each step and the other the concentration at each step. As the NaDos dosimeters sample every 3 minutes, many step durations were 0.05 hours. Successive periods of time spent at the same concentration (usually 0 ppm) were consolidated into one longer step to save lines in the arrays. Non-work hours were set to 0 ppm and lasted from the final dosimeter reading at night to the first dosimeter reading the next morning. On the last day of exposure in the simulation, the non-work hours stretched from the final dosimeter reading until the time of the urine sample the following morning. Individual subjects had as many at 501 steps in their arrays.

Predictions for each of the nine subjects are found in the Figures 10 through 18. Sex, height, body weight and age were input for each subject, along with their time and concentration arrays. Predictions for each include (A) a graph of the individual exposure concentrations in air, (B) a blood concentration time course, (C) a range of combined naphthols concentration in the urine compared to observed data, and (D) a range of combined naphthols concentration corrected to predicted creatinine production. The ranges are set at 10 to 20 percent of liver metabolites and 5.5 to 11 percent of lung metabolites, as discussed above. Full sets of predictions for the three exempt subjects are included in Appendix A.

The model is able to predict urine naphthol concentrations for some individuals (Figures 12, 13, 15, 16) and creatinine corrected concentrations for other subjects (Figures 10, 11, 18). Some subjects' data are in less accord with predictions (Figures 14 and 17). The graphs that make up these figures are on different scales (Y-axes).

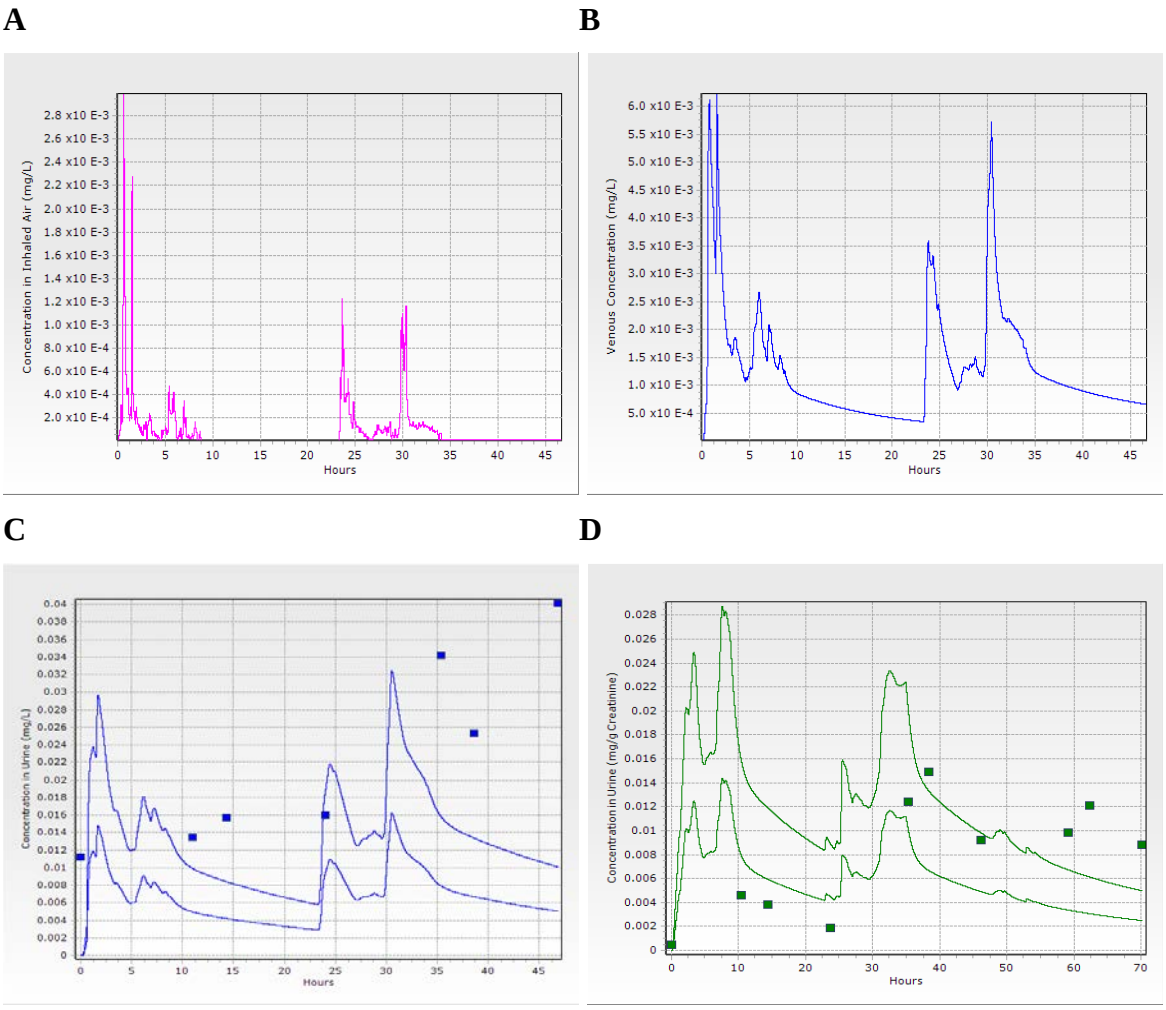

Figure 10. Predictions for Subject 01

Individual model predictions (lines) compared to observed data (squares) for: (A) Naphthalene exposure concentrations in inhaled air (mg/L), (B) Venous naphthalene blood concentration time course (mg/L); (C) A range of combined naphthols concentrations over time in the urine (mg/L) using predicted urine production (Hays et al., 2015); and (D) A range of combined naphthols concentrations over time corrected to predicted creatinine production (mg/g creatinine), based on the work of Forni Ogna et al. (2015).

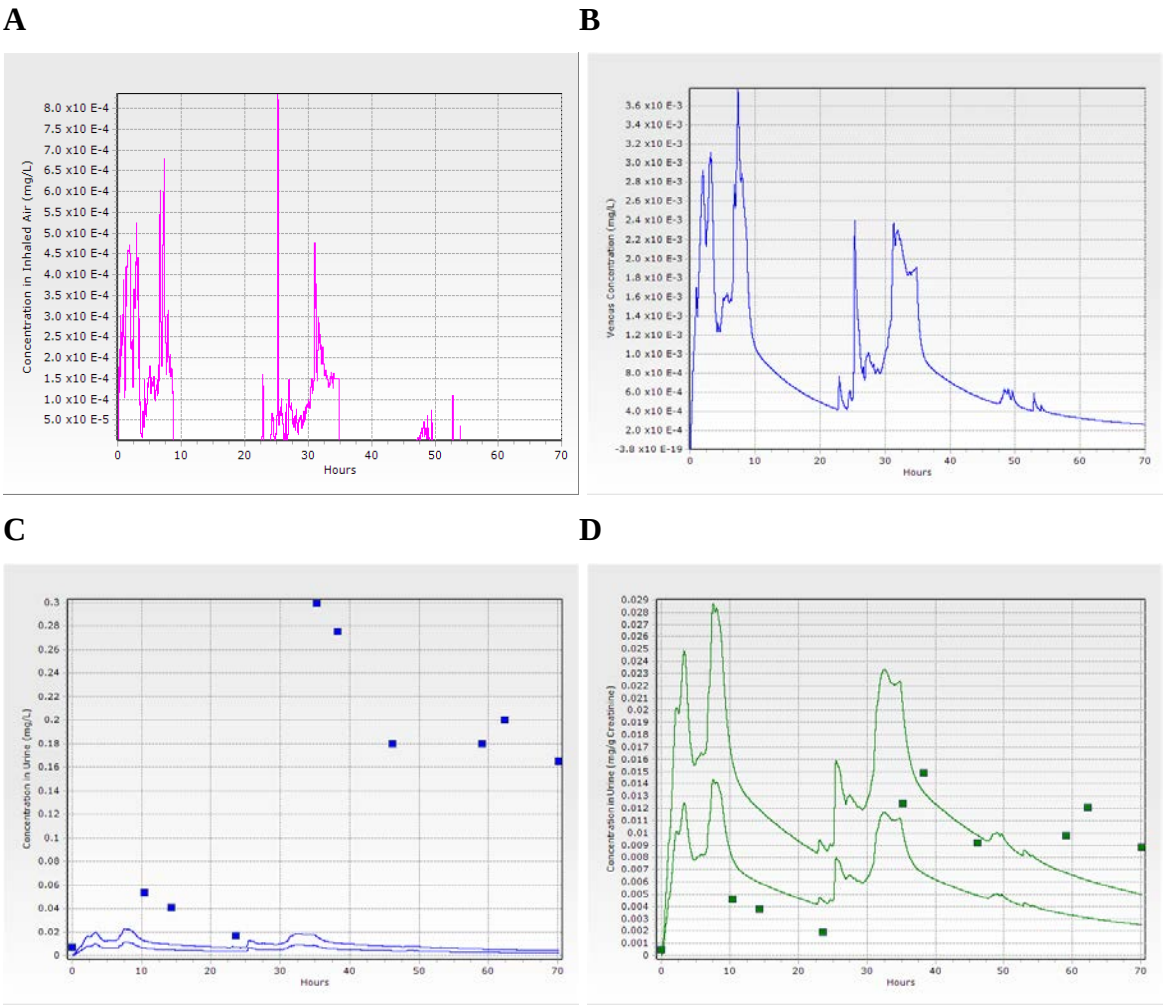

Figure 11. Predictions for Subject 04

Individual model predictions (lines) compared to observed data (squares) for: (A) Naphthalene exposure concentrations in inhaled air (mg/L), (B) Venous naphthalene blood concentration time course (mg/L); (C) A range of combined naphthols concentrations over time in the urine (mg/L) using predicted urine production (Hays et al., 2015); and (D) A range of combined naphthols concentrations over time corrected to predicted creatinine production (mg/g creatinine), based on the work of Forni Ogna et al. (2015).

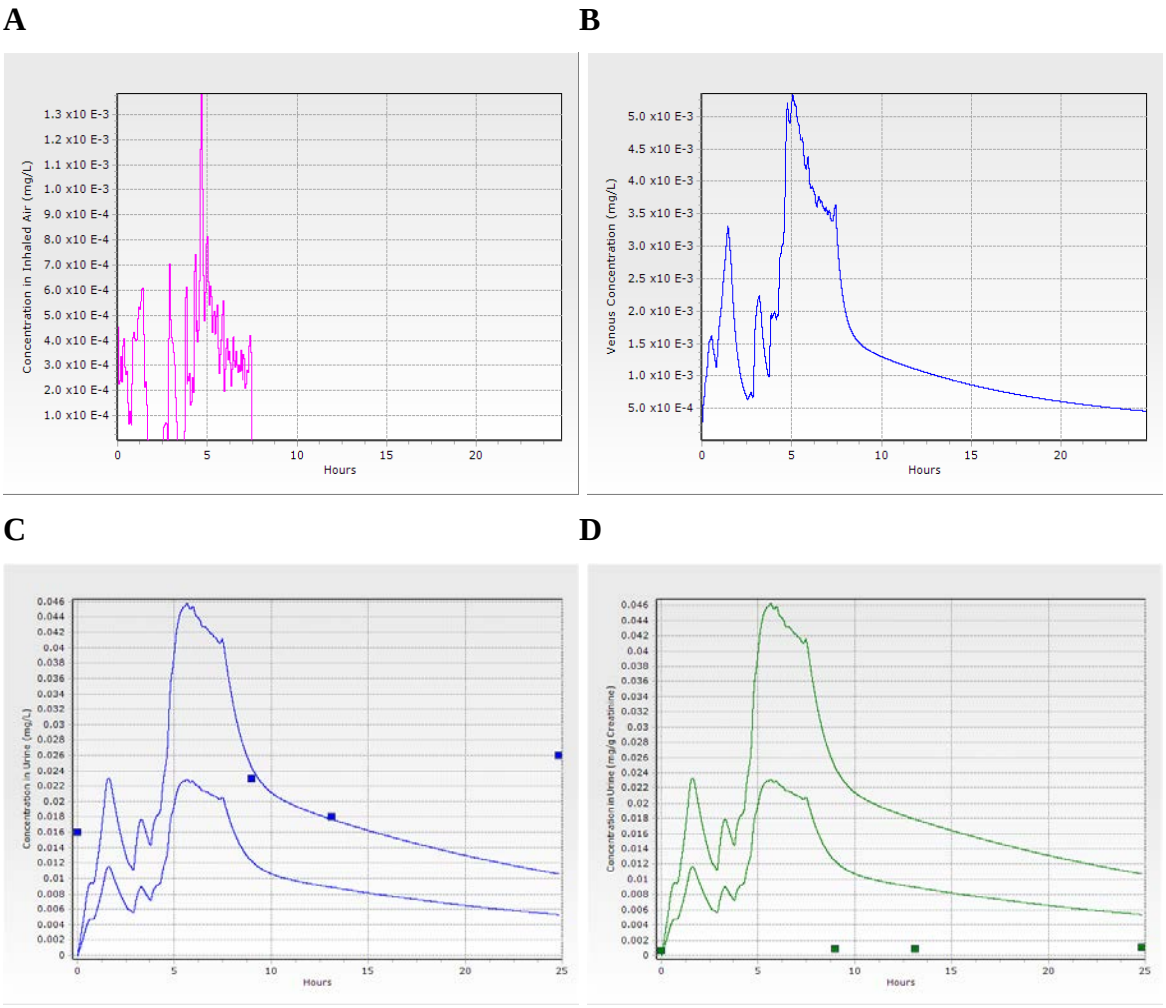

Figure 12. Predictions for Subject 05

Individual model predictions (lines) compared to observed data (squares) for: (A) Naphthalene exposure concentrations in inhaled air (mg/L), (B) Venous naphthalene blood concentration time course (mg/L); (C) A range of combined naphthols concentrations over time in the urine (mg/L) using predicted urine production (Hays et al., 2015); and (D) A range of combined naphthols concentrations over time corrected to predicted creatinine production (mg/g creatinine), based on the work of Forni Ogna et al. (2015).

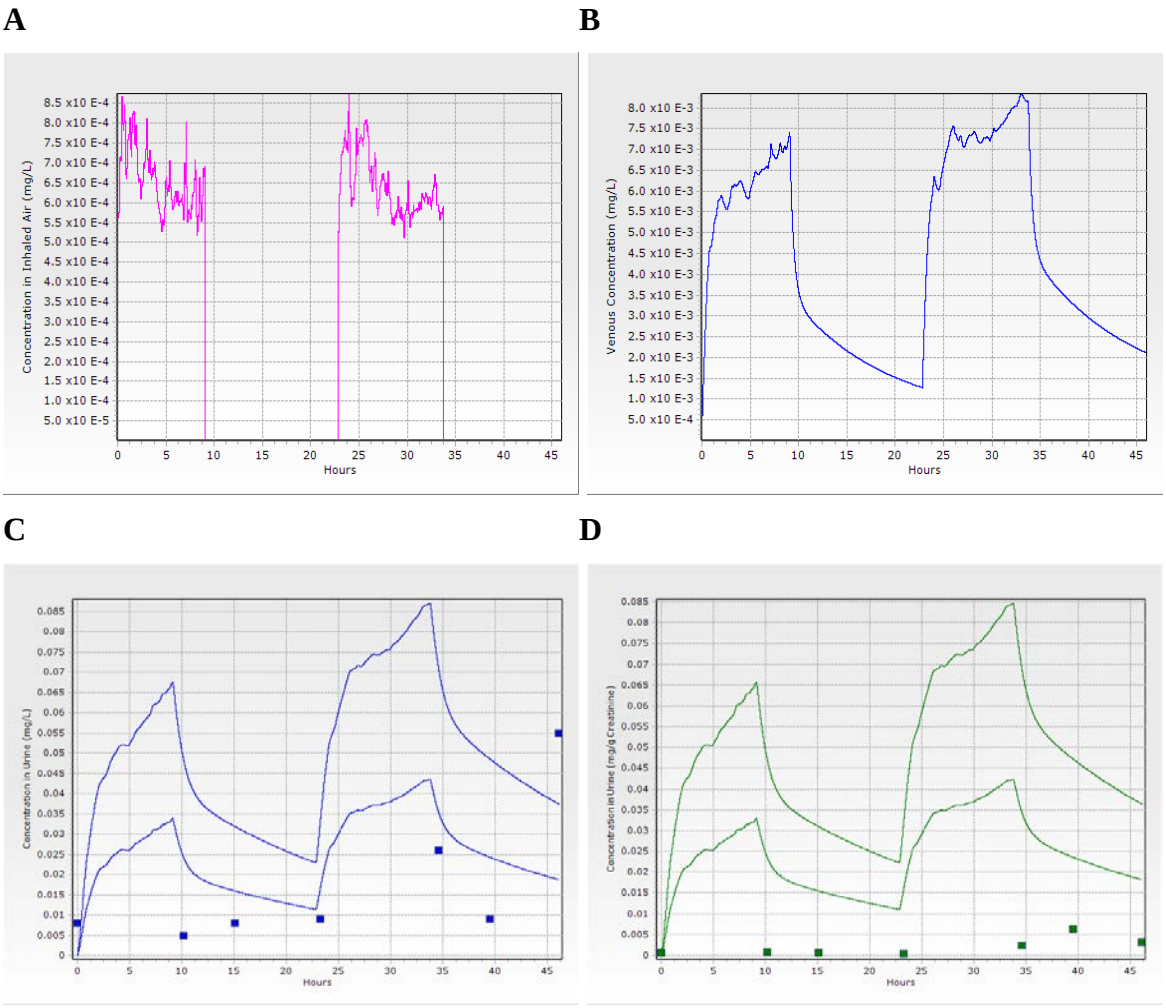

Figure 13. Predictions for Subject 06

Individual model predictions (lines) compared to observed data (squares) for: (A) Naphthalene exposure concentrations in inhaled air (mg/L), (B) Venous naphthalene blood concentration time course (mg/L); (C) A range of combined naphthols concentrations over time in the urine (mg/L) using predicted urine production (Hays et al., 2015); and (D) A range of combined naphthols concentrations over time corrected to predicted creatinine production (mg/g creatinine), based on the work of Forni Ogna et al. (2015).

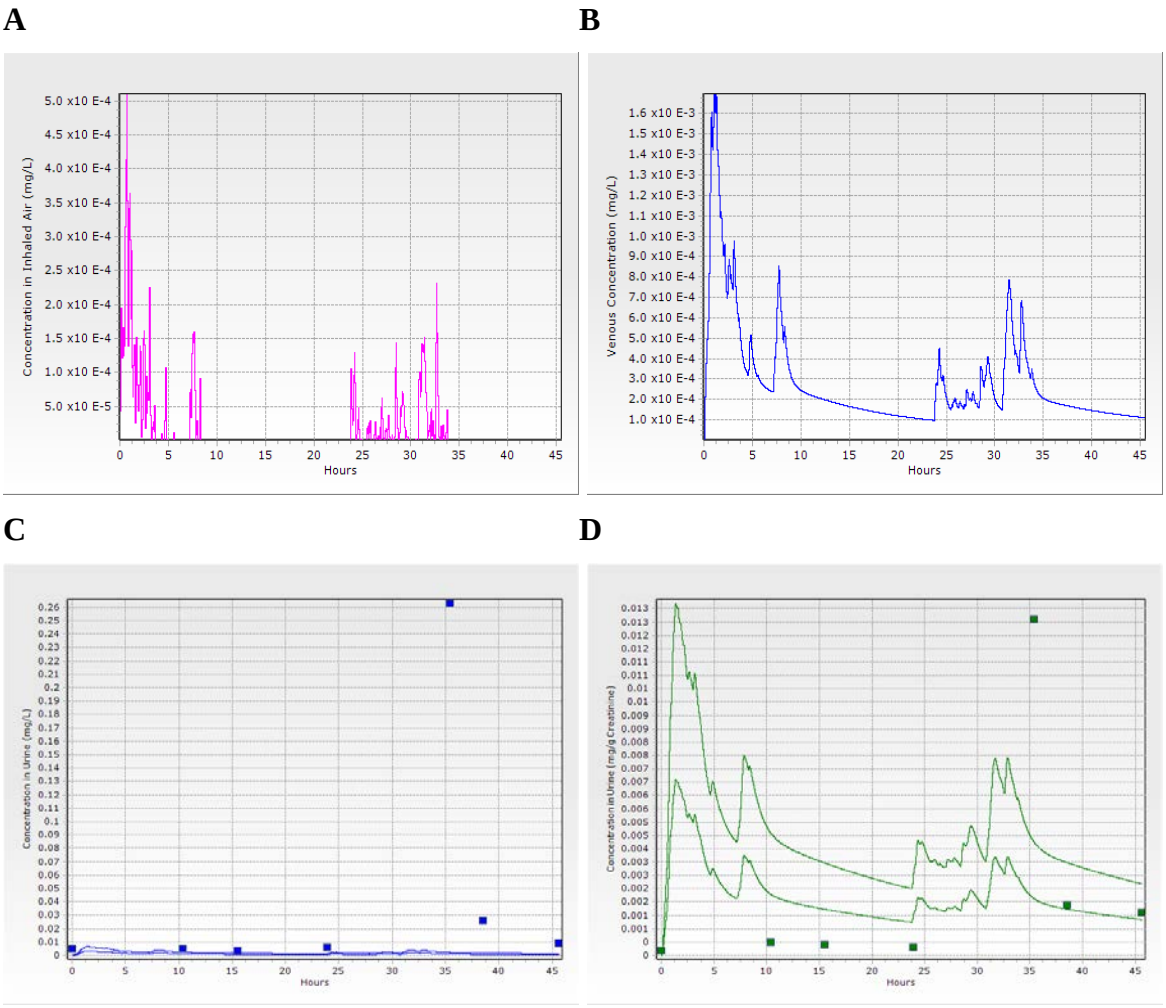

Figure 14. Predictions for Subject 08

Individual model predictions (lines) compared to observed data (squares) for: (A) Naphthalene exposure concentrations in inhaled air (mg/L), (B) Venous naphthalene blood concentration time course (mg/L); (C) A range of combined naphthols concentrations over time in the urine (mg/L) using predicted urine production (Hays et al., 2015); and (D) A range of combined naphthols concentrations over time corrected to predicted creatinine production (mg/g creatinine), based on the work of Forni Ogna et al. (2015).

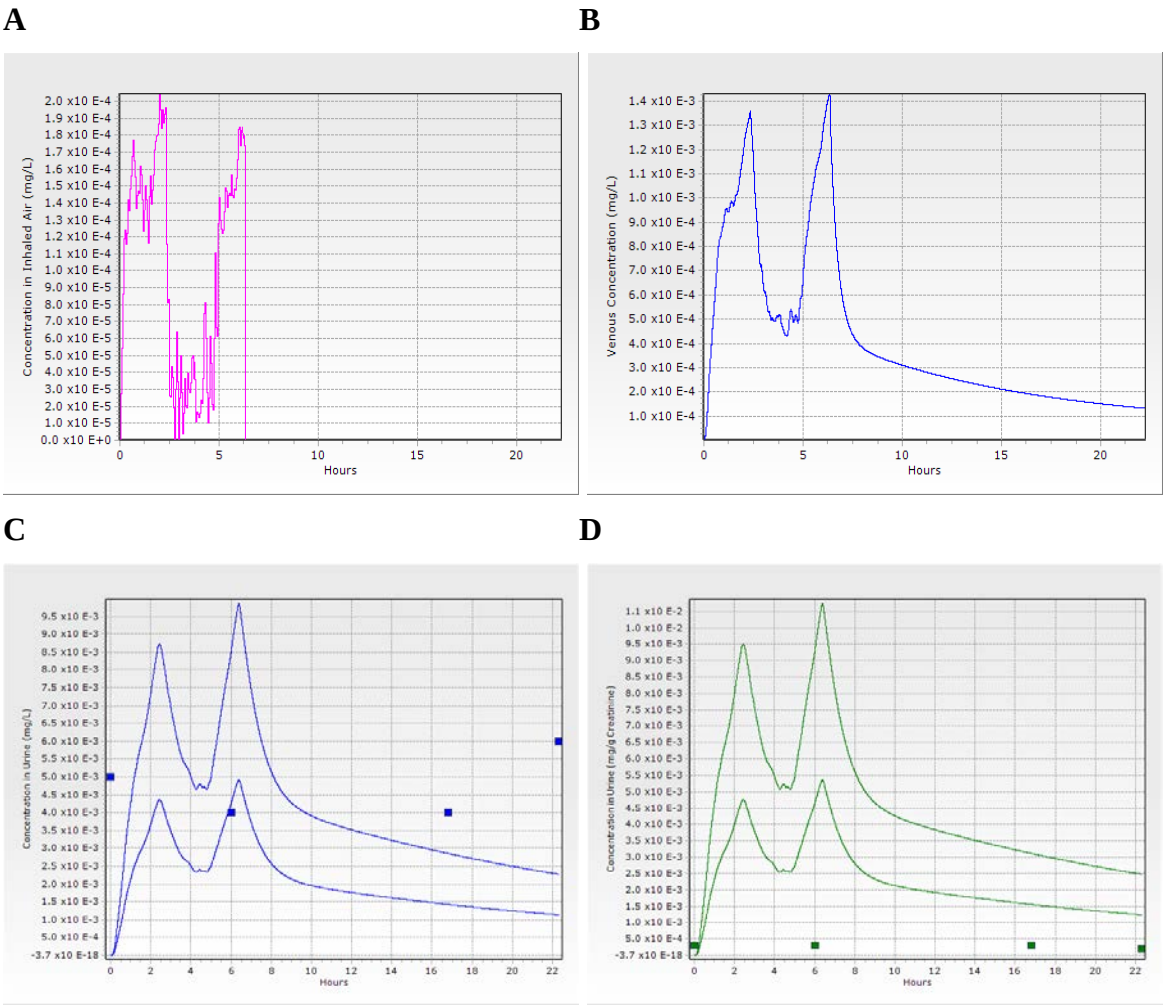

Figure 15. Predictions for Subject 10

Individual model predictions (lines) compared to observed data (squares) for: (A) Naphthalene exposure concentrations in inhaled air (mg/L), (B) Venous naphthalene blood concentration time course (mg/L); (C) A range of combined naphthols concentrations over time in the urine (mg/L) using predicted urine production (Hays et al., 2015); and (D) A range of combined naphthols concentrations over time corrected to predicted creatinine production (mg/g creatinine), based on the work of Forni Ogna et al. (2015).

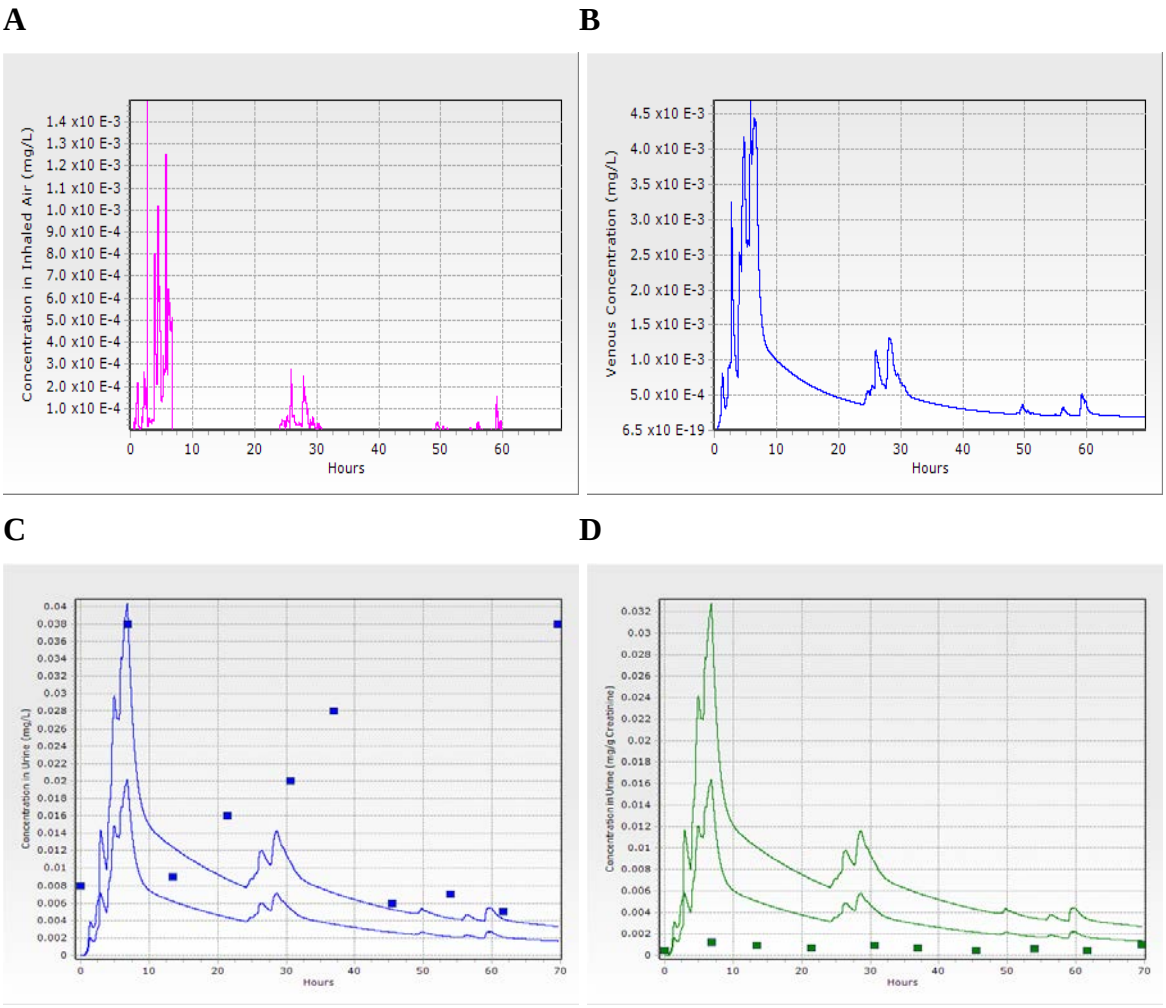

Figure 16. Predictions for Subject 11

Individual model predictions (lines) compared to observed data (squares) for: (A) Naphthalene exposure concentrations in inhaled air (mg/L), (B) Venous naphthalene blood concentration time course (mg/L); (C) A range of combined naphthols concentrations over time in the urine (mg/L) using predicted urine production (Hays et al., 2015); and (D) A range of combined naphthols concentrations over time corrected to predicted creatinine production (mg/g creatinine), based on the work of Forni Ogna et al. (2015).

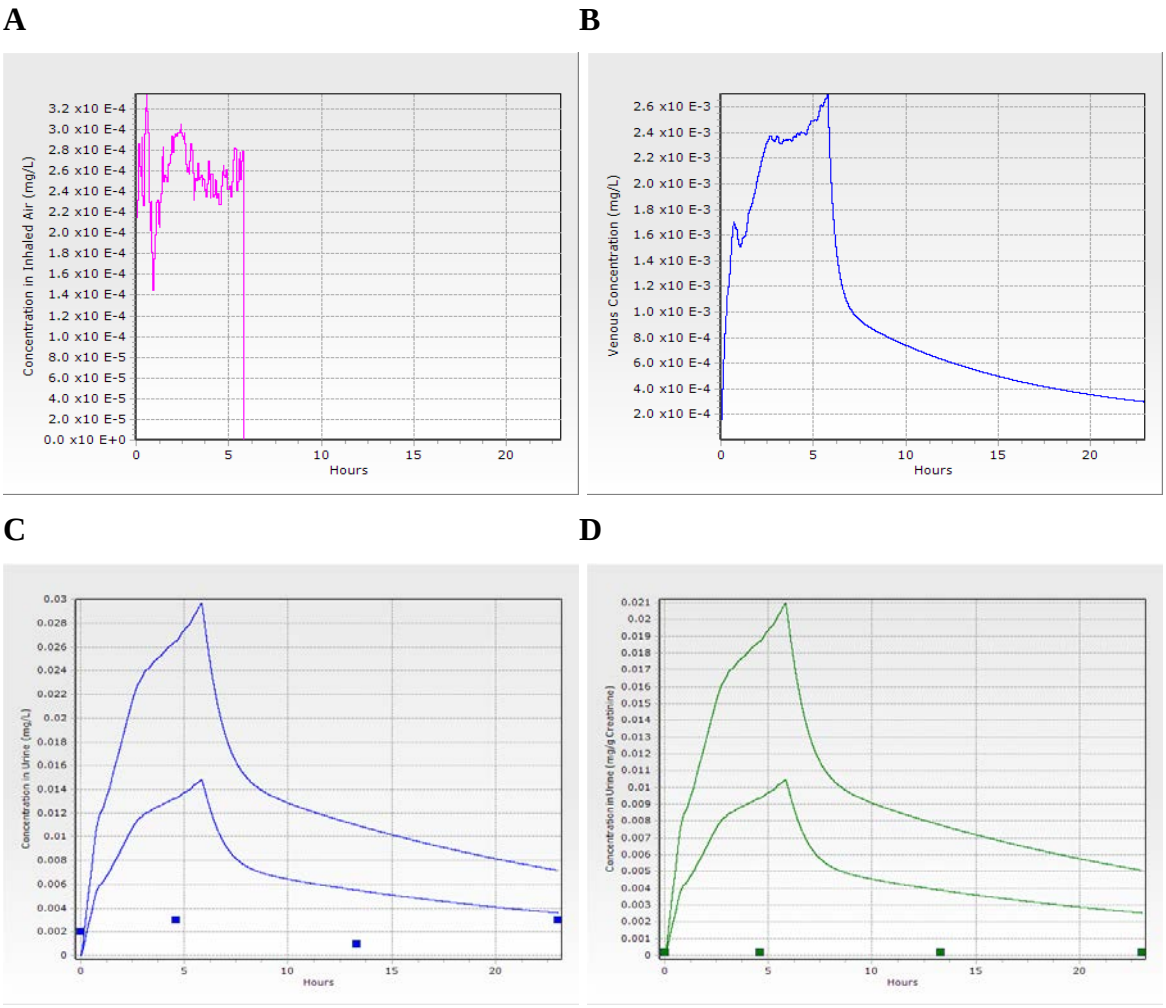

Figure 17. Predictions for Subject 13

Individual model predictions (lines) compared to observed data (squares) for: (A) Naphthalene exposure concentrations in inhaled air (mg/L), (B) Venous naphthalene blood concentration time course (mg/L); (C) A range of combined naphthols concentrations over time in the urine (mg/L) using predicted urine production (Hays et al., 2015); and (D) A range of combined naphthols concentrations over time corrected to predicted creatinine production (mg/g creatinine), based on the work of Forni Ogna et al. (2015).

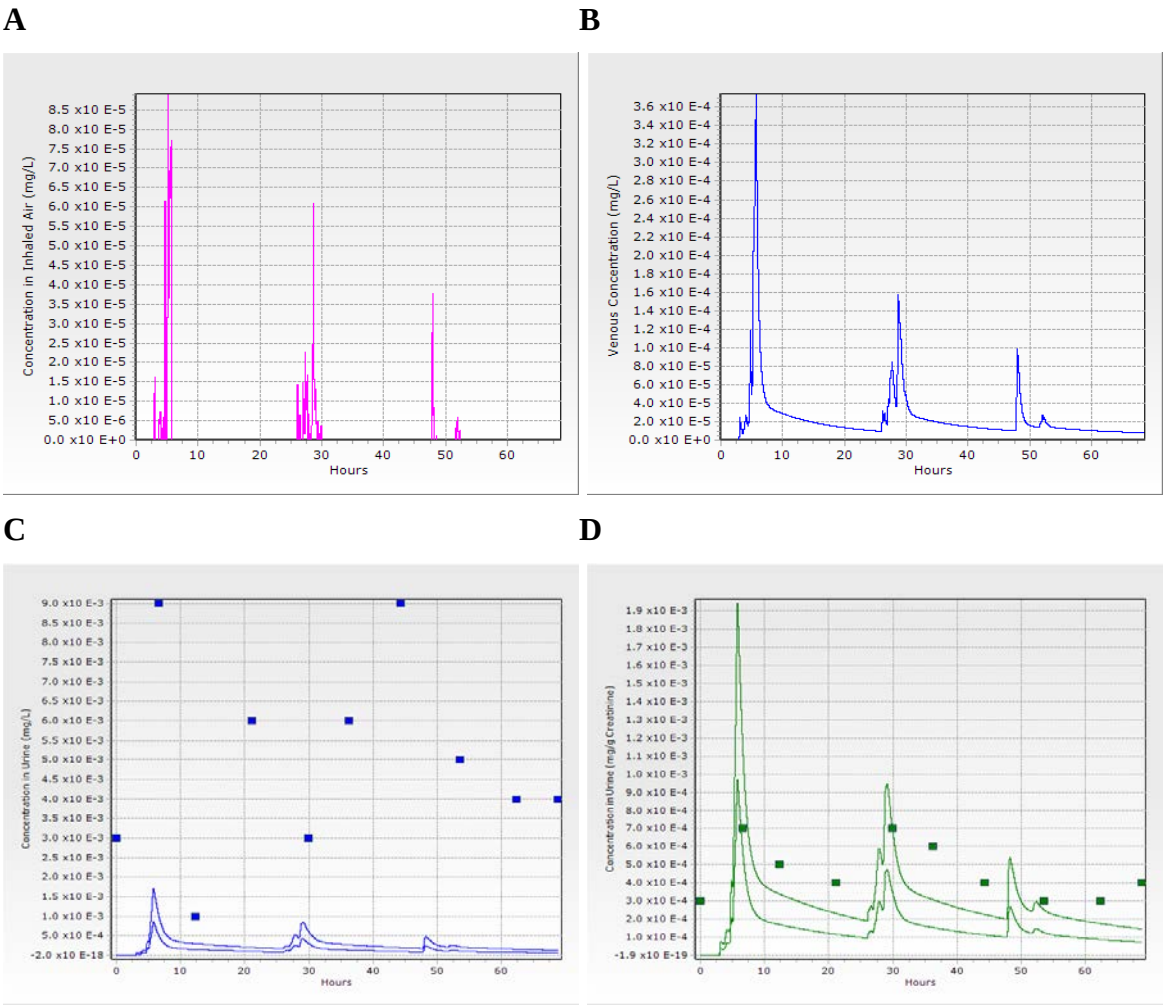

Figure 18. Predictions for Subject 14

Individual model predictions (lines) compared to observed data (squares) for: (A) Naphthalene exposure concentrations in inhaled air (mg/L), (B) Venous naphthalene blood concentration time course (mg/L); (C) A range of combined naphthols concentrations over time in the urine (mg/L) using predicted urine production (Hays et al., 2015); and (D) A range of combined naphthols concentrations over time corrected to predicted creatinine production (mg/g creatinine), based on the work of Forni Ogna et al. (2015).

While conventional sorbent tube samples were taken for all subjects, continuous sampling times that matched real-time sampling durations only occurred for 4 subjects. For these subjects, the predicted area under the curve (AUC) values in venous blood for a steady exposure at the measured TWA and for the predicted AUC using the real-time data were noted on the individual graphs in Figure 19.

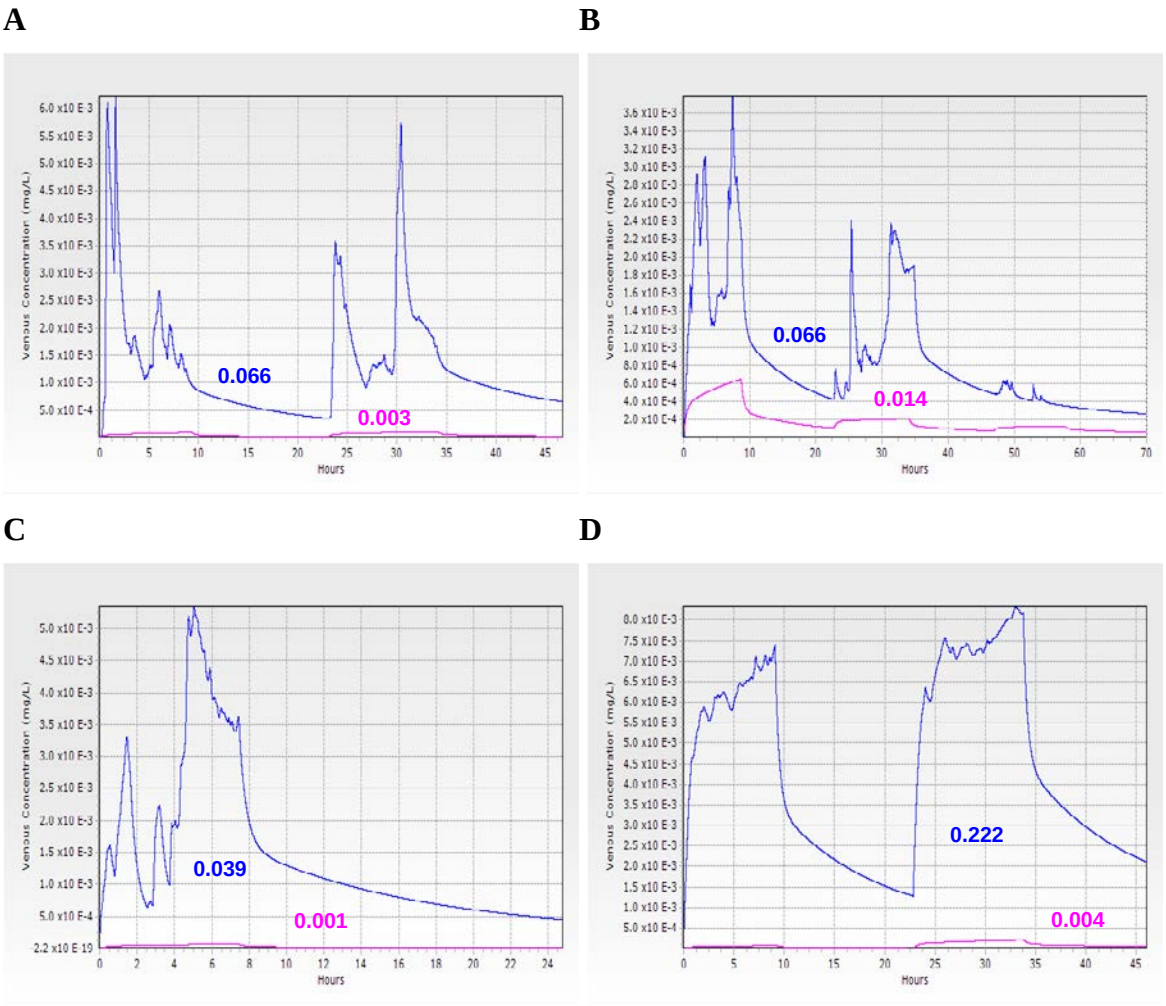

Figure 19. Real-time versus Time Weighted Average Naphthalene Venous Blood Predictions

*RT predictions are shown as a blue line. TWA predictions are shown as a magenta line. Calculated venous blood AUC values for the RT predictions are in blue text. TWA venous AUC values are in magenta text. AUC units are (mg/L)*hours. Individual predictions are included for: (A) Subject 01, (B) Subject 04, (C) Subject 05, and (D) Subject 06.*

5.0 DISCUSSION

5.1 Naphthalene PBPK Model

The nasal passages of rodents are very complex, likely related to the importance of superior olfaction for survival. Additionally, rodents are obligatory nose breathers and susceptible to injury from many xenobiotics (Harkema *et al.*, 2006). Campbell *et al.* (2014) developed a computational fluid dynamic model of naphthalene within the upper respiratory tract, which was validated in the rat. While the Campbell model represents the most comprehensive model in terms of risk-relevant dosimetry to the rat respiratory tract, the upper respiratory tract was not included in the current PBPK model. The nasal passages of humans are less complex and differ considerably in susceptibility to toxicants that are highly damaging to rodents (Harkema *et al.*, 2006). In the case of naphthalene, there are no case reports of human nasal tumors associated with occupational exposures to naphthalene (Lewis, 2012). Instead, inclusion of the lung was determined to be more relevant as a susceptible tissue in humans, as well as a site of metabolism (Figure 1). The liver was also included as it is the main site of naphthalene metabolism across species.

The model code includes 3 routes of exposure. Intravenous was preserved from the original model structure (Clewell *et al.*, 2001) to accommodate the RTI (1996) data and is typically felt to translate well to other routes of extrapolation (Kuepfer *et al.*, 2016). Inhalation exposure was crucial as a main source of exposure for the subjects herein, as well as having rat (NTP, 2000) and human literature studies (Bieniek, 1994; Egeghy *et al.*, 2003) to allow for model fitting and parameter checking. Dermal dosing was included in the model code, provided in Appendix B, due to the original model structure (Clewell *et al.*, 2001). Although the dermal route is considered a major source of exposure to jet fuels (Chao *et al.*, 2005), the participants in this study wore personal protective clothing such as gloves and coveralls, limiting the dermal exposure; the majority of the hand wash wipes analyses were below the detection limit. Had significant dermal exposure occurred, naphthalene time-course data from rat (Turkall *et al.*, 1994) and human dermal exposures (Kim *et al.*, 2007) would have been utilized to parameterize the dermal exposure route.

Pharmacokinetic/pharmacodynamic models provide understanding of mechanisms through which an organism responds to a chemical. Model descriptions of absorption, distribution, metabolism/biotransformation and elimination form a basis for extrapolating effects or biomarkers. Utility and confidence of a model will depend on completeness of calibration data sets. Herein the data available for calibrating the model was extremely limited. Two resources were found for the routes of exposure most pertinent to this work, the RTI (1996) IV study and the NTP (2000) inhalation studies. An intraperitoneal (IP) study (O'Brien *et al.*, 1985) was also identified but not pursued as modeling an IP study requires multiple assumptions that don't translate well for route-to-route extrapolation (Steuperaert *et al.*, 2017). Published tissue:blood PCs measured in mouse tissues were used in the model; these were previously utilized in the Campbell *et al.* (2014) rat model as well.

Surprisingly, given the number of naphthalene PBPK models, metabolic K_m values were not available from rat *in vitro* studies. Each PBPK model published has taken a different route to filling this gap. Typically K_m values from *in vitro* sources work well in PBPK models as they are independent of enzyme concentration (Bale *et al.*, 2014). Herein, the lung K_m (Buckpitt *et al.*,

2013) worked well enough for the rat liver, as the K_m influences the venous concentration curve shape (Figure 2). The human liver K_m (Cho *et al.*, 2006) was also tried, but the lung K_m simply worked better. $V_{max}C$ values were a different matter. Unaltered *in vitro*-derived $V_{max}C$ values caused far too much metabolism to fit the NTP (2000) data. Successive scaling of the maximal velocities resulted in good peak data heights with 1/100 $V_{max}C$ values (Figure 2).

There were no tissue kinetic data available to determine if the model parameters and structure described the tissue concentrations well. Only venous concentrations were found with which to determine the involvement of distribution limitation in more fatty tissues (fat and slowly perfused tissue compartments). Given measured PCs and without diffusion limitation, the model could not achieve the width of the data peak (Figure 2). Incorporation of fitted *PA* values for these the fatty tissues resulted in the simulations showing suitable breadth of peak. The reasonable agreement between simulations of blood concentrations and measured experimental data provides confidence in the use of the model for dosimetry of naphthalene and its contribution to 1- and 2-naphthol in urine.

Willems *et al.* (2001) found that parameters used to fit the NTP (2000) data in their published model could not fit the RTI (1996) data. As inhalation as a route is much more important to occupational exposure than intravenous and as the inhalation data had smaller (tighter) standard deviations, the RTI (1996) data were utilized merely to determine if the naphthalene model parameters were "on track". While good fit was not achieved by the prediction in Figure 3, this graph does show appropriate metabolic removal of naphthalene, particularly in the lowest dose (1 mg/kg), a concentration more similar to occupational levels than the others in the study.

To simulate repeated naphthalene exposures (Figure 4), up-regulation of metabolism was required. To determine the potential magnitude of up-regulation and the capacity for up-regulation in liver and lung, a separate literature analysis of naphthalene metabolism following a single and multiple doses was located. Elovaara *et al.* (2007) measured induction of UDP-glucuronosyltransferase 1A in rats exposed to naphthalene and other polycyclic aromatic hydrocarbons (PAHs) over 3 days. 1-Naphthol is a substrate sensitive for the detection of this up-regulation. Maximal metabolic increases were measured at 6.4 fold in the rat liver and 1.9 fold in the rat lung. As this magnitude of induction was not observed in the repeated exposure rats (NTP, 2000), the ratio of liver:lung up-regulation (3.4:1) was held constant and applied during successive fitting of the $V_{Max}C$ in this PBPK model. Induction following two weeks of exposure in the rat was found to be on the order of 1.40 times the single exposure $V_{Max}C$ in the liver and 1.12 times in the lung (Figure 5).

Essentially no naphthalene kinetic data were located for humans. Therefore the human model was parameterized with human physiological values, rat model PCs and human *in vitro* study derived metabolic constants. Up-regulation was not assumed for the human subjects in this study. It is unknown if their repeated exposures are sufficient to result in metabolic up-regulation, as was seen in the NTP (2000) rat study with much higher exposure levels in a different species.

A few human data points were located in a study by Egeghy *et al.* (2003). Median and quartile expired (end-exhaled breath) data were documented resulting from 4-hour JP-8 jet fuel exposures (naphthalene exposure = 485 μg/m^3). The model predicted end-exhaled air shown in Figure 8 indicate good parameterization of the blood:air PC (571; Campbell *et al.*, 2014; NTP, 2000), a predominant factor in this prediction.

5.2 Naphthols PBPK Model

As with the parent compound, there were no data available on blood or tissue concentrations of different naphthalene metabolites in animals or humans, thereby making it impossible to check the model parameters involved in describing the distribution of 1- and 2- naphthol. Without measured PCs, a QSAR approach was used to estimate distribution of the naphthols into tissues (Ruark *et al.*, 2014). Available naphthol data for parameterizing urinary clearance was limited to two data sets published by Bieniek (1994). The first data set (Figure 6) featured data from naphthalene oil plant workers. This exposure is 73.6 percent naphthalene, but also includes 1-naphthol and probably other hydrocarbon carriers, in order to achieve a liquid from a compound that sublimes. The second data set (Figure 7) was urinary 1-naphthol from coke plant workers. The naphthalene exposures were much lower in the coke plant and workers were not exposed to 1-naphthol. However, many other hydrocarbons and PAHs would be represented in this mixture. A single urinary clearance value ($Cl_{Ur}C$ = 0.4 L/(hour*kg$^{0.75}$)) was fit that adequately but not ideally described the concentration of 1-naphthol in the urine for both data sets. As the data were only for 1-naphthol, the percentage of total metabolites in the urine was set to 5.5 for the lung and 10 for the liver (see Section 3.5 above). Bieniek noted in this publication that estimated urinary half-lives for the two groups were very different (4 and 14 hours). The author attributed this to the 1-naphthol contributing to a shorter half-live in the naphthalene oil workers. PAH metabolic competition among the coke plant workers, conversely, has the potential to slow metabolism. Given the complex nature of each Bieniek exposure, and the complex exposure to JP-8 among fuel cell maintenance military members, it is not possible to say which exposure is more representative than the other. Therefore, a single urinary clearance value was settled upon that was adequate for both data sets.

5.3 NaDos Real-time Data

In preparation for modeling, the NaDos data from the human field study were examined and criteria established for its use in the modeling effort. The process, described in the Methods section, included steps to select only subjects with appropriate real-time, conventional and urinary data. Three subjects (Appendix A) were excluded solely on the proportion of exempt real-time data. A large proportion of data points for the Navy participants studied aboard the aircraft carrier were listed as exempt, owing to temperature and/or humidity exceeding the NaDos internal lookup table constraints. This issue indicates more development should be considered in order for the dosimeter to be used successfully to monitor occupational exposures under the wide range of environmental conditions in which military members work.

The urine data highlighted several issues inherent with excretion data. First, all subjects entered the study with measureable combined naphthols concentrations; the modeling "Time 0" average concentration was 0.0146 ± 0.0230 mg naphthols/L urine, equivalent to 0.00130 ± 0.00195 mg naphthols/g creatinine (mean ± SD). The urine collection began on a Tuesday of a standard work week for the AF personnel; Navy participants had been on the carrier with daily duties prior to the study initiation, which would have included naphthalene (fuels) exposures. Additionally, naphthalene exposures occur in many common settings (Jia and Batterman, 2010). The Centers for Disease Control (CDC, 2019) reports a geometric mean and 95 percent confidence interval of 0.00574 (0.00532 – 0.00618) mg combined naphthols/L for the general

U.S. population during the years 2013 and 2014, which correspond to the first two sampling events in this study. The statistics for creatinine corrected concentration for this population were 0.00666 (0.00628 – 0.00706) mg naphthols/g creatinine. Figure 20 shows these background levels and the study mean at Time 0 for modeling superimposed on an example (Subject 01) simulation of two days of occupational exposure. In terms of urinary naphthols concentration (Figure 20A), the study mean is higher than the population mean. In terms of urinary concentration corrected to creatinine (Figure 20B), the study mean falls considerably below the population mean.

A **B**

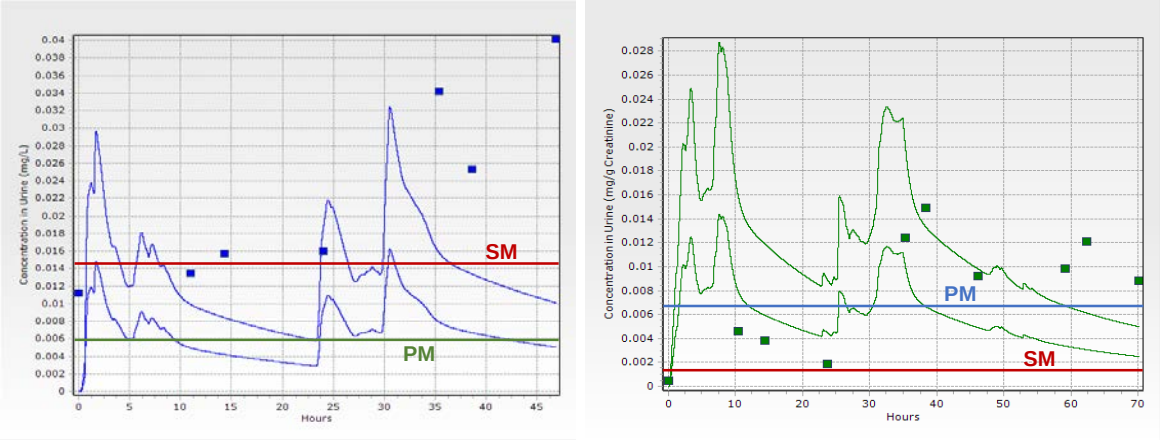

Figure 20. Predictions for Subject 01 Overlaid with Initial Subject and Population Background Concentrations of Naphthols in the Urine

(A) Measured urine concentrations of total naphthols (squares) and predicted time course (curve) of naphthols concentration in the urine (mg/L) using predicted urine production (Hays et al., 2015). (B) Measured concentrations of naphthols corrected to creatinine excretion (squares) and predicted time course of naphthols concentration corrected to predicted creatinine production (mg/g creatinine) based on the work of Forni Ogna et al. (2015). SM denotes the study mean concentration at Time 0 for the modeling effort. PM denotes the general population mean of combined naphthols as published by CDC (2019).

Second, creatinine excretion was found to vary widely among intra- and extra-individual samples. This is a known deficit of creatinine normalization; however, given that individuals vary, it is a useful normalization factor in medicine (Miller *et al.*, 2004). Forni Ogna and others (2015) developed an algorithm to predict daily creatinine production reference values based on empirical data. The training set for this work was 1137 Swiss people of European descent, aged 18 to more than 60 years old; the participants exceeded an estimated glomerular filtration rate of 60 mL per minute per 1.73 m^2. Figure 9 indicates that predicted daily creatinine production generated using this algorithm does not correlate with the average creatinine excretion measured for each individual in this study. Additional factors besides age, sex and body composition (BMI) which may affect creatinine excretion include race, physical health, kidney health, diet, supplement use (creatine protein supplements) and level of hydration (Mage *et al.*, 2008; Williamson and New, 2014). Individuals in this study were, on average, 25 years old (range: 20

to 39 years) and in good physical health; 4 of the 18 subjects listed a racial or ethnic heritage inconsistent with the Forni Ogna training set. Study subjects may have produced more creatinine that the training set population, which in turn decreased the relative urinary naphthols concentration following normalization (Figure 20B).

Third, the ratios of urinary 1- to 2-naphthol were not consistent across subjects. An *in vitro* metabolic study with human liver cells (Cho *et al.*, 2006) indicated a 10 to 1 ratio of 1-naphthol being produced, as compared to 2-naphthol. Of 17 subjects, 11 had measured concentrations of 2-naphthol that were higher than the 1-naphthol concentration. The variation in magnitude and whether a greater proportion of 2-naphthol is produced likely reflects inter-individual differences in metabolism. Sams (2017) measured 1- and 2-naphthols in the urine of occupationally exposed carbamate and naphthalene workers in the United Kingdom; he observed an average 1- to 2-naphthol ratio of 1.4 among 233 study participants, with a minimum ratio of 0.07 and maximum of 33.6. Dermal exposures to naphthalene have been known to result in increased 2-naphthol production (Chao *et al.*, 2006). Additionally, individuals may also be exposed to other naphthol forming compounds, such as the ubiquitous carbamate pesticides (Sams, 2017; Meeker *et al.*, 2007). By study design, efforts were made to screen participants for non-occupational exposures.

The solution to this third issue was to predict a range of naphthol production. The lower bound was set for the model from work by Cho *et al.* (2006) who found that 1- and 2-naphthol combined were produced at about 10 percent of liver metabolites with *in vitro* human liver cell microsomes. The lung lower bound was set at 5.5 percent of lung metabolites based on 1-naphthol in NHP lung cell microsomes (Buckpitt *et al.*, 2013). The liver value is similar to the product of mouse liver microsomal incubations (approximately 11 percent 1-naphthol, Buckpitt and Bahnson, 1986). These authors consider 1-naphthol to be the spontaneous rearrangement product of the naphthalene epoxide intermediate, which may be why there's some consistency across species under common *in vitro* microsomal preparation conditions.

The upper bound of the range was set at 20 percent of liver metabolites and 9.5 percent of lung metabolites for modeling. Observations made on the urinary data from the military subjects herein indicate that the majority of the workers excrete more 2-naphthol than 1-naphthol. Certainly, genetics and metabolic variation can affect the predominance of one metabolite over another (Sams, 2017). It could also be speculated that low level dermal absorption, not consistently quantifiable in the hand wipes, may be playing a role in the formation of higher 2-naphthol levels, given the work of Chao *et al.* (2006). The upper bounds for liver and lung production of naphthols was arbitrarily set as twice the respective lower bounds, to accommodate the production of 2-naphthol, which is so rarely measured in these studies.

5.4 NaDos Simulations and Urinary Naphthols Predictions

One of the most unique features of the model is the exposure dosing code. PBPK models utilizing complex real-time data were not found in the literature. Model inhalation exposures tend to represent a single concentration over a specific period. Use of arrays to assign a different concentration to a specific duration is a unique approach that was able to simulate the temporal fluctuations in exposure recorded by the RT NaDos monitor (Figures 10 through 18, part A).

Overall, either the urine concentration or the creatinine normalized concentration adequately predicted the urinary data in most subjects (6 out of 9). Given that these concentrations were developed using grab samples, predicted average urinary volume (Hays *et al.*, 2015), and predicted creatinine production (Forni Ogna *et al.*, 2015), the model is considered a success. Given the limitations of creatinine normalization, cumulative urine samples or even complete catches with urine volume and time since the last void likely would have improved the predictions.

Finally, the model was used to compare the predicted AUCs for venous blood, a common measure of internal dose in PBPK models (Travis, 2011), for the real-time data versus the TWA collected using conventional sorbent tubes. These simulations of blood concentrations capture temporal changes including spikes and lows in exposures and often result in blood AUCs that are much higher than those which could be simulated from a traditional constant TWA for the same period. In this comparison, the NaDos AUC was 4.7 to 56 times higher than the TWA AUC. It appears that a real-time monitor would be more protective of worker health, both in the speed at which results are generated and in the capture of brief fluctuations in naphthalene levels. Given that the model was able to predict urine concentrations in 7 of 9 subjects using a single set of parameters (except for individual physiological description, like height and weight), indicates that the human body absorbs and reacts to the fluctuations of naphthalene in this occupational exposure.

5.5 Recommendations

Individuals metabolize naphthalene differently. Reasons for these differences may be attributed to genetic factors, age or even normal variations in physiology across the general population. Because metabolism is the primary elimination route for naphthalene, the metabolic constants used are sensitive parameters. A formal sensitivity analysis would identify this and other parameters that most greatly influence urinary metabolite predictions. Based upon *a priori* information regarding the sensitive parameters, those with the most inherent uncertainty can be identified for probability analysis. Probability distributions are a much more realistic way of describing uncertainty in those parameters.

The individual variability of the subject data in this study would be better described through Monte Carlo (MC) analysis of sensitive parameters, now that the basic model is complete. MC analysis would enhance the model's performance with individual data by predicting a range of reasonable physiological concentrations that reflects the population diversity in metabolism, clearance, and other identified sensitive parameters.

The subjects in this study were performing normal duties as fuel cell workers. By default, PBPK models use resting physiological parameters. Additional information about subject workload would provide improvements to the individual predictions given by the model. Without subject-specific information, exercise sensitive parameters could be varied during MC analysis, based on known physiological changes during exercise. Any future studies on the kinetics, metabolism and elimination of naphthalene in human subjects would benefit from a full 24-hour urine collection, especially if blood draws are not possible.

6.0 CONCLUSIONS

The fit-for-purpose RT PBPK model developed for this project successfully simulates the limited available rat and human data, demonstrating interspecies extrapolation capability. The majority of parameters utilized within the model are based on literature studies with minimal fitted values. The ability of the model to extrapolate across species and routes (intravenous and inhalation) with so few fit parameters, gives confidence in the model predictions. The model is able to predict individual metabolite urinary concentrations in 7 of 9 subjects. Individual variability inherent in real-time occupational monitoring data preclude a better performance without additional work to incorporate MC analysis.

One objective of this modeling exercise was to determine if RT data could be used to predict urinary naphthol concentrations in occupationally exposed personnel. Analysis of the RT data in conjunction with the spot urine samples indicate the possibility of additional occupational or non-occupational naphthalene or naphthol-producing exposures that affect urinary output of naphthols. While the measured exposures describe urinary profiles for several individuals, utilizing urinary profiles to back-calculate occupational exposures may not be completely accurate. Therefore, urinary naphthols are a good indicator of exposure to naphthalene or other naphthol generating compounds, but care should be taken when relying on these as a biomarker exclusively of occupational naphthalene exposure.

7.0 REFERENCES

ATSDR. 2005. Toxicological Profile for Naphthalene, 1-methylnaphthalene and 2-methylnaphthalene. Atlanta GA: U.S. Department of Health and Human Services, Public Health Service, Agency for Toxic Substances and Disease Registry.

Bale AS, Kenyon E, Flynn TJ, Lipscomb JC, Mendrick DL, Hartung T, Patton GW. 2014. Correlating *in vitro* data to *in vivo* findings for risk assessment. ALTEX 31: 79-90.

Bieniek G. 1994. The presence of 1-naphthol in the urine of industrial workers exposed to naphthalene. Occup Environ Med. 51:357-359.

Brown RP, Delp MD, Lindstedt SL, Rhomberg LR, Beliles RP. 1997. Physiological parameter values for physiologically based pharmacokinetic models. Toxicol Ind Health. 13:407-484.

Buckpitt A, Boland B, Isbell M, Morin D, Shultz M, Baldwin R. Chan K, Karlsson A, Lin C, Taff A, West J, Fanucchi M, van Winkle L, Plopper C. 2002. Naphthalene-induced respiratory tract toxicity: metabolic mechanisms of toxicity. Drug Metab Rev. 34:791-820.

Buckpitt A, Morin D, Murphy S, Edwards P, Van Winkle L. 2013. Kinetics of naphthalene metabolism in target and non-target tissues of rodents and in nasal and airway microsomes from the Rhesus monkey. Toxicol Appl Pharmacol. 270:97-105.

Buckpitt AR and Bahnson LS. 1986. Naphthalene metabolism by human lung microsomal enzymes. Toxicology. 41:333-341.

Buckpitt AR and Franklin RB. 1989. Relationship of naphthalene and 2-methylnaphthalene metabolism to pulmonary bronchiolar epithelial cell necrosis. Pharmac Ther. 41:393-410.

Buckpitt AR, Castagnoli N, Nelson SD, Jones AD, Bahnson LS. 1987. Stereoselectivity of naphthalene epoxidation by mouse, rat, and hamster pulmonary, hepatic, and renal microsomal enzymes. Drug Metab Disposit. 15:491-498

Campbell JL, Andersen ME, Clewell HJ. 2014. A hybrid CFD-PBPK model for naphthalene in rat and human with IVIVE for nasal tissue metabolism and cross-species dosimetry. Inhal Toxicol. 333-344.

CDC. 2019. Fourth National Report on Human Exposure to Environmental Chemicals. Updated Tables, January 2019, Volume One. Atlanta GA: U.S. Department of Health and Human Services, Centers for Disease Control and Prevention. <https://www.cdc.gov/exposurereport/pdf/FourthReport_UpdatedTables_Volume1_Jan2019-508.pdf>

Chao YE, Gibson RL, Nylander-French LA. 2005. Dermal Exposure to Jet Fuel (JP-8) in US Air Force Personnel. Ann Occup Hyg. 49:639-645.

Chao YE, Kupper LL, Serdar B, Egeghy PP, Rappaport SM, Nylander-French LA. 2006. Dermal exposure to jet fuel JP-8 significantly contributes to the production of urinary naphthols in fuel-cell maintenance workers. Environ Health Perspect. 114:182-185.

Cho TM, Rose RL, Hodgson E. 2006. *In vitro* metabolism of naphthalene by human liver microsomal cytochrome P450 enzymes. Drug Metab Dispos. 34:176-183.

Clewell HJ, Gentry PR, Gearhart JM, Covington TR, Banton MI, Andersen ME. 2001. Development of a physiologically based pharmacokinetic model of isopropanol and its metabolite acetone. Toxicol Sci. 63: 160-172.

Dodd DE, Wong BA, Gross EA, Miller RA. 2012. Nasal epithelial lesions in F344 rats following a 90-day inhalation exposure to naphthalene. Inhal Toxicol. 24:70-79.

Egeghy PP, Hauf-Cabalo L, Gibson R, Rappaport SM. 2003. Benzene and naphthalene in air and breath as indicators of exposure to jet fuel. Occup Environ Med. 60:969-976.

Elovaara E, Mikkola J, Stockmann-Juvala H, Luukkanen L, Keski-Hynnila H, Kostiainen R, Pasanen M, Pelkonen O, Vainio H. 2007. Polycyclic aromatic hydrocarbon (PAH) metabolizing enzyme activities in human lung, and their inducibility by exposure to naphthalene, phenanthrene, pyrene, chrysene, and benzo(a)pyrene as shown in the rat lung and liver. Arch Toxicol. 81:169-182.

Forni Ogna V, Ogna A, Vuistiner P, Pruijm M, Ponte B, Ackermann D, Gabutti L, Vakilzadeh N, Mohaupt M, Martin PY, Guessous I, Pechere-Bertschi A, Paccaud F, Bochud M, Burnier M. 2015. New anthropometry-based age- and sex-specific reference values for urinary 24-hour creatinine excretion based on the adult Swiss population. BMC Med. 13:40.

Harkema JR, Carey S, Wagner JG. 2006. The nose revisited: a brief review of the comparative structure, function, and toxicologic pathology of the nasal epithelium. Toxicol Pathol. 34:252-269.

Hays SM, Aylward LL, Blount BC. 2015. Variation in urinary flow rates according to demographic characteristics and body mass index in NHANES: potential confounding of associations between health outcomes and urinary biomarker concentrations. Environ Health Perspect. 123(4):293-300.

Hu XS, Arredondo MM, Gomba M, Confer N, DaSilva AF, Johnson TD, Shalinsky M, Kovelman I. 2015. Comparison of motion correction techniques applied to functional near-infrared spectroscopy data from children. J Biomed Opt. 20:126003. doi: 10.1117/1.JBO.20.12.126003.

Jia C, Batterman S. 2010. A critical review of naphthalene sources and exposures relevant to indoor and outdoor air. Int J Environ Res Public Health. 7:2903-39.

Kim D, Andersen ME, Chao YC, Egeghy PP, Rappaport SM, Nylander-French LA. 2007. PBTK modeling demonstrates contribution of dermal and inhalation exposure components to end-exhaled breath concentrations of naphthalene. Environ Health Perspect. 115:894-901.

Kuepfer L, Niederalt C, Wendl T, Schlender JF, Willmann S, Lippert J, Block M, Eissing T, Teutonico D. 2016. Applied Concepts in PBPK Modeling: How to Build a PBPK/PD Model. CPT Pharmacometrics Syst Pharmacol. 5:516-531.

Lanza DL, Code e, Crespi CL, Gonzalez FJ, Yost GS. 1999. Specific dehydrogenation of 3-methylindole and epoxidation of naphthalene by recombinant human CYP2F1 expressed in lymphoblastoid cells. Drug Metab Dispos. 27:798–803.

Lee MG, Phimister A, Morin D, Buckpitt A, Plopper C. 2005. In situ naphthalene bioactivation and nasal airflow cause region-specific injury patterns in the nasal mucosa of rats exposed to naphthalene by inhalation. J Pharmacol Exp Ther 314(1):103-110.

Lewis JR. 2012. Naphthalene Animal Carcinogenicity and Human Relevancy: Overview of Industries with Naphthalene-containing Streams. Reg Toxicol Pharmacol. 62: 131-137

Li L, Wei Y, Van Winkle L, Zhang QY, Zhou X, Hu J, Xie F, Kluetzman K, Ding X. 2011. Generation and characterization of a Cyp2F2-null mouse and studies on the role of CYP2F2 in naphthalene-induced toxicity in the lung and nasal olfactory mucosa. J Pharmacol Exp Ther. 339:62-71.

Mage DT, Allen RH, Kodali A. 2008. Creatinine corrections for estimating children's and adult's pesticide intake doses in equilibrium with urinary pesticide and creatinine concentrations. J Expos Sci Environ Epidemiol. 18:360-368.

Meeker JD, Barr DB, Serdar B, Rappaport SM, Hauser R. 2007. Utility of urinary 1-naphthol and 2-naphthol levels to assess environmental carbaryl and naphthalene exposure in an epidemiology study. J Expo Sci Environ Epidemiol. 17:314-20.

Miller RC, Brindle E, Holman DJ, Shofer J, Klein NA, Soules MR, O'Connor KA. 2004. Comparison of specific gravity and creatinine for normalizing urinary reproductive hormone concentrations. Clin Chem. 50:924-32.

National Research Council (NRC). 2003. Toxicologic Assessment of Jet-Propulsion Fuel 8. Washington, D.C.: National Academies Press. 207 pp.

Negi I, Tsow F, Tanwar K, Zhang L, Iglesias RA, Chen C, Rai A, Forzani ES, Tao N. 2011. Novel monitor paradigm for real-time exposure assessment. J Expos Sci Environ Epidemiol. 21:419-426.

NTP. 2000. NTP Technical Report on the Toxicology and Carcinogenesis Studies of Naphthalene (CAS NO. 91-20-3) in F344/N Rats (Inhalation Studies). Research Triangle Park NC: National Toxicology Program. NTP TR 500.

O'Brien KAF, Smith LL, Cohen GM. 1985. Differences in naphthalene-induced toxicity in the mouse and rat. Chem Biol Interact. 55:109-122.

Quick DJ, Shuler ML. 1999. Use of *in vitro* data for construction of a physiologically based pharmacokinetic model for naphthalene in rats and mice to probe species differences. Biotechnol Prog. 15:540-55.

Reid M, Reid RD, Oswal P, Sullivan K, Bhartia R, Hug WF. 2018. NaDos: A real-time, wearable, personal exposure monitor for hazardous organic vapors. Sens. Actuators B Chem. 255:2996-3003.

RTI. 1996. The Toxicokinetics of Naphthalene - Protocol RTI-518: The Toxicokinetics of Intravenously Administered Naphthalene (NAP) in Male and Female B6C3F1 Mice and F344 rats. Research Triangle Park NC: Research Triangle Institute.

Ruark CD, Hack CE, Robinson PJ, Mahle DA, Gearhart JM. 2014. Predicting Passive and Active Tissue:Plasma Partition Coefficients: Interindividual and Interspecies Variability. J Pharm Sci., 103:2189-2198. doi:10.1002/jps.24011

Sams C. 2017. Urinary naphthol as a biomarker of exposure: results from an oral exposure to carbaryl and workers occupationally exposed to naphthalene. Toxics. 6; 5. doi:10.3390/toxics5010003.

Serdar B, Egeghy PP, Waidyanatha S, Gibson R, Rappaport SM. 2003. Urinary biomarkers of exposure to jet fuel (JP-8). Environ Health Perspect. 111:1760-1764.

Steuperaert M, Debbaut C, Segers P, Ceelen W. 2017. Modeling drug transport during intraperitoneal chemotherapy. Pleura Peritoneum. 2(2):73-83.

Sweeney LM, Shuler ML, Quick DJ, Babish JG. 1996. A preliminary physiologically based pharmacokinetic model for naphthalene and naphthalene oxide in mice and rats. Ann Biomed Eng. 24:305-20.

Travis CC. 2011. On the definition of internal dose metrics. Human Ecolog Risk Assess. 17:467-477.

Turkall RM, Skowronski GA, Kadry AM, Abdel-Rahman MS. 1994. A comparative study of the kinetics and bioavailability of pure and soil-adsorbed naphthalene in dermally exposed male rats. Arch Environ Contam Toxicol. 26:504-9.

U.S. EPA. 1998. Naphthalene CASRN 91-20-3. Washington D.C.: U.S. Environmental Protection Agency. Assessment updated 09/17/1998. <https://cfpub.epa.gov/ncea/iris2/chemicalLanding.cfm?substance_nmbr=436.>

Van Winkle LS, Buckpitt AR, Nishio SJ, Isaac JM, Plopper CG. 1995. Cellular response in naphthalene-induced Clara cell injury and bronchiolar epithelial repair in mice. Am J Physiol. 269:L800-18.

Willems BA, Melnick RL, Kohn MC, Portier CJ. 2001. A physiologically based pharmacokinetic model for inhalation and intravenous administration of naphthalene in rats and mice. Toxicol Appl Pharmacol. 176:81-91.

Williamson L, New D. 2014. How the use of creatine supplements can elevate serum creatinine in the absence of underlying kidney pathology. BMJ Case Rep. Sep 19, 2014.

APPENDIX A. EXEMPT SUBJECT PREDICTIONS

A **B**

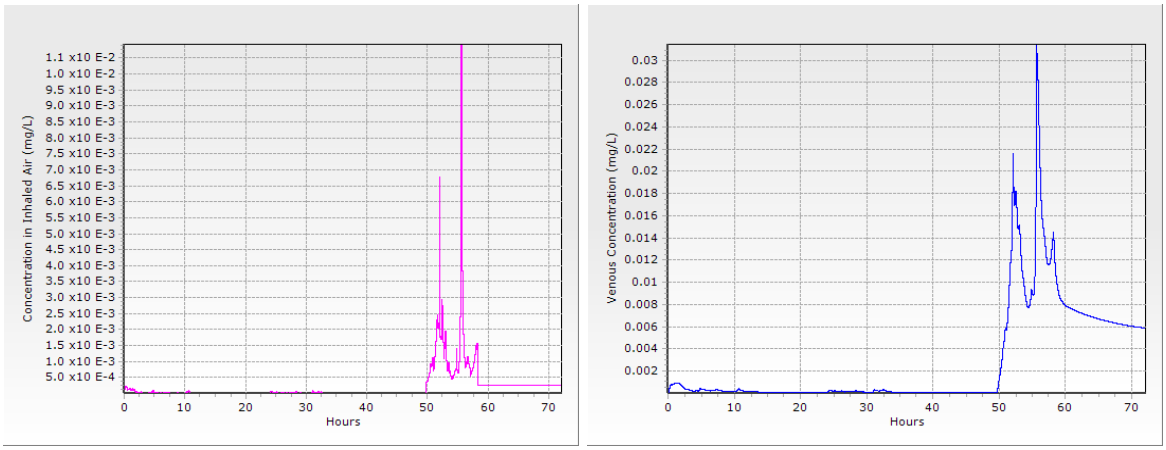

C **D**

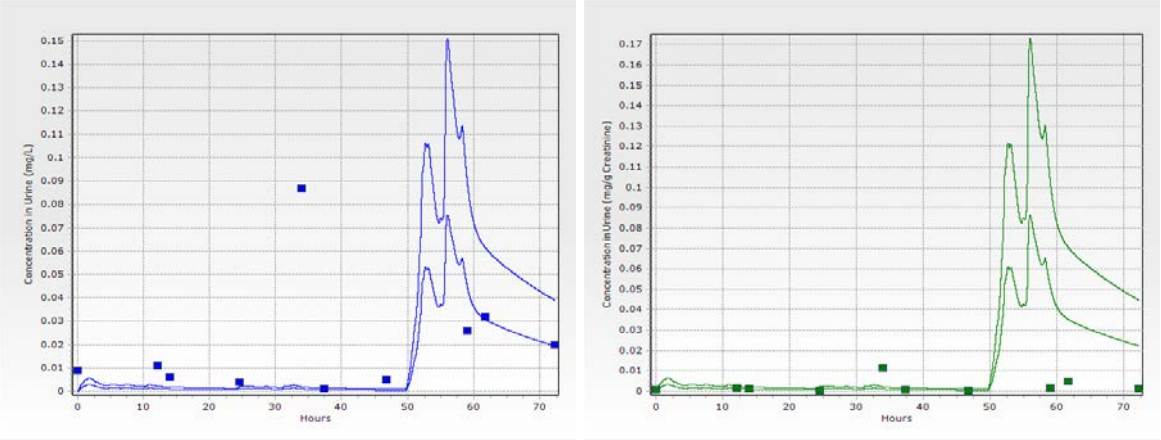

Predictions for Subject 17. Individual model predictions (lines) compared to observed data (squares) for: (A) Naphthalene exposure concentrations in inhaled air (mg/L), (B) Venous naphthalene blood concentration time course (mg/L); (C) A range of combined naphthols concentrations over time in the urine (mg/L) using predicted urine production (Hays *et al.*, 2015); and (D) A range of combined naphthols concentrations over time corrected to predicted creatinine production (mg/g creatinine), based on the work of Forni Ogna *et al.* (2015).

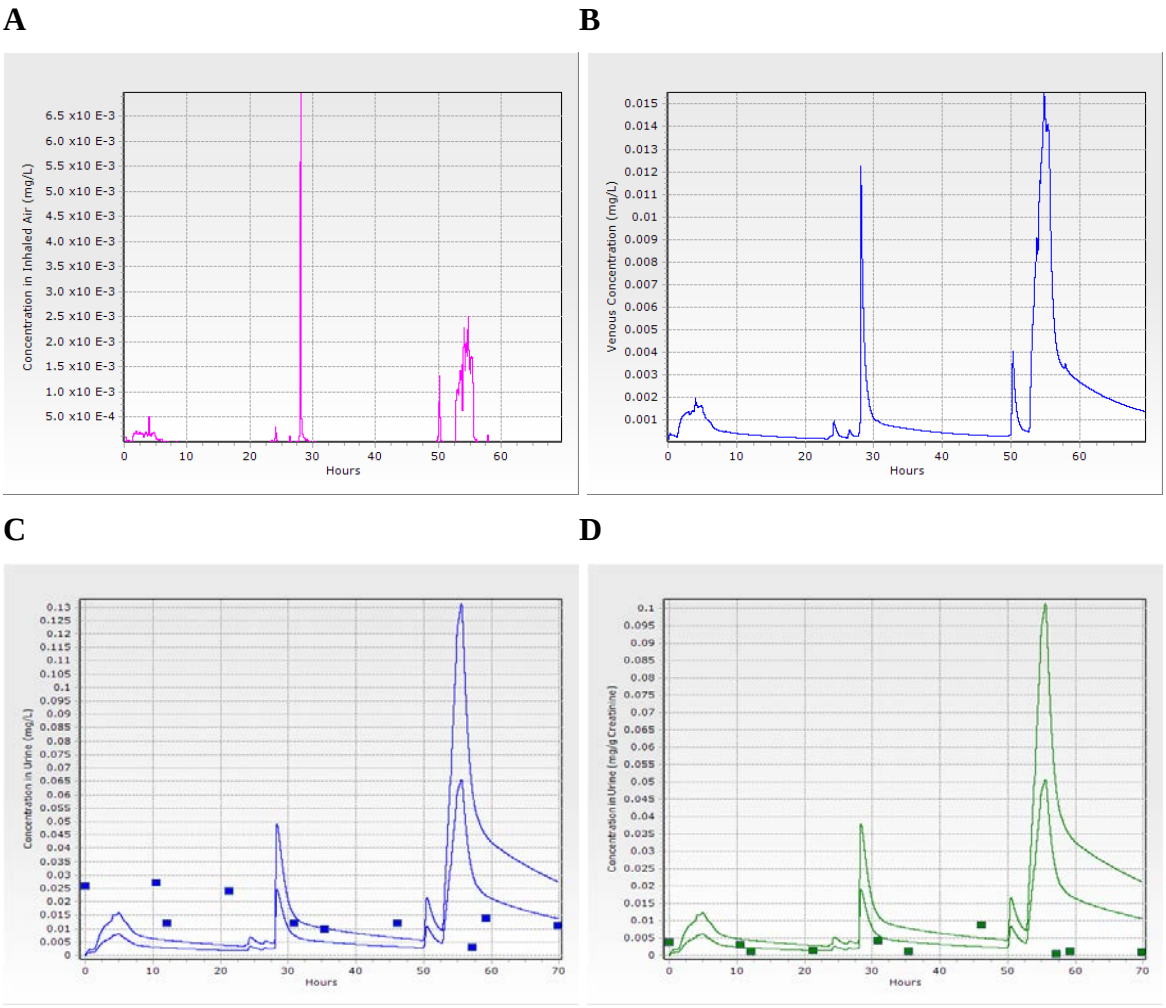

Predictions for Subject 18. Individual model predictions (lines) compared to observed data (squares) for: (A) Naphthalene exposure concentrations in inhaled air (mg/L), (B) Venous naphthalene blood concentration time course (mg/L); (C) A range of combined naphthols concentrations over time in the urine (mg/L) using predicted urine production (Hays *et al.*, 2015); and (D) A range of combined naphthols concentrations over time corrected to predicted creatinine production (mg/g creatinine), based on the work of Forni Ogna *et al.* (2015).

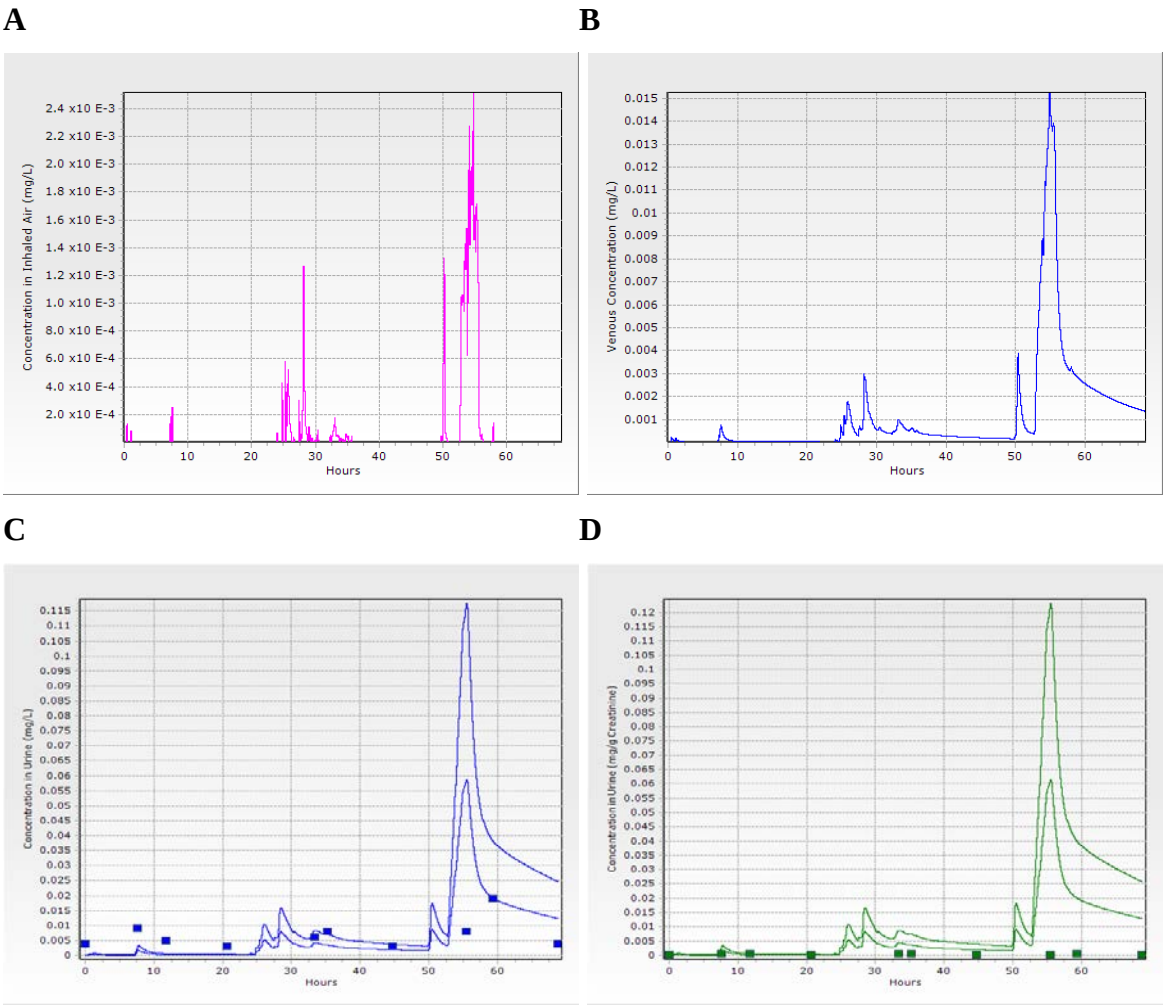

Predictions for Subject 19. Individual model predictions (lines) compared to observed data (squares) for: (A) Naphthalene exposure concentrations in inhaled air (mg/L), (B) Venous naphthalene blood concentration time course (mg/L); (C) A range of combined naphthols concentrations over time in the urine (mg/L) using predicted urine production (Hays *et al.*, 2015); and (D) A range of combined naphthols concentrations over time corrected to predicted creatinine production (mg/g creatinine), based on the work of Forni Ogna *et al.* (2015).

APPENDIX B. ACSLX CSL MODEL FILE

"NCONC" is set to 501 in the code below. M files included in other appendices need an NCONC value specific to the number of exposure concentration in that file. This value ranges from 3 to 501. The M file may run with an NCONC higher than needed but will produce odd results if run with a lower value. Further, acslX tends to crash if the NCONC number is far greater than needed (e.g., using NCONC=501 for a simulation only needing NCONC=3 or even NCONC=300).

Note: Report formatting introduces extraneous line breaks not in the original code.

PROGRAM: NaDoRT4a.csl

```
! Naphthalene Dosimeter Real Time data model by Teri Sterner and Elaine Merrill, Feb
2019

! Model time is hours
! States (i.e., tissue amounts) have units mg
! Tissue concentrations have units mg/L
! Inhalation concentrations MUST be in PPM

! NOTE - YOU MUST SET NCONC BEFORE RUNNING EACH M FILE AND THEN BUILD THE
CSL!!!!!!!!!!!
!      - SET INIT.M TO EXECUTE AT LOAD-TIME!!!!!!!!!!!!!!!

INITIAL

  INTEGER NConc, i
  PARAMETER (NConc=375)   ! Integer set equivalent to # of concentrations in ConcList
(= # of time points in StTList)
             !Minimum of 2 (not 2.0 - it's an integer) as the first time and conc need
to be 0.0 each for most RT data

  DIMENSION ConcList(NConc), StTList(NConc)
            ! ConcList = List of concentrations to which the subjects are exposed
including all non-exposures (0.0 ppm)
            ! StTList = Start times for each concentration in units of # of hours for
corresponding concentration from end of previous step

  LOGICAL  AdjQCQP   ! Adjust QC and QP (QAlv) with exercise
  LOGICAL  StartAdj  ! Switch to start adjusting ventilation and blood flows with
exercise
  LOGICAL  CC        ! To control whether closed or open chamber

! Chamber Parameter
  CONSTANT      CC = .FALSE.      ! Default to open chamber
  CONSTANT    VChC = 9.1          ! Volume of closed chamber (L)
  CONSTANT    kLCC = 0.0          ! Chamber loss
  CONSTANT     PCh = 1.0          ! Chamber/atmospheric pressure (atm)
  CONSTANT       R = 0.0821       ! Universal gas constant (L-atm/K-mol)
  CONSTANT    Temp = 298.15       ! Air temperature (for inhalation exposure) (K)

! Rat Total Pulmonary Ventilation Rate (L/hr/kg^0.75)
  CONSTANT     QPC = 24.75        ! Total pulmonary ventilation (L/hr - 1 kg)

! Rat Blood Flows (fraction of cardiac output)
  CONSTANT     QCC = 14.6         ! Cardiac output (L/hr/kg^0.75)
```

```
  CONSTANT   QFatC = 0.07         ! Fat
  CONSTANT   QLivC = 0.183        ! Liver
  CONSTANT    QLuC = 0.021        ! Lung (Brown et al 1997)
  CONSTANT   QRapC = 0.556        ! Rapidly perfused (lung removed)
  CONSTANT   QSknC = 0.058        ! Skin
  CONSTANT   QSlwC = 0.17         ! Slowly perfused (includes skin)

! Rat Tissue Volumes (fraction of body weight)
  CONSTANT      BW = 0.22         ! Body weight (kg)
  CONSTANT   BWSTD = 0.22         ! Standard BW for normalizing urinary outputs (kg)
  CONSTANT     SEX = 0.0          ! Sex correction for females to males based on Forni
Ogna et al. 2015, F = 1.0, M = 0.0
  CONSTANT      HT = 0.15         ! Height (m)
  CONSTANT     AGE = 0.25         ! Age (years)
  CONSTANT   VAlvC = 0.007        ! Alveolar blood
  CONSTANT   VFatC = 0.10         ! Fat
  CONSTANT   VLivC = 0.034        ! Liver
  CONSTANT    VLuC = 0.005        ! Lung (Brown et al 1997)
  CONSTANT   VMucC = 0.0001       ! Mucous
  CONSTANT   VRapC = 0.045        ! Rapidly perfused (lung removed)
  CONSTANT   VSlwC = 0.65         ! Slowly perfused (includes skin)
  CONSTANT   Depth = 0.10         ! Skin thickness (cm)
  CONSTANT      DS = 0.15         ! Dead space volume (fraction)

! Rat Tissue Capillary Volumes (fractions of tissues)
       CONSTANT   VFatBC = 0.02    !Fraction of fat volume that is blood
       CONSTANT   VBrBC = 0.03    !Fraction of brain that is blood
       CONSTANT   VLivBC = 0.21    !Fraction of liver that's blood
  CONSTANT   VSlwBC = 0.033       !Fraction of Slowly perfused that's blood

! Molecular Weights
  CONSTANT      MW = 60.09        ! Isopropanol
  CONSTANT     MW1 = 58.08        ! Acetone
             Stoch = MW1/MW

! Parent Tissue/Blood Partition Coefficients
  CONSTANT      PB = 1290.0       ! Blood/air
  CONSTANT     PLq = 1500.0       ! Saline/air
  CONSTANT    PMuc = 1290.0       ! Mucous/air (usually the same as PB)
  CONSTANT    PFat = 0.21         ! Fat
  CONSTANT    PLiv = 0.76         ! Liver
  CONSTANT     PLu = 2.1          ! Lung (toluene, human, Fiserova-Bergerova and Diaz,
1986)
  CONSTANT    PRap = 0.79         ! Rapidly perfused tissue
  CONSTANT    PSlw = 0.85         ! Slowly perfused tissue

! Permeability Area Cross Products (PAs) for diffusion limitation
  CONSTANT    PAFatC = 1.0                    ! Diffusion limitation for fat
  CONSTANT    PASlwC = 1.0              ! Diffusion limitation for fat

! Metabolite Tissue/Blood PCs
  CONSTANT     PB1 = 275.0        ! Blood/air
  CONSTANT    PLu1 = 0.50         ! Lung
  CONSTANT   PFat1 = 0.31         ! Fat
  CONSTANT   PLiv1 = 0.60         ! Liver
  CONSTANT   PRap1 = 0.53         ! Rapidly perfused tissue
  CONSTANT   PSlw1 = 0.55         ! Slowly perfused tissue

! PAs for metabolite
       CONSTANT    PAFat1C = 1.0                    ! Diffusion limitation for fat
  CONSTANT    PASlw1C = 1.0                   ! Diffusion limitation for fat

! Dermal Exposure Parameters
```

```
  CONSTANT    Area = 4.3          ! Exposed area (cm^2)
  CONSTANT      KP = 0.0          ! Permeability constant (cm/hr)
  CONSTANT   ICSFC = 0.0          ! Initial concentration on skin (mg/mL)
  CONSTANT   IVSFC = 0.0          ! Initial volume on skin surface (mL)

! Metabolism Parameters
  CONSTANT     KFC = 0.0         ! First order rate constant (kg^0.25/hr)
  CONSTANT VMaxLivC = 7.5        ! Maximum reaction rate Liver (mg/hr/kg^0.75)fitted
and scaled or (mg/hr/kg) in vitro derived
  CONSTANT    KMLiv = 75.0       ! Michaelis-Menten constant Liver(mg/L)
  CONSTANT     KFC1 = 0.0        ! First order rate constant (liver) (kg^0.75/hr)
  CONSTANT  VMaxLuC = 0.1                ! Maximum reaction rate Lung
(mg/hr/kg^0.75)fitted and scaled or (mg/hr/kg) in vitro derived
  CONSTANT     KMLu = 1.0         ! Michaelis-Menten constant Lung (mg/L)
  CONSTANT    KUrnC = 0.047       ! Urinary excretion rate, humans, El-Masri et al.
2018, (0.00065 L/hr)/kg
  CONSTANT    FOHLu = 0.095       ! Fraction of naphthols produced in lung (1-naphthol
+ diols, Buckpitt13)
  CONSTANT   FOHLiv = 0.2         ! Fraction of naphthols produced in liver (1-naphthol
fract x2, Cho16)

! Uptake and Clearance Parameters
  CONSTANT   ClUrC = 0.004        ! Urinary clearance of parent (L/hr/kg^0.75)
  CONSTANT  ClUrC1 = 0.004        ! Urinary clearance of metabolite (L/hr/kg^0.75)
  CONSTANT   kUrtC = 11.0         ! URT uptake (L/hr/kg^0.75)
  CONSTANT     kAD = 0.5          ! Absorption from duodenum (/hr)
  CONSTANT     kAS = 2.0          ! Absorption from stomach (/hr)
  CONSTANT     kTD = 0.25         ! Excretion (/hr)
  CONSTANT    kTSD = 3.0          ! Transfer - stomach to duodenum (/hr)

! Dosing Parameters
  CONSTANT ConcList = NConc*0.0       ! Inhaled concentration (array) (ppm)
  CONSTANT  StTList = NConc*0.0       ! Time of concentration (array) (hr)
  CONSTANT   TStart = 1000.0          ! Time to start first inhalation exposure (hr)
  CONSTANT   IVDose = 0.0          ! IV dose (mg/kg)
  CONSTANT    TChng = 0.0          ! Length of inhalation exposure (hrs)
  CONSTANT     TInf = 0.20         ! Length of IV injection (hrs)
  CONSTANT     Rats = 1.0          ! Number of animals in experiment

! Simulation Control Parameters
  CONSTANT AdjQCQP = .FALSE.      ! Switch to adjust QC and QP for exercise
  CONSTANT   TExer = 0.5          ! Time to start exercise (hrs)
  CONSTANT   LExer = 0.25         ! Length of exercise period (hrs)
  CONSTANT  RampUp = 0.05         ! Time frame to ramp up QC and QP (hrs)
  CONSTANT  RampDn = 0.1          ! Time frame to ramp down QC and QP (hrs)
  CONSTANT   TStop = 24.0
  CONSTANT   CIntC = 0.005

  IF (.NOT.CC) THEN       ! Large chamber = open chamber
      VCh = 1.0e+20
      kLC = 0.0
  ELSE
      VCh = VChC - (Rats*BW)          ! Calculate net chamber volume
      kLC = kLCC
  ENDIF

! Calculate Total Area of Skin (cm^2)
     TArea = 9.1 * ((BW*1000.0)**0.666)

! Scaled Pulmonary Ventilation Rate (L/hr)
    QPInit = QPC * (BW**0.75)
      QAlv = 0.67 * (QPC * (BW**0.75))
        QP = QPInit
```

```
! Scaled Cardiac Output (L/hr)
       QCN = QCC * (BW**0.75)

! If dermal dosing, adjust volume and flow to slowly perfused for separate skin
exposed
      VSlw = 0.0         ! initalization in case of dermal dose
  IF (ICSFC.GT.0.0) THEN
      VSkn = (Area * Depth) / 1000.0
      VSlw = (VSlwC * BW) - VSkn
      QSknC2 = QSknC * (Area/TArea)
  ELSE
      VSkn = -1.0    ! flag for no dermal
      VSlw = VSlwC * BW
      QSknC2 = 0.0
  ENDIF

! Scaled Blood Flows (L/hr)
      QFat = QFatC * QCN
      QLiv = QLivC * QCN
       QLu = QLuC * QCN
      QRap = QRapC * QCN
      QSkn = QSknC2 * QCN
      QSlw = (QSlwC * QCN) - QSkn
        QC = QFat + QLiv + QLu + QRap + QSkn + QSlw

! Scaled Tissue Volumes (L)
      VAlv = VAlvC * BW
      VFatX = VFatC * BW                !Vol includes fat and capillary bed
                  VFatB = VFatBC * VFatx  !Vol of fat capillary bed
                  VFat = VFatX - VFatB        !Vol of Fat  without capillary bed
      VLiv = VLivC * BW
       VLu = VLuC * BW
      VMuc = VMucC * BW
      VRap = VRapC * BW
      VSlwX = VSlwC *BW
      VSlwB = VSlwX * VSlwBC  !volume of slow's capillary bed
      VSlw = VSlwX - VSlwB       !volume of slow without capillary bed
      VTot = VAlv + VFat + VFatB + VLiv + VLu + VMuc + VRap + VSlw + VSlwB + max(0.0,
VSkn)

! Scaled Permeability Area X products
      PAFat = PAFatC * BW**0.75
      PASlw = PASlwC * BW**0.75
      PAFat1 = PAFat1C * BW**0.75
      PASlw1 = PASlw1C * BW**0.75

! Calculation of Skin Partition Coefficients
      PSkn = (0.3*PFat*PB) + (0.7*PSlw*PB)        ! Skin/air partition
      PSkn1 = (0.3*PFat1*PB1) + (0.7*PSlw1*PB1)   ! Skin/air partition
      PSknB = PSkn / PB                           ! Skin/blood partition
      PSknB1 = PSkn1/PB
      PSknL = PSkn / PLq                          ! Skin/saline partition

! Initial Amounts of parent (mg)
     IAArt = 0.0
     IAFat = 0.0
     IALiv = 0.0
      IALu = 0.0
     IARap = 0.0
     IASkn = 0.0
     IASlw = 0.0
   InitTot = IAArt + IAFat + IALiv + IALu + IARap + IASkn + IASlw
```

```
! Initial Amounts of metabolite (mg)
     IAFat1 = 0.0
     IALiv1 = 0.0
      IALu1 = 0.0
     IARap1 = 0.0
     IASkn1 = 0.0
     IASlw1 = 0.0
   InitTot1 = IAFat1 + IALiv1 + IALu1 + IARap1 + IASkn1 + IASlw1

! Scaled Metabolism Parameters: Use for Fit and Extrapolated Values
!        KF = KFC / (BW**0.25)
!     VMaxLiv = VMaxLivC * (BW**0.75)         ! mg/hr
!       KF1 = KFC1 / (BW**0.25)
!             VmaxLu = VmaxLuC * (BW**0.25)

! Metabolism Parameters: Use for In Vitro Derived Metabolic Values for Rodent & Human
!   No allometric scaling needed
        KF = KFC / BW
     VMaxLiv = VMaxLivC * BW         ! mg/hr
       KF1 = KFC1 / BW
      VmaxLu = VmaxLuC * BW           ! mg/hr

! Scaled Clearance Rates
      ClUr = ClUrC * (BW**0.75)
     ClUr1 = ClUrC1 * (BW**0.75)
      kUrt = (min(kUrtC, QPC)) * (BW**0.75)

! Scaled urinary production rate equation from El-Masri, normalized to 70 kg person,
L/hr
      KUrn = KUrnC * BW * (BW/BWSTD)

! Scaled Excretion of creatinine based on Forni Ogna et al 2015 (units = umol
creat/(kg BW x dy)), converted to g creat/hr)
!   MW creatinine = 113.2 g/mol
    KCreat = (266.16+(-47.71*SEX)+(-2.33*(BW/HT))+(0.66*AGE)+(-
0.017*AGE*AGE))*0.0001132/24.0*BW

! Initialize Starting Values
  StartAdj = .FALSE.
      CINT = CIntC
        IV = 0.0
         i = 1         ! Integer, exposure counter
     CIppm = 0.0
      CInh = 0.0
     DDose = ICSFC * IVSFC        ! Initial dermal dose (mg)
   TotDose = 0.0
    PerEnd = 0.0
    PerMix = 0.0
  PAUCCBld = 0.0
  PAUCCUrn = 0.0
       AI0 = (ConcList(i)*VCh*MW)/24450.0         !Initial amount in chamber (mg)
 ! CUrnMet1 = 0.0

  SCHEDULE ConcOn .AT. TStart
END               ! End of Initial

DYNAMIC
  ALGORITHM  IALG = 2             ! Gear stiff method

DISCRETE DoseOff
  CINT = CIntC
  IV = 0.0
```

```
END

DISCRETE DoseOn    ! Start dosing
 INTERVAL DoseInt = 24.0         ! Interval to repeat dosing

 SCHEDULE DoseOff .AT. T + TInf
   IF (T.LE.TInf) THEN
      IF (IVDose.GT.0.0) CINT = MIN(CIntC, (TInf/10.0))
      IF (IVDose.GT.0.0) IV = (IVDose * BW) / TInf   ! Rate of intravenous dosing
(mg/hr)
 ENDIF
END

DISCRETE ConcOn  !Inhalation dosing
   SCHEDULE ConcOn .AT. T+StTList(i)
   CIppm = ConcList(i)
   i = i+1
END

DISCRETE Calc      ! Calculate daily average AUC
   INTERVAL CalcInt = 24.0

   DAUCCBld = (AUCCBld - PAUCCBld) / (CalcInt/24.0)
   DAUCCUrn = (AUCCUrn - PAUCCUrn) / (CalcInt/24.0)

   IF (T.GT.0.0) THEN
       PAUCCBld = AUCCBld
       PAUCCUrn = AUCCUrn
ENDIF
END      ! End of Calc

DERIVATIVE
     Hours = T
   Minutes = T * 60.0
      Days = T / 24.0

! Amount in Inhaled Air
      RACh = (Rats*((-QAlv*CInh) + (QAlv*CAlv) + RAMucX)) - (kLC*ACh)
       ACh = INTEG(RACh, AI0)
        CP = (CInh * 24450.0) / MW

PROCEDURAL (CInh = CC, ACh, VCh, CIppm, MW)
      CInh = CIppm * MW/24450.0                  ! mg/L
      IF (CC) CInh = ACh / VCh                   ! mg/L
END

! Amount in Mucous
    RAMucI = kUrt * (CInh - (CMuc/PMuc))
    RAMucX = kUrt * ((CMuc/PMuc) - CAlv)
     RAMuc = RAMucI - RAMucX
      AMuc = INTEG(RAMuc, 0.0)
      CMuc = AMuc / VMuc

! Amount in Arterial Blood (mg)
     RAArt = (QAlv*CInh) - RAMucI - (QAlv*CAlv) + (QC*(CVen-CArt))
      AArt = INTEG(RAArt, IAArt)
      CArt = AArt / VAlv
      CAlv = CArt / PB
   CAlvPPM = CAlv * (24450.0 / MW)
   AUCCBld = INTEG(CArt, 0.0)

! Amount Exhaled (mg)
     RAExh = (QAlv * CAlv) + RAMucX
```

```
      AExh = INTEG(RAExh, 0.0)

! Concentration in End-Exhaled Air (mg/L)
      CEnd = RAExh / QAlv
   CEndPPM = CEnd * (24450.0 / MW)
  IF (CIppm.GT.0.0) PerEnd = (CEnd / ((CIppm * MW) / 24450.0)) * 100.0

! Concentration in Mixed Exhaled Air (mg/L)
      CMix = ((1.0 - DS) * CEnd) + (DS * CInh)
   CMixPPM = CMix * (24450.0 / MW)
  IF (CIppm.GT.0.0) PerMix = (CMix / ((CIppm * MW) / 24450.0)) * 100.0

! Amount in Lung (mg)
  RALu = QLu * (CArt - CVLu) - RAMetLu
   ALu = INTEG(RALu, IALu)
   CLu = ALu / VLu
  CVLu = CLu / PLu

! Amount Metabolised in Lung -- Saturable (mg)
    RAMetLu = (VMaxLu * CVLu) / (KMLu + CVLu)
     AMetLu = INTEG(RAMetLu, 0.0)

! Amount in Fat (mg)
     RAVFat = QFat*(CArt-CVFat) +PAFat*(CFat/PFat-CVFat)
     AVFat = INTEG(RAVFat,0.0)
     CVFat = AVFat/VFatB
     RAFat = PAFat*(CVFat-CFat/PFat)
      AFat = Integ(RAFat,0.0)
      CFat = AFat/VFat

! Amount in Liver (mg)
     RALiv = (QLiv * (CArt - CVLiv)) - RAMet1 - RAMet2
      ALiv = INTEG(RALiv, IALiv)
      CLiv = ALiv / VLiv
     CVLiv = CLiv / PLiv

! Amount Metabolised in Liver -- Saturable (mg)
    RAMet1 = (VMaxLiv * CVLiv) / (KMLiv + CVLiv)
     AMet1 = INTEG(RAMet1, 0.0)

! Amount Metabolised in Liver -- 1st Order (mg)
    RAMet2 = KF * CVLiv * VLiv
     AMet2 = INTEG(RAMet2, 0.0)

! Amount in Rapidly Perfused Tissue (mg)
     RARap = QRap * (CArt - CVRap)
      ARap = INTEG(RARap, IARap)
      CRap = ARap / VRap
     CVRap = CRap / PRap

! Amount on Skin Surface (mg)
   CSFZone = RSW(T.LT.TChng, 1.0, 0.0)
     RASFC = ((KP * Area)/1000.0) * ((CSkn/PSknL) - CSFC)
      ASFC = INTEG(RASFC, DDose)
      CSFC = 1000.0 * ICSFC * CSFZone

! Amount in Skin (mg)
     RASkn = ((KP * Area)/1000.0) * (CSFC - (CSkn/PSknL)) + (QSkn * (CArt - CVSkn))
      ASkn = INTEG(RASkn, IASkn)
      CSkn = ASkn / VSkn
     CVSkn = CSkn / PSknB

! Amount in Slowly Perfused Tissue (mg)
```

```
    RAVSlw = QSlw*(CArt-CVSlw) +PASlw*(CSlw/PSlw-CVSlw)
     AVSlw = INTEG(RAVSlw,0.0)
     CVSlw = AVSlw/VSlwB
     RASlw = PASlw*(CVSlw-CSlw/PSlw)
      ASlw = Integ(RASlw,0.0)
      CSlw = ASlw/VSlw

! Concentration in Mixed Venous Blood (mg/L)
      CVen = (QLu*CVLu + QFat*CVFat + QLiv*CVLiv + QRap*CVRap + QSkn*CVSkn +
QSlw*CVSlw + IV - RAUrn) / QC

! Amount in Urine (mg)
     RAUrn = ClUr * CArt
      AUrn = INTEG(RAUrn, 0.0)

! ----------------- METABOLITE MODEL --------------------------------
! Amount in Arterial Blood (mg)
     RAArt1 = QC*(CVen1 - CArt1) - RAUrn1
     AArt1 = INTEG(RAArt1, 0.0)
     CArt1 = AArt1/VAlv
     CAlv1 = CArt1 / PB1

! Amount Exhaled (mg)
     RAExh1 = (QAlv * CAlv1)
      AExh1 = INTEG(RAExh1, 0.0)

! Amount in Lung (mg)
!  RALu1 = QLu * (CArt1 - CVLu1) + 0.055*(Stoch * RAMetLu)
   RALu1 = QLu * (CArt1 - CVLu1) + FOHLu*(Stoch * RAMetLu)
   ALu1 = INTEG(RALu1, IALu1)
   CLu1 = ALu1 / VLu
  CVLu1 = CLu1 / PLu1

! Amount in Fat (mg)
     RAVFat1 = QFat*(CArt1-CVFat1) +PAFat1*(CFat1/PFat1-CVFat1)
     AVFat1 = INTEG(RAVFat1,0.0)
     CVFat1 = AVFat1/VFatB
     RAFat1 = PAFat1*(CVFat1-CFat1/PFat1)
      AFat1 = Integ(RAFat1,0.0)
      CFat1 = AFat1/VFat

! Amount in Liver (mg) - 0.1=in vitro liver value (Cho et al.)
!     RALiv1 = (QLiv * (CArt1 - CVLiv1)) + 0.1*(Stoch * (RAMet1 + RAMet2))
     RALiv1 = (QLiv * (CArt1 - CVLiv1)) + FOHLiv*(Stoch * (RAMet1 + RAMet2))
      ALiv1 = INTEG(RALiv1, IALiv1)
      CLiv1 = ALiv1 / VLiv
     CVLiv1 = CLiv1 / PLiv

! Amount in Rapidly Perfused Tissue (mg)
     RARap1 = QRap * (CArt1 - CVRap1)
      ARap1 = INTEG(RARap1, IARap1)
      CRap1 = ARap1 / VRap
     CVRap1 = CRap1 / PRap1

! Amount in Skin (mg)
     RASkn1 = QSkn * (CArt1 - CVSkn1)
      ASkn1 = INTEG(RASkn1, IASkn1)
      CSkn1 = ASkn1 / VSkn
     CVSkn1 = CSkn1 / PSknB1

! Amount in Slowly Perfused Tissue (mg)
    RAVSlw1 = QSlw*(CArt1-CVSlw1) +PASlw1*(CSlw1/PSlw1-CVSlw1)
     AVSlw1 = INTEG(RAVSlw1,0.0)
```

```
     CVSlw1 = AVSlw1/VSlwB
     RASlw1 = PASlw1*(CVSlw1-CSlw1/PSlw1)
      ASlw1 = Integ(RASlw1,0.0)
      CSlw1 = ASlw1/VSlw

! Concentration in Mixed Venous Blood (mg/L)
      CVen1 = (QLu*CVLu1 + QFat*CVFat1 + QLiv*CVLiv1 + QRap*CVRap1 + QSkn*CVSkn1 +
QSlw*CVSlw1 - RAUrn1) / QC

! Amount in Urine (mg)
     RAUrn1 = (ClUr1*CArt1)
      AUrn1 = INTEG(RAUrn1, 0.0)
! Metabolite Concentration in Urine using average excretion rate (mg/L)
    CUrnMetOH = RAUrn1/KUrn                !(mg/L)
! Metabolite Concentration and AUC in Urine Normalized to Creatinine using average
creatinine rate (mg/mg creatinine)
   CUrnNormOH = RAUrn1/KCreat                ! (mg/hr) / (mg creat/hr)
    AUCCUrn = INTEG(CUrnNormOH, 0.0)

! ----------------- CHECK MASS BALANCE ------------------------------
     TDose = INTEG((QAlv*CInh), 0.0) + INTEG(IV, 0.0) + (DDose - ASFC)
  Parent = AMuc + AArt + ALu + AFat + AVFat + ALiv + ARap + ASkn + ASlw + AVSlw + AExh
+ AUrn + AMet1 + AMet2 + AMetLu - InitTot
  Metabo = AArt1 + ALu1 + AFat1 + AVFat1 + ALiv1 + ARap1 + ASkn1 + ASlw1 + AVSlw1 +
AExh1 + AUrn1 - InitTot1
 MassBal = TDose - Parent
  MetBal = ((AMetLu + AMet1 + AMet2)*Stoch)- Metabo

TERMT(T.GT.TStop, 'Simulation Finished')

END               ! End of Derivative
END               ! End of Dynamic
END ! PROGRAM
```

APPENDIX C. ACSLX M FILES FOR MODEL OPERATIONS

Init.m

```
% Initial requirements

%Set to Execute at Load-Time

prepare T HOURS MINUTES DAYS MASSBAL CART CVEN CMIX CMIXPPM CENDPPM CALVPPM AURN
prepare QC QP QALV QFAT QLIV QRAP QSKN QSLW MINUTES
prepare CLU CLIV CRAP CSLW CFAT CVFAT CVSLW
prepare AMET1 AMETLU
prepare CIPPM AI0 CINH  CMUC
prepare AUCCBLD AUCCURN
prepare CURNMETOH CURNNORMOH CEND
prepare METABO
prepare CLU1 CLIV1 CRAP1 CFAT1 CVFAT1 CSLW1 CVSLW1 CVEN1 CART1

xerror (["ACh", "AMuc", "AExh"], [1.0e-11, 1.0e-11, 1.0e-11])
xerror (["AArt", "ALu", "AVFat", "AFat"], [1.0e-8, 1.0e-8, 1.0e-8, 1.0e-8])
xerror (["ALiv", "ARap", "AVSlw", "ASlw"], [1.0e-8, 1.0e-8, 1.0e-8, 1.0e-8])
xerror (["ASFC", "ASkn"], [1.0e-8, 1.0e-8])
xerror (["AMetLu", "AMet1", "AMet2", "AUrn"], [1.0e-8, 1.0e-8, 1.0e-8, 1.0e-8])

HVDPRN=0;
WESITG=0;
CINTC=0.001;

disp("Initialization Complete")
```

ResetDoses.m

```
% Reset all doses to default values

%Inhalation parameters
%STTLIST=NCONC*0.0; CONCLIST=NCONC*0.0;
TSTART=1000.0;
CC=0; RATS=1.0;

%IV parameters
IVDOSE=0.0; TINF=0.20;

%Dermal parameters
KP = 0.0; ICSFC = 0.0; IVSFC = 0.0;
```

APPENDIX D. ACSLX M FILES FOR PHYSIOLOGICAL PARAMETERS

Note: Report formatting introduces extraneous line breaks not in the original code.

Human.m

```
% Human physiological parameters

% Values from published Clewell IPA model unless noted otherwise
  BW=70.0; BWSTD=70.0;
  QCC=12.89; QPC=27.75;
     QFATC=0.052; QLIVC=0.227; QLUC=0.025;
     QRAPC=0.419; QSKNC=0.058; QSLWC=0.188;
  VALVC=0.0079; VMUCC=0.0001;
     VFATC=0.214; VLIVC=0.026; VLUC=0.0076;
     VRAPC=0.0484; VSLWC=0.536;
  VFATBC=0.02; VSLWBC=0.04;
  DEPTH=0.1; KP=0.0;

% Urinary Flow Rate for ages 20-59 yr (Hays)
  KURNC = 0.00065        % (L/hr)/kg, El-Masri
                         % 95% CI for KUrnC = 0.00063, 0.00067 (L/hr)/kg

  SEX = 0.0;   % Sex correction for females to males based on Forni Ogna, F = 1.0, M =
0.0
  HT = 1.77;   % Height (m), Average for male population in Forni Ogna
  AGE = 48.1;  % Age (years), Average for male population in Forni Ogna

% VRapC = Clewell VRapC + Clewell VBrnC - Brown VLuC (0.036 + 0.02 - 0.0076 = 0.0484

% VLuC, QLuC, VFatBC, VSlwBC from Brown
% VSlwBC is mean of all slowly perfused tissues reported excluding fat

% Brown RP, Delp MD, Lindstedt SL, Rhomberg LR, Beliles RP. Physiological
%   parameter values for physiologically based pharmacokinetic models. Toxicol Ind
%   Health. 1997 Jul-Aug;13(4):407-84.
% Clewell HJ 3rd, Gentry PR, Gearhart JM, Covington TR, Banton MI, Andersen ME.
%   Development of a physiologically based pharmacokinetic model of isopropanol and
%   its metabolite acetone. Toxicol Sci. 2001 Oct;63(2):160-72.
% Hays SM, Aylward LL, Blount BC. Variation in urinary flow rates according to
%   demographic characteristics and body mass index in NHANES: potential confounding
%   of associations between health outcomes and urinary biomarker concentrations.
%   Environ Health Perspect. 2015 Apr;123(4):293-300.
% El-Masri HA, Hong T, Henning C, Mendez W Jr, Hudgens EE, Thomas DJ, Lee JS.
%   Evaluation of a Physiologically Based Pharmacokinetic (PBPK) Model for Inorganic
%   Arsenic Exposure Using Data from Two Diverse Human Populations. Environ Health
%   Perspect. 2018 Jul 16;126(7):077004.
% Forni Ogna V, Ogna A, Vuistiner P, Pruijm M, Ponte B, Ackermann D, Gabutti L,
%   Vakilzadeh N, Mohaupt M, Martin PY, Guessous I, P??ch??re-Bertschi A, Paccaud F,
%   Bochud M, Burnier M; Swiss Survey on Salt Group. New anthropometry-based age- and
%   sex-specific reference values for urinary 24-hour creatinine excretion based on
%   the adult Swiss population. BMC Med. 2015 Feb 27;13:40.
```

Rat.m

```
% Rat physiological parameters

% Parameter values from Clewell IPA model

  BW=0.22; BWSTD=0.22;
```

```
  QCC=14.6; QPC=24.75;
     QFATC=0.07; QLIVC=0.183; QLUC=0.021;
     QRAPC=0.557; QSKNC=0.058; QSLWC=0.17;
  VALVC=0.007; VMUCC=0.0001;
     VFATC=0.10; VLIVC=0.034; VLUC = 0.005;
     VRAPC=0.045; VSLWC=0.65;
  VFATBC=0.02; VSLWBC=0.033;
  DEPTH=0.1; KP=0.0;

% Constants added to calculate urinary excretion normalized to creatinine production;
NOT FOR RATS
  KURNC = 0.00065;    % Urinary production rate, HUMAN VALUE, El-Masri (0.00065
L/hr)/kg
  SEX = 0.0;          % Sex correction for HUMAN females to males based on Forni Ogna,
F = 1.0, M = 0.0
  HT = 0.15;          % Height (m)
  AGE = 0.25;         % Age (years)

% VRapC = Clewell VRapC + Clewell VBrnC - Brown VLuC (0.044 + 0.006 - 0.005 = 0.045

% Brown RP, Delp MD, Lindstedt SL, Rhomberg LR, Beliles RP. Physiological
%   parameter values for physiologically based pharmacokinetic models. Toxicol Ind
%   Health. 1997 Jul-Aug;13(4):407-84.
%Clewell HJ 3rd, Gentry PR, Gearhart JM, Covington TR, Banton MI, Andersen ME.
%   Development of a physiologically based pharmacokinetic model of isopropanol and
%   its metabolite acetone. Toxicol Sci. 2001 Oct;63(2):160-72.
% El-Masri HA, Hong T, Henning C, Mendez W Jr, Hudgens EE, Thomas DJ, Lee JS.
%   Evaluation of a Physiologically Based Pharmacokinetic (PBPK) Model for Inorganic
%   Arsenic Exposure Using Data from Two Diverse Human Populations. Environ Health
%   Perspect. 2018 Jul 16;126(7):077004.
% Forni Ogna V, Ogna A, Vuistiner P, Pruijm M, Ponte B, Ackermann D, Gabutti L,
%   Vakilzadeh N, Mohaupt M, Martin PY, Guessous I, P??ch??re-Bertschi A, Paccaud F,
%   Bochud M, Burnier M; Swiss Survey on Salt Group. New anthropometry-based age- and
%   sex-specific reference values for urinary 24-hour creatinine excretion based on
%   the adult Swiss population. BMC Med. 2015 Feb 27;13:40.
```

APPENDIX E. ACSLX M FILES FOR PHYSICOCHEMICAL PARAMETERS

Note: Report formatting introduces extraneous line breaks not in the original code.

Human_Naph.m

```
% Sets human naphthalene parameters

MW=128.1705;  %NIST

  %------------------PCs--------------------
  %PCs from Campbell (PLU = PRAP)
  PB=571.0; PMUC=571.0; PLU=3.5; PFAT=49.0; PLIV=1.6; PRAP=3.5; PSLW=3.5;

  %Predicted average PCs for 1- and 2-naphthol by Ruark
  PB1=10000.0; PLU1=(0.88+0.54)/2; PFAT1=(10.2+7.3)/2; PLIV1=(0.88+0.55)/2;
PRAP1=(0.72+0.46)/2; PSLW1=(0.45+0.24)/2;

  %------------------PAs-----------------
  %Diffusion limitation default is inactive = 10000.0

  PAFATC = 2.0;                  %0.2 Rat fit
  PASLWC = 2.0;                  %2.0 Rat fit

  PAFAT1C = 10000.0;
  PASLW1C = 10000.0;

  %----------Metabolism/urinary clearance parameters--------
    % Units are VMaxC (mg/hr/kg^0.75), KM (mg/L), KFC (kg^0.25/hr)

  VMAXLIVC=0.775;  % Cho06, human microsomes, sum of metabolite VMax values/100
  KMLIV=2.94;       % 2.94 Cho06, diol value (lowest)

  VMAXLUC=0.0035; % 0.0035 Buckpitt13, lowest value (Campbell14)
  KMLU=8.7;     % 8.7 Buckpitt13, NHP airways, weighted average of metabolic pathway
Km values, based on paired VMax fraction of whole

  KFC=0.0;
  KFC1=0.0;
  CLURC=0.0;         %L/hr/kg^0.75
  CLURC1=0.4;   %L/hr/kg^0.75
  FOHLU=0.095;    %0.095 Buckpitt13 1-naphthol + diol in NHP microsomes
  FOHLIV=0.2;     %0.2 Cho16 1-naphthol x2 in hmn microsomes

  KFC=0.0;
  KFC1=0.0;
  CLURC=0.0;         %L/hr/kg^0.75
  CLURC1=0.4;   %L/hr/kg^0.75
  FOHLU=0.095;    %0.095 Buckpitt13 1-naphthol + diol in NHP microsomes
  FOHLIV=0.2;     %0.2 Cho16 1-naphthol x2 in hmn microsomes

   %----------------Upper respiratory-----------------
  KURTC=0.0;  %no scrubbing
  DS=0.15;  %Lung dead space, Clewell

  %----------------Dermal absorption-------------------
  KP=0.038; %Calculated by Peter Robinson using Wilschut et al. 1995 = 0.038 cm/hr

% Buckpitt A, Morin D, Murphy S, Edwards P, Van Winkle L. Kinetics of
%   naphthalene metabolism in target and non-target tissues of rodents and in nasal
```

```
%   and airway microsomes from the Rhesus monkey. Toxicol Appl Pharmacol. 2013 Jul
%   15;270(2):97-105.
% Campbell JL, Andersen ME, Clewell HJ. A hybrid CFD-PBPK model for naphthalene
%   in rat and human with IVIVE for nasal tissue metabolism and cross-species
%   dosimetry. Inhal Toxicol. 2014 May;26(6):333-44.
% Cho TM, Rose RL, Hodgson E. In vitro metabolism of naphthalene by human liver
%   microsomal cytochrome P450 enzymes. Drug Metab Dispos. 2006 Jan;34(1):176-83.
% Clewell HJ 3rd, Gentry PR, Gearhart JM, Covington TR, Banton MI, Andersen ME.
%   Development of a physiologically based pharmacokinetic model of isopropanol and
%   its metabolite acetone. Toxicol Sci. 2001 Oct;63(2):160-72.
% NIST Chemistry Webbook
(https://webbook.nist.gov/cgi/cbook.cgi?Name=naphthalene&Units=SI)
% Ruark CD, Hack CE, Robinson PJ, Mahle DA, Gearhart JM. Predicting passive and
%   active tissue:plasma partition coefficients: interindividual and interspecies
%   variability. J Pharm Sci. 2014 Jul;103(7):2189-2198.
% Wilschut, A., Berge, ten, W. F., Robinson, P. J., & McKone, T. E. (1995). Estimating
skin permeation. The validation
%   of five mathematical skin permeation models. Chemosphere, 30(7), 1275-1296
```

Rat_Naph.m

```
% Sets rat naphthalene parameters

  MW=128.1705;  %NIST

  %------------------PCs--------------------
  % PMuc is set equal to PB

% Rat_Naph.m
% Sets rat naphthalene parameters

  %PCs from Campbell (PLU = PRAP)
  PB=571.0; PMUC=571.0; PLU=3.5; PFAT=49.0; PLIV=1.6; PRAP=3.5; PSLW=3.5;

%Predicted average PCs for 1- and 2-naphthol by Ruark
  PB1=10000.0; PLU1=(0.88+0.54)/2; PFAT1=(10.2+7.3)/2; PLIV1=(0.88+0.55)/2;
PRAP1=(0.72+0.46)/2; PSLW1=(0.45+0.24)/2;

  %-------------------PAs------------------
  %Diffusion limitation default is inactive = 10000.0

  PAFATC = 0.2;
  PASLWC = 2.0;

  PAFAT1C = 10000.0
  PASLW1C = 10000.0

  %----------Metabolism/urinary clearance parameters--------
    % Units are VMaxC (mg/hr/kg^0.75), KM (mg/L), KFC (kg^0.25/hr)
  KFC=0.0;
  KFC1=0.0;
  CLURC=0.0;
  CLURC1=0.4;   %L/hr/kg^0.75
  FOHLU=0.095;    %0.095 Buckpitt13 1-naphthol + diol in NHP microsomes
  FOHLIV=0.2;     %0.2 Cho16 1-naphthol x2 in hmn microsomes

  VMAXLIVC=8.28; %Calc from Buckpitt13 with liver:lung ratio from Buckpitt87
  KMLIV=2.18;     %2.18 lung Km
  VMAXLUC=0.45;   %Buckpitt13, added 2 enzyme values
  KMLU=2.18;      %Buckpitt13, weighted average of 2 enzyme values

%-----------------Upper respiratory-----------------
  KURTC=0.0;  %no scrubbing
```

```
  DS=0.15;  %Lung dead space, Clewell

  %-----------------Dermal absorption-------------------
  KP=0.038; %Calculated by Peter Robinson using Wilschut = 0.038 cm/hr

% Buckpitt A, Morin D, Murphy S, Edwards P, Van Winkle L. Kinetics of
%   naphthalene metabolism in target and non-target tissues of rodents and in nasal
%   and airway microsomes from the Rhesus monkey. Toxicol Appl Pharmacol. 2013 Jul
%   15;270(2):97-105.
% Buckpitt AR, Castagnoli N Jr, Nelson SD, Jones AD, Bahnson LS. Stereoselectivity
%   of naphthalene epoxidation by mouse, rat, and hamster pulmonary, hepatic, and
%   renal microsomal enzymes. Drug Metab Dispos. 1987 Jul-Aug;15(4):491-8.
% Campbell JL, Andersen ME, Clewell HJ. A hybrid CFD-PBPK model for naphthalene
%   in rat and human with IVIVE for nasal tissue metabolism and cross-species
%   dosimetry. Inhal Toxicol. 2014 May;26(6):333-44.
% Cho TM, Rose RL, Hodgson E. In vitro metabolism of naphthalene by human liver
%   microsomal cytochrome P450 enzymes. Drug Metab Dispos. 2006 Jan;34(1):176-83.
% Clewell HJ 3rd, Gentry PR, Gearhart JM, Covington TR, Banton MI, Andersen ME.
%   Development of a physiologically based pharmacokinetic model of isopropanol and
%   its metabolite acetone. Toxicol Sci. 2001 Oct;63(2):160-72.
% NIST Chemistry Webbook
(https://webbook.nist.gov/cgi/cbook.cgi?Name=naphthalene&Units=SI)
% Ruark CD, Hack CE, Robinson PJ, Mahle DA, Gearhart JM. Predicting passive and
%   active tissue:plasma partition coefficients: interindividual and interspecies
%   variability. J Pharm Sci. 2014 Jul;103(7):2189-2198.
% Wilschut, A., Berge, ten, W. F., Robinson, P. J., & McKone, T. E. (1995). Estimating
skin permeation. The validation
%   of five mathematical skin permeation models. Chemosphere, 30(7), 1275-1296
```

APPENDIX F. ACSLX M FILES FOR RAT SIMULATIONS

Note: Column formatting introduces extraneous line breaks not in the original code.

NTP00_rat_singleihl.m

```
% NTP. 2000. NTP Technical Report on
the Toxicology and Carcinogenesis
Studies of Naphthalene
%  (CAS NO. 91-20-3) in F344/N Rats.
National Toxicology Program, Research
Triangle Park NC. NTP TR 500.

% Sprague-Dawley rats, n = 3 males
(data for female rats available too)
% 10, 30, or 60 ppm
%    6 hr single exposure
%    Chambers were allowed to empty for
12 min to reduce the concentration
enough to remove the rats
%    Therefore TChng = 6.1
%      (adding 6 min of full exposure
to average out 12 minutes of exposure
decrease from full to 10%)
% Male BW data from Table D5 = 125 g

% SET NCONC = 3 IN CSL
FILE!!!!!!!!!!!!!!!!!!!!!!!!!!!!!!

  resetdoses
  rat
  rat_naph

% Time, CVen for 10, 30, 60 ppm single
dose after 6.1 hours of exposure
% Values, top to bottom, are series of
average, -SE, +SE in mg/L
blood = [
6.10   0.463  1.387  5.360
6.10   0.497  1.439  6.026
6.10   0.429  1.335  4.694
6.60   0.308  0.911  3.193
6.60   0.317  0.962  3.529
6.60   0.299  0.860  2.857
7.10   0.171  0.661  2.227
7.10   0.179  0.720  2.615
7.10   0.163  0.602  1.839
7.60   0.094  0.476  1.143
7.60   0.103  0.494  1.399
7.60   0.085  0.458  0.887
8.10   0.100  0.239  0.838
8.10   0.111  0.267  0.987
8.10   0.089  0.211  0.689
10.1   0.051  0.138  0.380
10.1   0.053  0.145  0.422
10.1   0.049  0.131  0.338
12.1   0.029  0.071  0.252
12.1   0.030  0.072  0.261
12.1   0.028  0.070  0.243
14.1   0.014  0.060  0.174
14.1   0.017  0.063  0.197
14.1   0.011  0.057  0.151];

BW=0.125;  %Study specific rat

CONCLIST=[
0.0
10.0
0.0];

STTLIST=[
0.0
6.0
24.0];

TSTART=0.0;
TSTOP=24.0;
start @NoCallback

  plotcven = plot (0, blood(:,1),
blood(:,2), '+b', _t, _cven, '-b');
  plotcvenlo = plot (0, blood(:,1),
blood(:,2), '+b', _t, _cven, '-b');

CONCLIST=[
0.0
30.0
0.0];

  start @NoCallBack

  plot (plotcven, 1, blood(:,1),
blood(:,3), '+g', _t, _cven, '-g');

CONCLIST=[
0.0
60.0
0.0];

  start @NoCallBack

  plot (plotcven, 1, blood(:,1),
blood(:,4), '+m', _t, _cven, '-m');
```

RTI96_rat_iv.m

```
%Simulates data from RTI 1996
% SE and individual data are available
%Data used in publications by Quick and
Shuler (1999),
% Willems et al. (2001), Campbell et
al. (2014).

%male rats, 1, 3 and 10 mg/kg, time and
mean cvenbldna
```

```
male=[
0.03   1.980  3.580  9.330
0.03   3.080  8.280  11.030
0.03   0.880  0.000  7.630
0.08   0.668  2.310  5.050
0.08   0.707  4.610  6.150
0.08   0.629  0.010  3.950
0.17   0.322  2.120  2.700
0.17   0.337  3.920  2.830
0.17   0.307  0.320  2.570
0.33   0.106  0.720  0.787
0.33   0.128  1.250  0.897
0.33   0.084  0.190  0.677
0.67   0.039  0.245  0.447
0.67   0.059  0.312  0.487
0.67   0.019  0.178  0.407
1.00   0.338  0.158  0.186
1.00   0.341  0.180  0.210
1.00   0.335  0.136  0.162
2.00   0.017  0.123  0.086
2.00   NaN      0.220      0.093
2.00   NaN      0.026      0.078
4.00   0.014  0.053  0.048
4.00   NaN      0.101      0.058
4.00   NaN      0.005      0.038
6.00   0.011  0.091  0.036
6.00   NaN      NaN    0.039
6.00   NaN      NaN    0.032
8.00   0.007  0.021  0.014
8.00   NaN      NaN    0.018
8.00   NaN      NaN    0.010];

%female rats, 1, 3 or 10 mg/kg, time
and mean cvenbldna
fem=[
0.03   1.030  4.140  10.200
0.03   1.930  6.440  12.300
0.03   0.130  1.840  8.100
0.08   0.457  2.100  6.130
0.08   0.827  2.850  9.530
0.08   0.087  1.350  2.730
0.17   0.209  1.780  2.220
0.17   0.409  2.880  2.640
0.17   0.009  0.680  1.800
0.33   0.057  0.457  0.860
0.33   0.112  0.535  1.090
0.33   0.002  0.379  0.630
0.67   0.029  0.179  0.333
0.67   0.046  0.251  0.414
0.67   0.012  0.107  0.252
1.00   0.018  0.108  0.211
1.00   0.022  0.139  0.234
1.00   0.013  0.077  0.188
2.00   0.013  0.047  0.092
2.00   0.020  0.058  0.104
2.00   0.005  0.036  0.080
4.00   0.014  0.022  0.061
4.00   0.021  0.032  0.064
4.00   0.007  0.012  0.058
6.00   0.016  0.026  0.050
6.00   0.027  0.028  0.056
6.00   0.005  0.024  0.045
8.00   0.011  0.024  0.029
8.00   NaN      NaN    0.031
8.00   NaN      NaN    0.027];

ResetDoses
Rat
Rat_Naph

% MALE SIMULATIONS
IVDOSE=1.0; %1 mg/kg
BW=0.255; %male rats
TINF=0.008, TSTOP=8.0;
start @nocallback

plotcven = plot (0, _t, _cven, '-b',
male(:,1), male(:,2), '+b');
plotcvenlo = plot (0, _t, _cven, '-b',
male(:,1), male(:,2), '+b');

IVDOSE=3.0; %3 mg/kg
start @nocallback

plot (plotcven, 1,  _t, _cven, '-g',
male(:,1), male(:,3), '+g');

IVDOSE=10.0; %10 mg/kg
start @nocallback

plot (plotcven, 1,  _t, _cven, '-m',
male(:,1), male(:,4), '+m');

%FEMALE SIMULATIONS
BW=0.156; %female rats
IVDOSE=1.0; %1 mg/kg
TINF=0.008, TSTOP=8.0;
start @nocallback

plotcvenf = plot (0, _t, _cven, '-b',
fem(:,1), fem(:,2), '+b');
plotcvenflo = plot (0, _t, _cven, '-b',
fem(:,1), fem(:,2), '+b');

IVDOSE=3.0; %3 mg/kg
start @nocallback

plot (plotcvenf, 1,  _t, _cven, '-g',
fem(:,1), fem(:,3), '+g');

IVDOSE=10.0; %10 mg/kg
start @nocallback

plot (plotcvenf, 1,  _t, _cven, '-m',
fem(:,1), fem(:,4), '+m');
```

NTP00_rat_repeatihl_2wk.m

```
% NTP. 2000. NTP Technical Report on
the Toxicology and Carcinogenesis
Studies of Naphthalene
%  (CAS NO. 91-20-3) in F344/N Rats.
National Toxicology Program, Research
Triangle Park NC. NTP TR 500.
%
```

```
% Sprague-Dawley rats, n = 3 males
(data for female rats available too; if
n=1 or 2, no SE info)
% 10, 30, or 60 ppm
%    6 hr/d, 5 d/wk, 2 week timepoint
%    Chambers were allowed to empty for
12 min to reduce the concentration
enough to remove the rats
%    Therefore TChng = 6.1
%      (adding 6 min of full exposure
to average out 12 minutes of exposure
decrease from full to 10%)
% BW data from 1 and 4 weeks used to
calculate a rough 2 (or 2.5) wk BW of
0.169 kg

% SET NCONC = 21 IN CSL
FILE!!!!!!!!!!!!!!!!!!!!!!!!!!!!!

  resetdoses
  rat
  rat_naph

% Increased VMaxC values due to
metabolic upregulation
%Use for KmLiv = KmLu = 2.18
  VMAXLIVC = 8.28*1.4;
  VMAXLUC = 0.45*1.12;

% Time, CVen for 10, 30, 60 ppm after
day 12 exposures ended
% Values, top to bottom, are series of
average, -SE, +SE in mg/L

blood = [
270.10 0.331  1.540  3.730
270.10 0.299  1.473  3.525
270.10 0.363  1.607  3.935
270.60 0.192  0.765  1.640
270.60 0.177  0.724  1.590
270.60 0.207  0.806  1.690
271.10 0.118  NaN      NaN
271.10 0.111  NaN      NaN
271.10 0.125  NaN      NaN
271.60 NaN      0.210      0.544
271.60 NaN      0.190      0.488
271.60 NaN      0.230      0.600
272.10 0.045  NaN      NaN
275.10 0.015  0.047  NaN
275.10 0.011  0.043  NaN
275.10 0.019  0.051  NaN
276.10 NaN    NaN      0.069
276.10 NaN      NaN    0.066
276.10 NaN      NaN    0.072
278.10 NaN      0.020      NaN
278.10 NaN      0.016      NaN
278.10 NaN      0.024      NaN
282.10 NaN      0.007      0.022
282.10 NaN      0.007      0.019
282.10 NaN      0.007      0.025
286.10 NaN      NaN    0.008
286.10 NaN      NaN    0.006
286.10 NaN      NaN    0.010];
```

```
BW=0.169;  %Study specific rat

CONCLIST=[
0.0
10.0
0.0
10.0
0.0
10.0
0.0
10.0
0.0
10.0
0.0
10.0
0.0
10.0
0.0
10.0
0.0
10.0
0.0
10.0
0.0];

STTLIST=[
0.0
6.0
18.0
6.0
18.0
6.0
18.0
6.0
18.0
6.0
66.0
6.0
18.0
6.0
18.0
6.0
18.0
6.0
18.0
6.0
290.0];

TSTART=0.0;
TSTOP=290.0;

start @NoCallback

  plotcven = plot (0, blood(:,1),
blood(:,2), '+b', _t, _cven, '-b');
  plotcvenlo = plot (0, blood(:,1),
blood(:,2), '+b', _t, _cven, '-b');

 CONCLIST=[
 0.0
30.0
0.0
```

```
30.0
0.0
30.0
0.0
30.0
0.0
30.0
0.0
30.0
0.0
30.0
0.0
30.0
0.0
30.0
0.0
30.0
0.0];

  start @NoCallBack

  plot (plotcven, 1, blood(:,1),
blood(:,3), '+g', _t, _cven, '-g');

CONCLIST=[
0.0
60.0
0.0
60.0
0.0
60.0
0.0
60.0
0.0
60.0
0.0
60.0
0.0
60.0
0.0
60.0
0.0
60.0
0.0];

  start @NoCallBack

  plot (plotcven, 1, blood(:,1),
blood(:,4), '+m', _t, _cven, '-m');
```

APPENDIX G. ACSLX M FILES FOR HUMAN LITERATURE SIMULATIONS

Note: Column formatting introduces extraneous line breaks not in the original code.

Bieniek_hmn.m

```
% Bieniek G. 1994. The presence of 1-
naphthol in the urine of industrial
workers exposed to
%   naphthalene. Occup Environ Med
51:357-359.
%
% Naphthalene oil workers have a T1/2
in urine of 4 hours
%   73.6% naphthalene, plus naphthol
and the oil carrier (plus impurities)
% Coke workers have a T1/2 in urine of
14 hours
%   Coke does not contain naphthols
% Figure 1 indicates that exposures
were around 0.5 mg/m3 = 0.1 ppm on
average
%    FIRST GUESS ONLY - Fitted to data
somewhat to observe elimination
behavior
% Figure 2 indicates 3x the naphthol in
oil workers as compared to coke workers
%    First guess is 1.5 ppm = 0.3 ppm
for average exposure
% Data are for 1-naphthol only; Change
FOH values accordingly

% SET NCONC = 3 IN CSL
FILE!!!!!!!!!!!!!!!!!!!!!!!!!!!!!

coke=[
0.18   0.60
1.09   0.20
1.14   0.50
1.02   0.80
1.41   0.90
1.21   1.30
3.13   1.30
3.31   1.30
2.74   0.90
2.97   0.70
4.27   0.80
4.66   1.01
5.07   1.01
4.86   1.21
4.11   1.41
5.46   1.61
6.79   1.30
7.20   1.01
7.38   0.61
7.17   1.61
7.24   2.00
7.38   2.00
8.06   2.20
8.16   2.10
8.75   1.41
9.30   1.41
9.37   1.71
10.9   2.81
10.8   2.40
11.2   2.20
11.4   1.81
11.1   1.31
11.1   1.01
12.5   1.21
12.5   2.10
12.7   1.81
12.9   1.80
13.2   2.40
14.4   1.61
14.8   1.81
15.0   1.31
15.1   1.32
15.2   1.41
15.3   1.71
16.2   1.91
17.0   1.51
17.3   1.41
17.4   1.41
17.1   1.11];

oil=[
0.69   0.11
1.18   0.12
0.90   1.13
1.18   1.43
0.96   1.83
0.67   2.24
1.36   2.44
1.78   2.60
1.94   2.61
1.31   3.21
0.96   3.40
0.85   4.34
3.16   3.23
3.14   3.10
3.29   2.90
3.29   3.59
3.40   3.53
3.89   1.35
5.29   2.83
5.27   4.73
3.49   5.84
5.27   7.04
5.41   7.04
6.87   4.14
6.76   5.41
7.09   4.62
7.49   3.84
7.49   4.52
7.49   5.41
```

```
7.27   6.02
7.11   8.48
7.40   8.35
7.52   8.06
7.38   9.80
9.47   11.00
9.38   9.19
9.07   8.58
9.45   8.28
8.87   5.93
9.16   5.73
9.07   4.95
8.89   3.62
9.87   5.05
11.1   5.14
10.6   4.05
10.9   4.07
11.2   4.43
10.5   2.24
11.4   5.86
11.3   8.19
12.9   6.85
13.1   5.95
13.2   4.73
13.4   4.75
13.0   4.25
12.4   3.73
11.8   3.44
12.8   3.14
13.2   3.23
13.0   1.85
13.2   2.06
13.4   3.92
13.8   4.12
14.0   1.86
13.8   0.77
14.8   0.45
15.5   2.33
15.4   3.74
15.8   3.44
16.7   2.35
17.1   2.76
17.3   2.67
16.9   1.25
16.7   1.08];

  resetdoses
  human
  hmn_naph

BW=70.0;    %Generic
FOHLU=0.055;
FOHLIV=0.1;

%-----------------------Coke Exposure--
--------------------------
%NOTE: CURRENT PEL IS 10 MG/M3
CONCLIST=[
0.0
8.0
0.0];

STTLIST=[
0.0
8.0
18.0];

TSTART=0.0;
TSTOP=18.0;
start @NoCallback

  ploturn = plot (0, _t, _curnmetoh, '-
b',  coke(:,1), coke(:,2),'+b');
  ploturn2 = plot (0, _t, _curnnormoh,
'-g',  coke(:,1), coke(:,2),'+g');

%-----------------------Oil Exposure---
-------------------------
CONCLIST=[
0.0
22.0
0.0];

TSTART=0.0;
TSTOP=18.0;
start @NoCallback

  ploturno = plot (0, _t, _curnmetoh,
'-b',  oil(:,1), oil(:,2),'+b');
  ploturno2 = plot (0, _t, _curnnormoh,
'-g',  oil(:,1), oil(:,2),'+g');
```

Egeghy_hmn_hiconc.m

```
% Egeghy PP, Hauf-Cabalo L, Gibson R,
Rappaport SM. Benzene and naphthalene
in
%   air and breath as indicators of
exposure to jet fuel. Occup Environ
Med. 2003
%   Dec;60(12):969-76.

% Human data using median plus upper
and lower quartile breath values versus
median exposure concentration

% Assuming 70 kg std human

%    4 data points
% !!!!!!!!!!!!!!!!!!!!Change NConc = to
# of data points in csl file

% Breath concentrations
%    Top to Bottom: median, lower and
upper quartile values for times:
%      pre-expos at testing ctr,
immediately after 4 hour shift, post-
expos at testing ctr

%High exposure group only
breath = [
0.00   0.0000006
4.57   0.0000060
4.57   0.0000026
4.57   0.0000161
```

```
5.13   0.00000183
5.13   0.0000009
5.13   0.0000040];

  resetdoses
  human
  hmn_naph

BW=70.0;

% Note that these are the times until
the next change, in hours
%    Set the last value equal to TSTOP
in order to run out the clock at the
final concentration (usually 0.0)
STTLIST=[
0.00
0.57
4.00
6.00];

%  HIGH EXPOSURE
CONCLIST=[
0.000
0.000
0.093
0.000];

TSTART=0.0;
TSTOP=6.0;

start @NoCallback

plotexh = plot (0, _t, _cend, '-b',
breath(:,1), breath(:,4),'+b');

start @NoCallback
```

LIST OF ACRONYMS

AF	Air Force
AUC	area under the curve
BMI	body mass index
CDC	Centers for Disease Control
F344	Fischer 344
GC	gas chromatograph
HPLC	high performance liquid chromatography
IP	intraperitoneal
IV	intravenous
MC	Monte Carlo
MS	mass spectrometry
NaDos	naphthalene dosimeter
NHP	non-human primate
NIOSH	National Institute of Occupational Safety and Health
NTP	National Toxicology Program
ODE	ordinary differential equation
PA	permeability coefficient
PBPK	physiologically-based pharmacokinetic
PC	partition coefficient
PTFE	polytetrafluoroethylene
RT	real time
RTI	Research Triangle Institute
SD	standard deviation
SE	standard error
TWA	time weighted average
UV	ultraviolet